



Università degli Studi di Ferrara

DOTTORATO DI RICERCA IN
SCIENZE FARMACEUTICHE

CICLO XXV

COORDINATORE Prof. MANFREDINI STEFANO

**Identification and synthesis of 3,4-
isoxazolidiamides as new class of
Hsp90 inhibitors**

Settore Scientifico Disciplinare CHIM/06

Tutore

Dott. Marchetti Paolo

Dottorando

Dott. Mangiola Stefania

Anni 2009/2012

Contents

1	INTRODUCTION	1
1.1	Heat shock proteins in health and disease	2
1.2	Functions of molecular chaperone	3
1.3	Heat shock proteins classification	4
1.4	Hsp90	7
1.4.1	Molecular anatomy of Hsp90	8
1.4.2	ATPase cycle	10
1.5	Oncogenic Hsp90 client proteins and signaling pathways	15
1.5.1	Growth Factor Receptor	12
1.5.2	Steroid receptors	13
1.5.3	Bcr-Abl	13
1.5.4	Flt3	13
1.5.5	Protein Kinase	14
1.6	A high-affinity conformation of tumor Hsp90 confers drug selectivity	15
1.7	Inhibitors of Hsp90 C-terminal ATP-binding domain	17
1.7.1	Novobiocin and analogues	17
1.7.2	Other C-terminal inhibitors	18
1.8	Inhibitors of Hsp90 N-terminal ATP binding domain	18
1.8.1	Geldanamycin and its derivatives	19
1.8.2	Radicalol and its derivatives	21
1.8.3	Purine-based derivatives	22
1.8.4	<i>o</i> -Aminobenzoic acid derivatives and resorcinol derivatives	24
1.8.5	Pyrazoles and isoxazoles derivatives	26

2	AIM OF THESIS	32
3	CHEMISTRY	36
3.1	Synthesis of 3,4-isoxazolidiamides scaffold	37
3.1.1	Synthesis of chloro-resorcinol derivatives	37
3.1.2	Modification at C-3	38
3.1.3	Synthesis of isopropyl-resorcinol derivatives	38
3.1.4	Modification at C-4	39
3.1.5	Synthesis of 4-aminoisoxazole	42
3.2	Attempts to synthesize 4,5,6,7-tetrahydro-isoxazole-[4,5-c]pyridine scaffold	43
3.3	Synthesis 4,5,6,7-tetrahydro-isoxazolo-[4,5-c]pyridine scaffold	45
3.3.1	Synthesis of resorcinol acid	46
4	RESULTS AND DISCUSSION	48
4.1	In vitro studies of 3,4-isoxazolidiamides scaffold	49
4.1.1	Analysis of the degradation of Hsp90 client proteins in A431 cells	59
4.2	In vivo studies of 3,4-isoxazolidiamides scaffold	61
4.3	In vitro studies of 4,5,6,7-tetrahydro-isoxazolo-[4,5-c]pyridine scaffold	64
5	CONCLUSION	67
6	EXPERIMENTAL SECTION	69
6.1	Biological section	70
6.2	Molecular modeling	72
6.3	Materials and methods	73
6.4	Experimental procedures	74
7	REFERENCE	106

List of Figures

1.1 Structural domain organization of human Hsp90 protein	8
1.2 ATP-dependent molecular clamp	10
1.3 Hsp90 cycle	15
1.4 Hsp90 client proteins	12
1.5 Model for tumor selectivity of Hsp90 inhibitors and Hsp90-dependent malignant progression	15
1.6 Chemical structure of novobiocin and coumercyn A1	17
1.7 Chemical structure of A4 and DHN2	18
1.8 Chemical structure of cisplatin and EGCG	18
1.9 Chemical structure of geldanamycin	19
1.10 Chemical structure of geldanamycin derivatives	20
1.11 Chemical structure of radicicol	21
1.12 Chemical structure of radicicol derivatives	21
1.13 Chemical structure of PU3 and PU24FCI	22
1.14 Chemical structure of PU-H71 and CUDC-305	23
1.15 Chemical structure of CNF-2024/BIIB021 and derivatives	24
1.16 Chemical structure of SNX-2112 and SNX-5422	24
1.17 Chemical structure of benzoisoxazole derivatives	25
1.18 Chemical structure of resorcinol derivatives	25
1.19 Chemical structure of other N-terminal domain inhibitors	26
1.20 Chemical structure of pyrazole derivatives	26
1.21 Chemical structure of VER49009	27
1.22 X-ray structure of VER49009 and VER50589	28
1.23 Chemical structure of VER50589	29
1.24 Chemical structure of NVP-AUY922	30
2.1 General structure of new Hsp90 inhibitors used in these study	33
2.2 New 4,5,6,7-tetrahydro-isoxazolo-[4,5-c]pyridine scaffold	35

4.1 36 co-crystallized in Hsp90 active site and docking pose of compound 91 in Hsp90 active site	50
4.2 123b co-crystallized in Hsp90 active site and docking pose of compound 58 in Hsp90 active site	53
4.3 Analysis of Hsp90 client protein levels and Hsp70 in A431 tumor cells	60
4.4 Antitumor activity of the compounds 91 and 115	62
4.5 Analysis of Hsp90 client protein levels (EGFR, Akt, CDK-4, and Hsp70) in A431 tumor xenografts	63
4.6 Interaction between Hsp90 and resorcinol moiety	64

List of Schemes

3.1 Synthesis of chloro-resorcinol intermediate 44a	37
3.2 Synthesis of chloro-resorcinol intermediate 44b,c	38
3.3 Synthesis of isopropyl-resorcinol intermediate 44d	39
3.4 Synthesis of 3,4-isoxazolidiamides inhibitors	40
3.5 Synthesis of morpholine and piperazine derivatives	41
3.6 Synthesis of amines-isoxazole derivates 123a-d	42
3.7 Attempts to synthesize 4,5,6,7-tetrahydro-isoxazole-[4,5-c]pyridine scaffold	43
3.8 Synthesis of 4,5,6,7-tetrahydro-isoxazole-[4,5-c]pyridine	45
3.9 Synthesis of chloro-resorcinol acid	46
3.10 Synthesis of isopropyl-resorcinol acid	47

List of Tables

1.1 The most families of molecular chaperones	4
1.2 Members of the family of 90-kDa molecular chaperones	7
1.3 Relationship between Hsp90 client proteins and hallmarks of cancer	14
1.4 Values of IG ₅₀ of VER-49009 and VER-50589 in different cells line	29
1.5 Hsp90-binding drugs: many classes of natural, semisynthetic and synthetic inhibitors of Hsp90	31
2.1 Data of G-score of structures proposed	34
4.1 Data for isoxazole-3,4 diamides	54
4.2 Data for isoxazole-4-alkyl/cycloalkyl amides	55
4.3 Data for isoxazole-4-aryl/heteroaryl amides	57
4.4 Data for 4-amino isoxazole	59
4.5 Data of cytotoxicity on A431 epidermoid carcinoma cells of the compounds tested in vivo	61
4.6 Antitumor activity of compounds 91 and 115	62
4.7 Data of binding on Hsp90 and citotoxicity on NCI-H460 non small cell lung carcinoma cells	65
4.8 Cytotoxic and apoptotic effects of the Hsp90 inhibitors in K562 cells	66

List of Abbreviations

- Aha1:** activator of Hsp90 ATPase
- Akt:** Protein Kinase B
- Boc:** *tert*-butoxycarbonyl
- Cdk:** Cyclin-dependent kinases
- DCM:** dichloromethane
- Cdc37:** cell division cycle
- DMF:** dimethylformamide
- DMSO:** dimethylsulfoxide
- EDC:** N[']-(3-dimethylaminopropyl)-N-ethyl-carbodiimide
- EGF-R:** epidermal growth factor receptor
- EtOH:** ethanol
- Flt3:** FMS-like tyrosine kinase 3
- FP:** fluorescence polarization
- GRP:** glucose regulated protein94
- HER-2:** Human Epidermal Growth Factor Receptor 2
- HOBt:** 1-Hydroxybenzotriazole
- Hop:** Hsp70-organizing protein
- IGF-R:** insulin-like growth factor-1 receptor
- IP:** immunophilins
- kDa:** kilo Dalton
- PDGF-R:** platelet-derived growth factor receptor
- PhMe:** toluene
- PI3K:** phosphatidyl inositol-3 kinase
- TFA:** trifluoroacetic acid
- TPR:** tetratricopeptide repeat
- TRAP:** tumor necrosis factor receptor-associated protein
- p-TSA:** p-toluene sulfonic acid

Chapter 1

Introduction

Contents

1.1 Heat shock proteins in health and disease

1.2 Functions of molecular chaperone

1.3 Heat shock proteins classification

1.4 Hsp90

1.4.1 Molecular anatomy of Hsp90

1.4.2 ATPase cycle

1.5 Oncogenic Hsp90 client proteins and signaling pathways

1.5.1 Growth Factor Receptors

1.5.2 Steroid receptors

1.5.3 Bcr-Abl

1.5.4 Flt3

1.5.5 Protein Kinase

1.6 A high-affinity conformation of tumor Hsp90 confers drug selectivity

1.7 Inhibitors of Hsp90 C-terminal ATP-binding domain

1.7.1 Novobiocin and analogues

1.7.2 Other C-terminal inhibitors

1.8 Inhibitors of Hsp90 N-terminal ATP binding domain

1.8.1 Geldanamycin and its derivatives

1.8.2 Radicicol and its derivatives

1.8.3 Purine-based derivatives

1.8.4 *o*-Aminobenzoic acid derivatives and resorcinol derivatives

1.8.5 Pyrazoles and isoxazoles derivatives

1.1 Heat shock proteins in health and disease

Heat Shock Proteins (Hsps) are molecular chaperones that have emerged over the last few years as one of the hottest and most interesting topics in biology. It has also become increasingly recognized that they play an important role in oncogenesis and cell death.^{1,2}

Among chaperones, heat shock proteins are the most important. The heat shock response was discovered in 1962 by Ritossa, who observed a pattern of *Drosophila* salivary gland chromosome puffs that were induced in response to transient exposures to elevated temperatures. Since then, efforts from a large number of investigators have shown that the heat shock response is ubiquitous and highly conserved in all organisms (from bacteria to plants and animals) as an essential defense mechanism for protection of cells from a wide range of harmful conditions. Stress can be any sudden change in the cellular environment, to which the cell is not prepared to respond, such as heat shock, hypoxia, alcohols, inhibitors of energy metabolism, heavy metals, oxidative stress, fever, inflammation, DNA damage or UV radiation.³ The rationale behind this phenomenon is that after stress there is an increased need for the chaperone function of Hsp, which triggers their induction. This need is caused by the increased amount of damaged proteins, by the inhibition of their elimination via the proteasome as well as by the damage of the chaperones themselves. Hsp induction might help to renature chaperones and, therefore, Hsp induction might lead to a ‘cascading amplification’ of available chaperone activity.³⁻⁵

Cancer is a disease characterized by genetic instability. Although identification of novel therapeutic agents via molecular targeting offers the promise of great specificity coupled with reduced systemic toxicity, specific inhibition of individual proteins or signaling pathways faces the potential peril of being subverted by the inherent genetic plasticity of cancer cells. Cancer cells are very adept at adapting to noxious environments.

If one assumes that cancer cells are always under moderate to severe stress of one type or another, an approach to this apparent dilemma might be to target the basic machinery that allows cancer cells to adapt so successfully to stress. Cells respond to stress by increasing synthesis of a number of molecular chaperones (also known as heat shock proteins, or Hsps, because they were first observed in cells exposed to elevated temperature).⁶

A recent trend in cancer therapy has been to develop agents that “target” a single molecular alteration. As most cancers are a result of multiple transformation-specific regulatory alterations, targeting one abnormality may be insufficient in reversing the transformed

phenotype. Chaperones are proteins that allow cancer cells to tolerate the components of dysregulated pathways that otherwise would be lethal; thus, their inactivation may result in targeting multiple molecular alterations.^{7,8}

1.2 Functions of molecular chaperones

Molecular chaperones support protein synthesis *in vivo*. Their most important roles are:

- facilitate the folding of nascent proteins into a stable and functional conformation,
- maintain conformation, stability and function of client proteins within the cell,⁹
- protect other proteins against aggregation,
- maintain the cellular homeostasis,
- help to transport proteins from the cytoplasm into different intracellular compartments,
- maintain proper protein folding, and facilitate the assembly of protein polymers,¹⁰
- chaperones do not determine the tertiary structure of the folding proteins, but help them find their structure more efficiently.¹¹

Instead, under conditions of stress, where protein folding/assembly events may be compromised, the increased expression and accumulation of the stress proteins facilitates the ability of cells to both repair and synthesize new proteins to replace those that were damaged after the particular metabolic insult. Further, chaperones are upregulated in response to cellular stresses and serve as essential regulators of proteins by preventing misfolding. In the case of acute misfolding and aggregation, proteins may be targeted to the proteasome for degradation.^{12,13}

1.3 Heat shock proteins classification

Heat shock proteins are classified into six major families based on their molecular mass: Hsp100 (100-110 kDa), Hsp90 (83-90 kDa), Hsp70 (66-78 kDa), Hsp60, Hsp 40 and the small Hsp (15-30 kDa) (*Table 1.1*). Family members of Hsps are expressed either constitutively or regulated inductively, and are present in different subcellular compartments. High molecular weight Hsps are ATP-dependent chaperones, whereas small HSPs act in an ATP-independent fashion. The most studied stress inducible Hsps are Hsp90, Hsp70 and Hsp27.¹⁴

Table 1.1 The most families of molecular chaperones.

Eukaryotic molecular chaperones	Functions of chaperone
Hsp27, the small heat-shock proteins	Prevent aggregation of proteins and the release of proteins by aggregation
Hsp40	Help the folding proteins
Hsp60	Prevent aggregation of proteins and help the folding proteins
Hsp70,grp78	Prevent aggregation of proteins and help the folding proteins
Hsp 90, grp94	Prevent aggregation of proteins
Hsp100	Release proteins by aggregations

sHsp (small Heat shock proteins)

Small heat shock proteins have a molecular mass between 15 and 30 kDa. They exist as high molecular weight complexes in vertebrates, *Drosophila*, yeasts, fungi, and plants. The small mammalian Hsps are oligomeric structures of about 32 subunits, corresponding to a molecular mass of 800 kDa. They are present in the cytosol of most cells and tissues even in the absence of stress factors such as elevated temperatures.

All these proteins contain a rather conservative so called α -crystallin domain, containing 80-100 residues located as a rule in the C-terminal part of these proteins.¹⁵ Additional features attributed to small Hsps range from RNA storage in heat shock granules to inhibition of apoptosis, actin polymerization and contribution to the optical properties of the eye lens in the case of α -crystallin. At the moment, it is unclear how these seemingly different functions can be explained by a common mechanism. However, as most of the observed phenomena involve non-native protein, the repeatedly reported chaperone properties of Hsp might be a key feature for further understanding of their function.¹⁶

Hsp40

Also known as chaperone DnaJ in *E. Coli* or Hsp40 (heat shock protein 40 kD) in eukaryotic cells, Hsp40 is a molecular chaperone protein and is involved in stabilization processes and correct folding of nascent proteins. It is expressed in a wide variety of organisms from bacteria to humans.

This family of proteins contains a 70 amino acid consensus sequence known as the J domain. The J domain interacts with Hsp70 and plays a role in regulating the ATPase activity of Hsp70.¹⁷

Hsp60

Hsp60 (heat shock protein 60 kDa) is a mitochondrial chaperonin that is typically held responsible for the transportation and refolding of proteins from the cytoplasm into the mitochondrial matrix. In addition to its role as a heat shock protein, Hsp60 functions as a chaperonin to assist in folding linear amino acid chains into their respective three-dimensional structure. Hsp60 are divided into two general groups: the chaperonines of the first group are expressed in Eubacteria, in mitochondrial, in chloroplasts and in most Archae, instead the chaperonines of the second group are found in cytosol of Eukaryotes and Archaeobacteria. Under normal physiological conditions, Hsp60 is a 60 kDa oligomer composed of monomers that form a complex arranged as two stacked heptameric rings. This double ring structure forms a large central cavity in which the unfolded protein binds via hydrophobic interactions. Each subunit of Hsp60 has three domains: the apical domain, the equatorial domain, and the intermediate domain. Through the extensive study of groEL, Hsp60's bacterial homolog, Hsp60 has been deemed essential in the synthesis and transportation of essential mitochondrial proteins from the cell's cytoplasm into the mitochondrial matrix.

Hsp70

Hsp70 is a conserved molecular chaperone that assists a wide range of folding processes, including the folding and assembly of newly synthesized proteins, refolding of misfolded and aggregated proteins, membrane translocation of organellar and secretory proteins, and control of the activity of regulatory proteins. The role of Hsp70s in the

folding of non-native proteins can be divided into three related activities: prevention of aggregation, promotion of folding to the native state, and solubilization and refolding of aggregated proteins.¹⁸

All such functions are mediated by interaction of extended, hydrophobic regions of substrate proteins with the Hsp70 C-terminal substrate-binding domain (SBD). Hsp70 proteins all consist of the same working parts: a highly conserved NH₂-terminal ATPase domain of 44 kDa and a COOH-terminal region of 25 kDa, divided into a conserved substrate binding domain of 15 kDa and a less-conserved immediate COOH-terminal domain of 10 kDa.¹⁹ The dynamic closing and reopening of the base onto the lid is regulated by ATP hydrolysis in the nucleotide binding domain. In the mammalian system, the molecular chaperones Hsp70 and Hsp90 are involved in the folding and maturation of key regulatory proteins, like steroid hormone receptors, transcription factors, and kinases, some of which are involved in cancer progression. Hsp70 and Hsp90 form a multichaperone complex, in which both proteins are connected by a third one called Hop.²⁰

Hsp90

Heat shock protein 90 (Hsp90) is one of the most abundant chaperone proteins, and has been recently shown to interact with a variety of proteins involved in cell proliferation. Of interest to cancer researchers, Hsp90 is constitutively expressed at 2 to 10 fold higher levels in tumor cells compared to their normal counterparts, suggesting that it may play a critical regulatory role in tumor cell growth and/or survival.²¹

The following section will focus on detailed description of the structure, function and clients oncogenic proteins of Hsp90.

Hsp100

The Hsp100 family of proteins has a wide distribution in both prokaryotes and eukaryotes. Members of the Hsp100 family were described first as components of the 2-subunit bacterial Clp protease system. The large-subunit ClpA represents an adenosine triphosphate (ATP)-dependent unfoldase, whereas the small-subunit ClpP is the protease. ClpA alone has no proteolytic activity, but it is able to prevent target proteins from aggregation. Interestingly, many ClpA-related proteins were characterized in bacteria and eukaryotes as stress-induced proteins, and hence, they are summarized as members of the Hsp100 family. A proteolytic subunit (ClpP) is only found in bacteria associated mainly or

exclusively with ClpA protein, whereas in eukaryotes, only the large subunit with chaperone function is observed. A peculiarity of the Hsp100 chaperones is their capability to promote dissociation of aggregated proteins in an ATP-dependent manner.²² Hsp100 (Clp family in *E. coli*) proteins are a family with a great diversity of functions, such as increased tolerance to high temperatures, promotion of proteolysis of specific cellular substrates and regulation of transcription. HSP100/Clp proteins are also synthesized in a variety of specific patterns and, in eukaryotes, are localized to different subcellular compartments. Recent data suggest that a common ability to disassemble higher order protein structures and aggregates unifies the molecular functions of this diverse family.²³ Hsp100 have been studied *in vivo* and *in vitro* for their ability to target and unfold tagged and misfolded proteins.

1.4 Hsp90

The 90-kDa heat shock protein, Hsp90, is a highly conserved molecular chaperone protein found in bacteria and all eukaryotes, exhibiting a 40% sequence identity between human and *Escherichia coli* protein.²⁴⁻²⁸ Under non-stress conditions, Hsp90 is present as 1-2% of the total cytosolic protein content, whereas under stress it is increased up to 4-6%.²⁹ This renders it one of the most abundant proteins of a typical eukaryotic proteome and has been shown to be essential for cell survival. Hsp90 is an ATP-dependent chaperone essential for the maturation and activity of a varied group of proteins involved in signal transduction, cell cycle regulation and apoptosis.³⁰

All the Hsp90 family members share a common general structural plan that likely reflects functional similarities in their mode of action. Currently, four forms are known in humans: the two major cytoplasmic isoforms Hsp90 α (inducible form) and Hsp90 β (constitutive form), glucose regulated protein94 (Grp94) in the endoplasmic reticulum and tumor necrosis factor receptor-associated protein1 (TRAP1/Hsp75) in the mitochondrial matrix. The four isomer forms are listed in *Table 1.2*.

Table 1.2 Members of the family of 90-kDa molecular chaperones.

Name	Location in cells
Hsp90 α , HSP90 β	Cytoplasm
Hsp75/TRAP-1	Mitochondrial
Grp94	Endoplasmic reticulum

The cytoplasmic forms exist predominantly as dimer within the cell and Hsp90 functions as a dimer, both homo and heterodimers, to maintain the appropriate folding and conformation of many other proteins.³¹

1.4.1 Molecular anatomy of Hsp90

Crystallization of full-length Hsp90 was first reported in the early 1990s.^{32,33} Functional Hsp90 is a homodimeric protein composed of two identical and symmetrical subunits.³⁴ Each monomer is divided into three highly conserved domains common to all members of the Hsp90 family, separated by a highly charged region of varying length.³⁵ These include the N-terminal domain (24-28 kDa), the C-terminal domain (11-15 kDa) and the middle domain (38-44 kDa) (*Figure 1.1*).³⁶

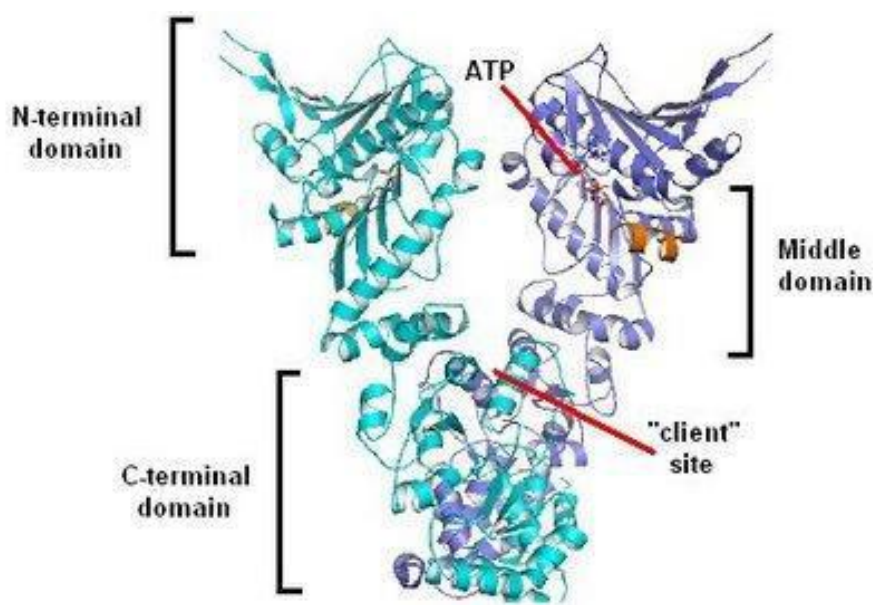


Figure 1.1 Structural domain organisation of human Hsp90 protein. The Hsp90 monomer is comprised of three domains: the N-terminal domain responsible for ATP-binding and inhibitor of Hsp90 as geldanamycin, radicicol (red), a core domain (green), and a C-terminal domain that facilitates homodimerization (blue). In eukaryotes, a "charged linker" region, that connects the N-terminus with the middle domain (not shown in figure).

The most studied is the 25kDa N-terminal domain, a proteolytically resistant core domain of approximately 220 amino acid residues containing both ATP-binding and ATP-hydrolytic activities. The three-dimensional crystal structure of human and yeast N-terminal fragments revealed the presence of an eight-stranded anti-parallel β -sheet and nine α -helices, which configure an α/β sandwich module and delimit the nucleotide-binding

pocket. This fold differs from the typical ATP-binding sites and shares high 3D homology with members of the ATPase/kinase GHHL (**G**yrase B, **H**sp90, **H**istidine Kinases, **MutL**) superfamily, in addition to other members of the Hsp90 family. These proteins are unrelated in function, but all of them require ATPase activity and contain an unusual adenine-nucleotide-binding pocket known as “Bergerat fold” for binding ATP.^{37,38}

A second ATP binding site is near the C-terminal domain, a 12kDa structural lobe that provides strong dimerization interface, necessary for both constitutive homodimerization and target substrate binding, which is absolutely essential for the implementation of HSP90 chaperone activities. The C-terminal of Hsp90 is the site of dimerization. This region contains a pentapeptide domain (MEEVD) implicated in binding to co-chaperones of Hsp90 such as Hop and Sti1 which contain tetratricopeptide repeats (TPR). Thus, the C-terminal domain is also involved in the formation of active Hsp90 multiprotein complexes.³⁹⁻⁴³

Most of the Hsp90 family members contain a highly charged linker region that joins the N-terminal with the flexible middle domain of 35kDa. This middle domain plays a crucial role in modulating ATP hydrolysis, through interaction with the N-terminal pocket. The isolated ATP-domain shows low intrinsic ATP-ase activity, which is enhanced by the cooperation of C-terminal sequence.⁴⁴

1.4.2 ATPase cycle

The structural mechanism for the chaperone activity of Hsp90 has been likened to a ‘molecular clamp’. In the absence of bound nucleotide, the N-termini of the Hsp90 homodimer maintain an open-state, facilitating the ‘capture’ of client proteins. Association with ATP induces modest changes in the conformation of Hsp90 that permit a transitory interaction between the opposing N-terminal domains. This produces the closed form of Hsp90 where clamping of the substrate protein occurs (*Figure 1.2*). It is through this ATPase-driven cycle that Hsp90, with the assistance of several co-chaperones, induces the activation of its ‘clientelle’.

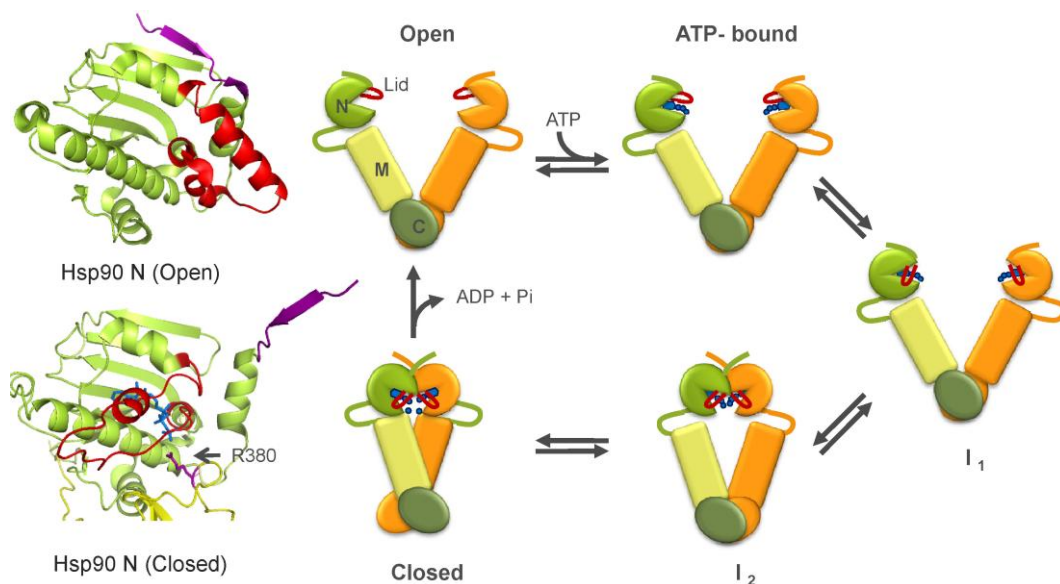


Figure 1.2 ATP-dependent molecular clamp: ATP-driven molecular clamp cycle of Hsp90. C-termin domain (C), N-termin domain (N), middle domain (M).

In eukaryotic plasma, Hsp90 is considered to mediate the folding, stabilization, activation and assembly of its client proteins, including steroid receptors, protein kinases and transcription factors. Hsp90 is not capable of autonomously functioning as a protein chaperone. Instead, it serves at the core of various multiprotein complexes that incorporate other chaperones, such as Hsp70, and an assortment of co-chaperones. Three dynamic steps have been observed in this assembly process (*Figure 1.3*). In a typical chaperone cycle, a client protein initially binds to a Hsp70/Hsp40 which is transferred onto the ADP-bound Hsp90 via the TPR (tetratricopeptide repeat) to form an *early complex*. Then Hsp90 with the co-chaperone Hop binds to this early complex to form an *intermediate complex*,

while the protein Hip binds to hsp70. When ADP is replaced by ATP, Hsp90 undergoes a conformational change which releases Hsp70/Hsp40 and Hop, thus allowing the ATP-dependent association of other co-chaperones, including p50, p23, CDC37, AHA1 which increases the ATPase activity of HSP90 and the immunophilins (IP) to form a *mature complex*.⁴⁵ When the ATP-binding site of Hsp90 is occupied by competitive inhibitors, the formation of the mature complex is disrupted and the client proteins can be degraded through the ubiquitination-proteasome pathway.^{46,47}

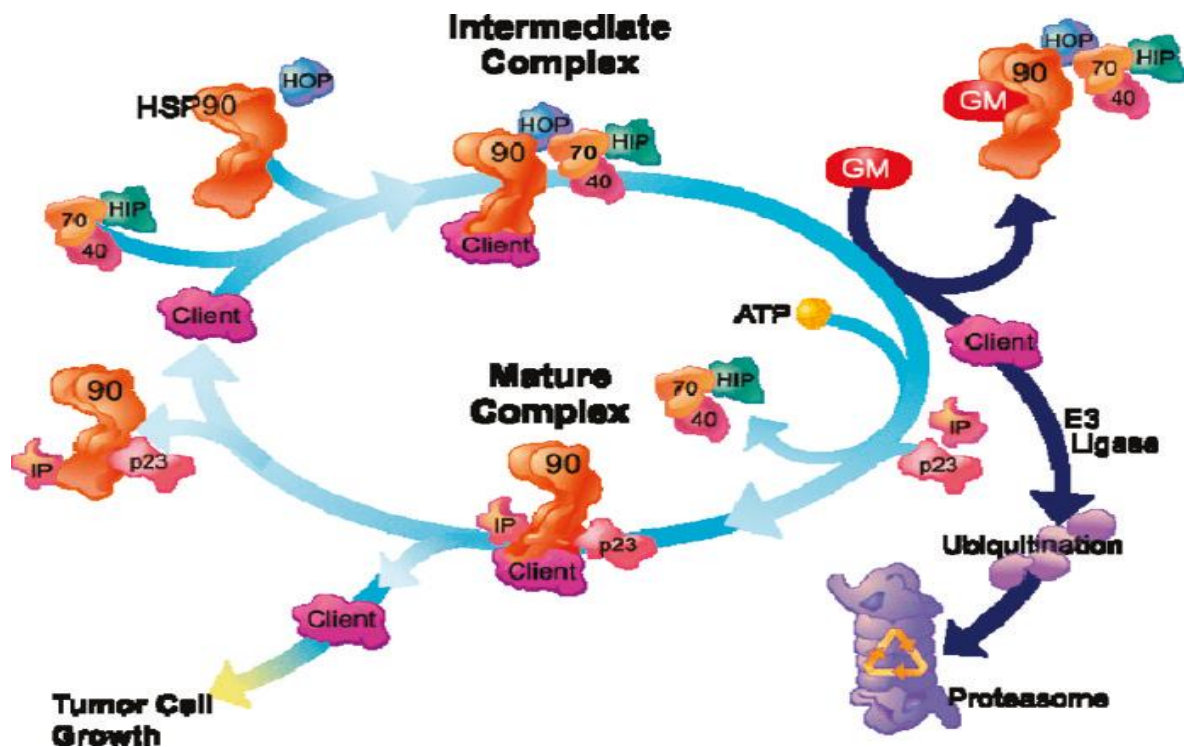


Figure 1.3 Hsp90 cycle: GM = geldanamycin analogue; 40 = HSP40; 70 = HSP70; IP = immunophilin; HIP = HSP70-interacting protein; HOP=HSP70/HSP90 organizing protein. Cdc37 and Aha1 are not shown.

1.5. Oncogenic Hsp90 client proteins and signaling pathways

By the early 1990s, several groups reported the observation that Hsps in general, and Hsp90 in particular, were over-expressed in a wide variety of cancer.⁴⁸ Cancer is a disease associated with genetic instability which allows cancer cells to acquire distinguishing characteristics, including self-sufficiency in growth signaling, resistance to apoptosis, insensitivity to growth inhibitory signaling, sustained angiogenesis, tissue invasion and metastasis, and limitless proliferative potential. Many signaling proteins

(more than 100 are known) related to these hall marks of cancer are client proteins of Hsp90. Most of these proteins play important roles in the control of cell cycle, growth and apoptosis and their dysregulated function might lead to transformation. Examples include such EGFR, HER-2, Akt, Raf-1, Cdk4, mutant p53, the estrogen and androgen receptor, mutant Raf, Bcr-Abl and Flt3 (Figure 1.4 and Table 1.3). The following section will focus on certain critical oncogenic proteins and pathways that are affected by Hsp90.

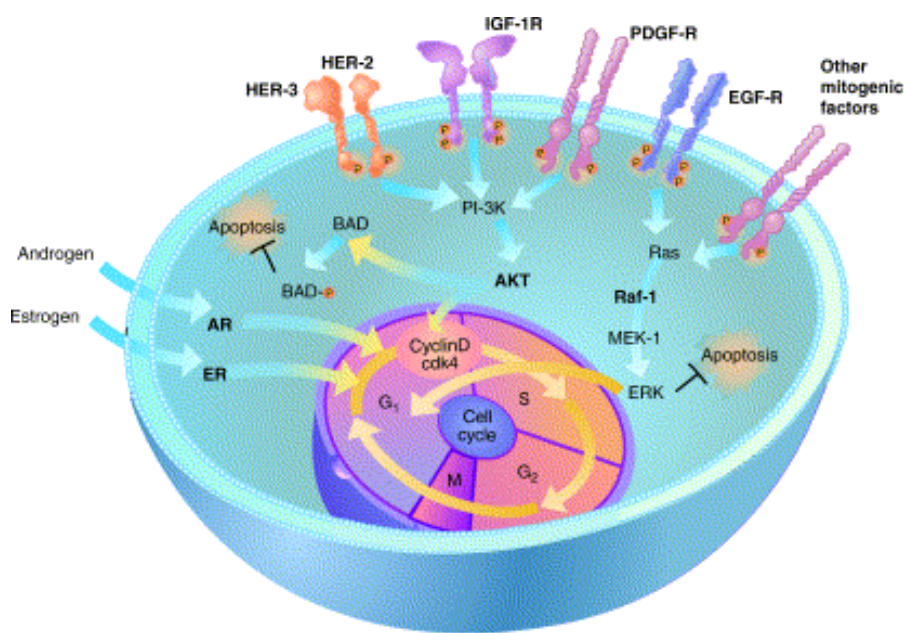


Figure 1.4 Hsp90 client proteins. Hsp90 client proteins regulate multiple signal transduction pathways that are deregulated in cancers. Hsp90 client proteins (shown in bold) include key components of the mitogenic signaling pathway that drives cell-cycle progression, as well as survival signal transduction pathways that inhibit apoptosis. Hsp90 client proteins include growth factor receptors (HER-2, IGF-1R, EGF-R and PDGF-R), signaling kinases (Akt and Raf-1), cell-cycle regulators (cdk4) and nuclear steroid receptors (AR and ER).

1.5.1. Growth Factor Receptors

EGFR and HER-2 are receptor tyrosine kinases of HER family that play critical roles in cell proliferation. Overexpression or mutation of either protein has been recorded in a variety of malignancies, including glioblastoma, breast and ovarian cancer. In the past, great efforts have been made in developing HER-2 and EGFR inhibitors (Herceptin, Tarceva, Iressa, Erbitux), but beneficial responses were limited. Studies in resistant cell lines revealed that major downstream signaling pathways, including Akt and Raf-1 pathways, were still active due to the expression of compensatory receptor tyrosine kinases or other mutation. These adaptations bypassed the suppression of the target and maintained

tumor growth, indicating that tumor cells can circumvent inhibition of one target and activate an alternative pathway to proliferate and survive. Hsp90 inhibitors inhibit tumor cell growth in HER-2 cell and may provide more robust and long-lasting antitumor effects by inhibiting multiple signaling pathways.⁴⁹

1.5.2. Steroid Receptors

Hsp90 inhibitors also inactivate steroid receptors, such as the androgen receptor and estrogen receptor, which, when bound to their cognate ligands, translocate to the nucleus and act as transcription factors.

1.5.3. Bcr-Abl

The fusion protein Bcr-Abl, known as Philadelphia Chromosome, is expressed in approximately 95% of cases of Chronic Myeloid Leukemia (CML) and is the target of the first small molecule tyrosine kinase inhibitor, Imatinib (Gleevec). Patients become resistant to the drug due to mutations in the kinase domain. Both wild type and mutant Bcr-Abl are Hsp90 clients and its inhibition causes degradation of Bcr-Abl and suppresses tumor growth in a variety of hematopoietic tumor lines.⁴⁹

1.5.4. Flt3

FMS-like tyrosine kinase 3 (Flt3) is a receptor tyrosine kinase which plays a crucial role in several hematopoietic malignancies as acute myeloid leukemia (AML), acute lymphoblastic leukemia (ALL) and myeloid lymphoblastic leukemia (MLL). It can mutate in two different points, both mutations cause constitutive Flt3 activation and are associated with poor prognosis. Even in this case both wild type and mutant proteins are sensitive to Hsp90 inhibitors which induce cell cycle arrest and apoptosis.⁴⁹

1.5.5. Protein Kinase

Hsp90 inhibitors inactivate multiple kinases, such as Raf-1, Akt and cdk4. Inactivation of the Ras-Raf-1-Mek-ERK and phosphatidyl inositol-3 kinase-Akt pathways by Hsp90 inhibitors causes the downregulation of cyclin D1 and the functional inactivation of Cdk4, both of which are important for the G1-S cell cycle transition (Figure 4).⁵⁰

- **PI3K/Akt Pathway**

PI3K/Akt pathway has a central role in cell proliferation and survival and it has attracted a lot of attention in drug development for anticancer therapy. Akt is abnormally activated in human tumors including breast, prostate, lung, pancreatic, ovarian and colorectal carcinomas. Several studies have shown that Akt relies on Hsp90 for its stability and activity: in animal models, Hsp90 inhibitors block the growth of tumors with active Akt when administered at doses capable of suppressing Akt phosphorylation.⁴⁹

- **Ras/Raf/MEK**

The Ras/Raf/MEK pathways occupies center stage in cell proliferation and survival; mutations of Ras and Raf are the most common in human tumors (35% in melanomas and 70% in papillary thyroid tumors). Raf isoforms and its downstream effector, MEK, are both HSP90 clients, and Hsp90 inhibitors deplete both proteins from tumor cells.⁴⁹

Table 1.3 Relationship between Hsp90 client proteins and hallmarks of cancer.

Hallmark of cancer	Hsp90 client protein
Evasion of apoptosis	Akt, Rip, p53, Survivin, Apaf-1, Bcl-2, IGF-IR
Sustained angiogenesis	VEGFR, HIF1, Akt, Fit-3,FAK, Src
Limitless replicative potential	n-TERT, telomerase
Tissue invasion and metastasis	c-MET, MMP2
Self-sufficiency in growth signals	EGFR/Her-2, Raf, Bcr-Abl, ErbB-2, Src, Akt, MEK
Insensitivity to anti-growth signals	Plk-1,Cdk4,Cdk6, Myt-1,cyclin D

Therefore, Hsp90 inhibitors simultaneously destabilize many oncoproteins in multiple signaling pathways, suggesting that the inhibition of Hsp90 could be particularly beneficial in attacking late-stage cancer cells, which can easily circumvent the blockade of a single target or pathway. Because of the wide array of Hsp90 client proteins, Hsp90 inhibitors can

be used to target diverse cancers in which an Hsp90 client protein is necessary for cancer proliferation, survival or progression.

1.6. A high-affinity conformation of tumor Hsp90 confers drug selectivity

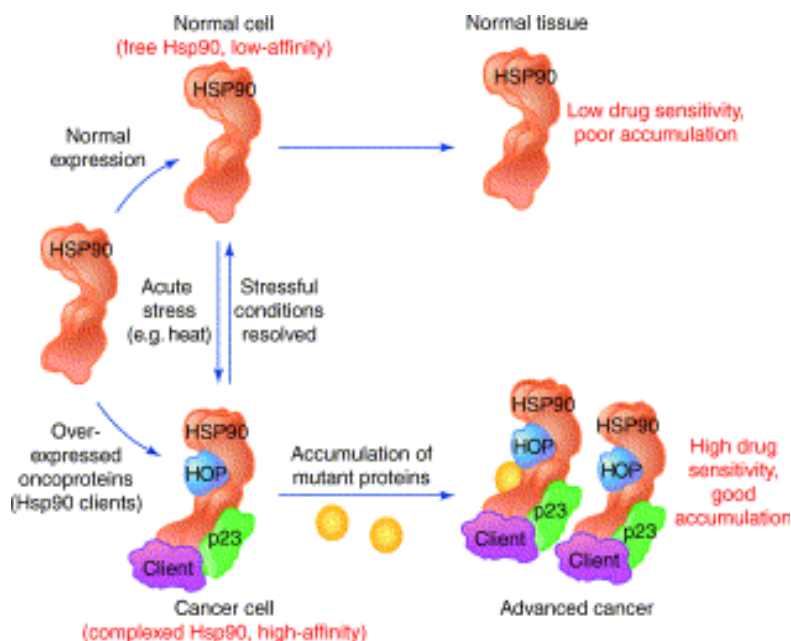


Figure 1.5 Model for tumor selectivity of Hsp90 inhibitors and Hsp90-dependent malignant progression.

Even though Hsp90 is an abundant protein in the cell, Hsp90 inhibitor drug selectively destroys tumor cells over normal cells. Hsp90 in normal cells exists in an uncomplexed form ('latent state') that has low affinity for Hsp90 inhibitor drugs, which accumulate poorly in normal tissues, and normal cells exhibit poor drug sensitivity. By contrast, the Hsp90 in cancer cells is involved in the active chaperoning of overexpressed oncoproteins and exists in a complexed form ('activated state') with co-chaperone proteins (include Hsp70, Hop, p23, cdc37, immunophilins and Aha1). Complexed Hsp90 in cancer cells exhibits high-affinity binding to Hsp90 inhibitor drugs, which accumulate in tumor tissues, and tumor cells exhibit good drug sensitivity. This model predicts that the accumulation of mutant proteins in advanced cancer would further increase Hsp90 usage and make tumor cells more Hsp90 dependent. Furthermore, this model suggests that the high-affinity change of Hsp90 can be driven by the overexpression of oncoproteins, as well as by stressful conditions in normal cells.^{4,51-54}

The *Figure 1.5* schematically depicts Hsp90 and its possible interaction partners and does not represent timely complexes.

Box 1: Potential mechanisms of selectivity of Hsp90 inhibitors for cancer versus normal cells:

- Hsp90 inhibitors cause simultaneous combinatorial depletion of oncogenic client proteins, including kinases, hormone receptors and transcription factors.
- Cancer cells might be especially dependent on Hsp90 to ensure the correct folding and function of the large quantities of mutated and overexpressed oncoproteins.
- Malignant cells are likely to acquire greater dependence on these cancer-causing client proteins compared with normal cells through the process of multistep oncogenesis, selection and 'oncogene addiction'.
- Cancer cells might also be especially dependent on Hsp90 and other molecular chaperones to survive the hostile tumor microenvironment owing to hypoxia, nutrient deprivation, acidosis, and so on.
- Effects of Hsp90 inhibitors on multiple oncogenic clients and pathways will cause antagonism of all six 'hallmark traits' of cancer. By analogy with its role in morphological evolution, Hsp90 might act as a buffer against mutations that accumulate in cancer cells, and its inhibition might uncover synthetic lethal effects.
- Some Hsp90 inhibitors, such as 17AAG, might accumulate to a great extent in cancer versus normal cells and tissues.
- New evidence shows that Hsp90 is present in cancer cells in heightened multichaperone complexes with increased ATPase activity and 100-fold greater binding affinity for 17AAG compared with the largely uncomplexed and less-active form of Hsp90 that is found in normal cells.²⁵

1.7 Inhibitors of Hsp90 C-terminal ATP-binding domain

1.7.1 Novobiocin and analogues

Novobiocin (**1**, NB) and coumermycin A1 (**2**) (Figure 1.6) are members of the coumermycin family of antibiotics isolated from *Streptomyces* strains and are well-established inhibitors of DNA gyrase and topoisomerase II.

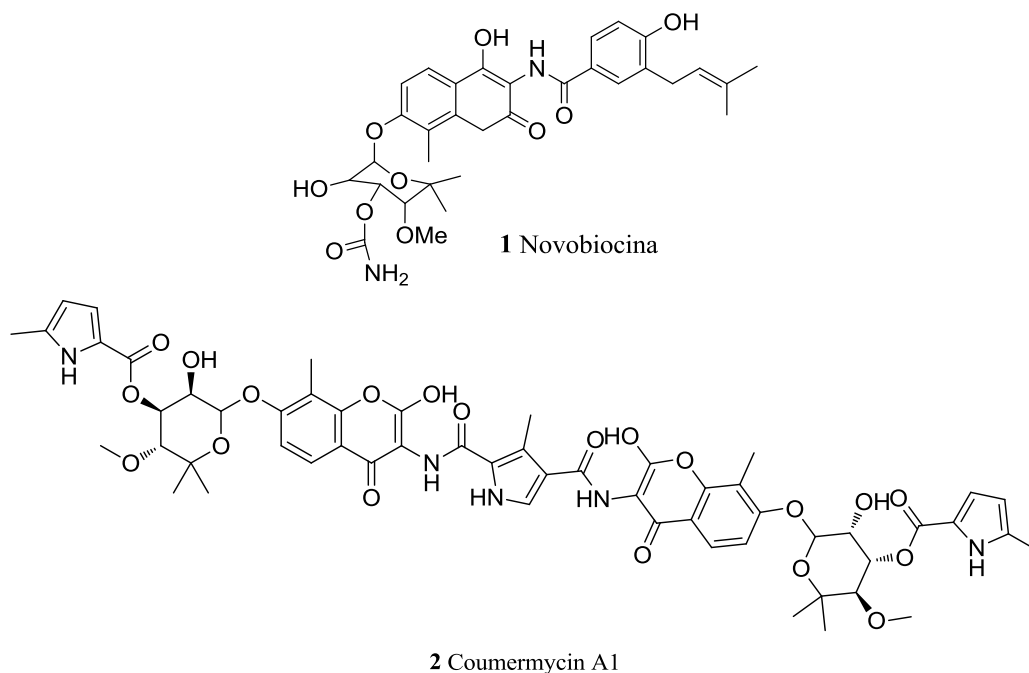


Figure 1.6 Chemical structure of novobiocin and coumermycin A1.

They also interact with Hsp90 causing *in vitro* and *in vivo* depletion of key regulatory Hsp90-dependent kinases including v-Src and Raf-1 at 700 μM and 70 μM , respectively. These compounds inhibit HSP90 by disrupting or preventing formation of dimer required for Hsp90 function.

In order to improve the affinity for HSP90 and the potency against cancer cells, two research groups synthesized more analogues based on the coumarin scaffold.

NB derivatives A4 (**3**) and DHN2 (**4**) (Figure 1.7), both lacking the 4-hydroxyl on the coumarin moiety, showed improved IC_{50} values of 10 μM and 0.5 μM against SKBr3 cells, while the coumermycin analogue **5** had an IC_{50} value of 1.9 μM .^{55,56}

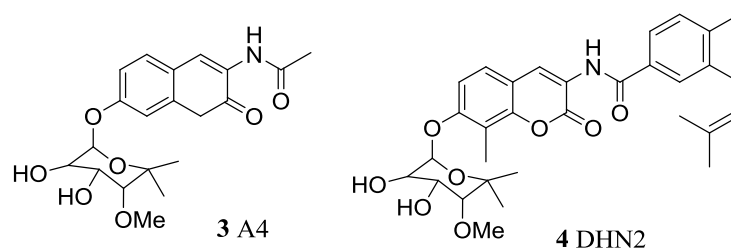


Figure 1.7 Chemical structure of A4 and DHN2.

1.7.2 Other C-terminal inhibitors

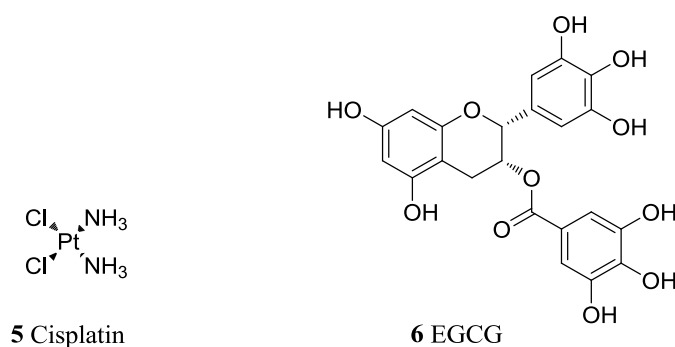


Figure 1.8 Chemical structure of cisplatin and EGCG.

Cisplatin (5), a platinum-based anticancer drug known to crosslink DNA, and epigallocatechin-3-gallate (EGCG, 6), the major component of green tea, are able to bind the C-terminal domain. Cisplatin interacts in a region proximal to the C-terminal nucleotide binding site; EGCG inhibits transcription mediated by aryl hydrocarbon receptor (AhR) through binding to Hsp90.

1.8 Inhibitors of Hsp90 N-terminal ATP binding domain

Two general classes of natural product inhibitors of Hsp90 have been discovered which bind to the N-terminal ATP pocket, and are based on geldanamycin (GM) and radicicol (RD). Interestingly, each was originally isolated as an antibiotic from fermentation broths. They affect Hsp90 chaperone function in a similar manner and possess comparable biological activity.

1.8.1 Geldanamycin and its derivatives

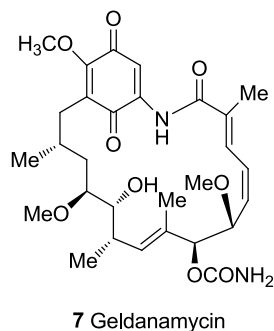


Figure 1.9 Chemical structure of geldanamycin.

Geldanamycin (GM, **7**) is a benzoquinone ansamycin that was first isolated as an antibiotic in 1970 by scientists at Upjohn by fermentation of *Streptomyces hygroscopicus*.⁵⁷

The crystal structure showed that GM binds tightly to the ATP pocket of the N-terminal domain and inhibits Hsp90-mediated protein conformation/refolding, resulting in a depletion of oncogenic kinases through the proteosomal degradation of immature protein. This process subsequently down-regulates expression of many oncogenes in cancer cells.^{58,59} Its structure includes a benzoquinone ring fused to a macrocyclic ansa ring. The benzoquinone ring is found near the entrance of the binding pocket and the ansa ring is directed towards the bottom of the pocket. When bound to Hsp90, GM adopts a C-shaped conformation similar to that of ADP. GM shows a potency in the micromolar concentration range *in vivo* ($K_d = 1.2 \mu\text{M}$) that increases 50 to 100-fold *in vitro*.^{60,61}

GM is a potent anticancer antibiotic but its potential clinical utility is hampered by its severe toxicity. First, it exhibits severe hepatotoxicity, which has been associated with the benzoquinone ring and imposes strict dosing limitations. Secondly, it is metabolically and chemically unstable. Also, it has very low solubility in aqueous media resulting in formulations requiring DMSO.

For this reason, a substantial effort has been made to modify its structure, generating a number of analogues in attempts to improve safety, stability, potency and water solubility.⁶²

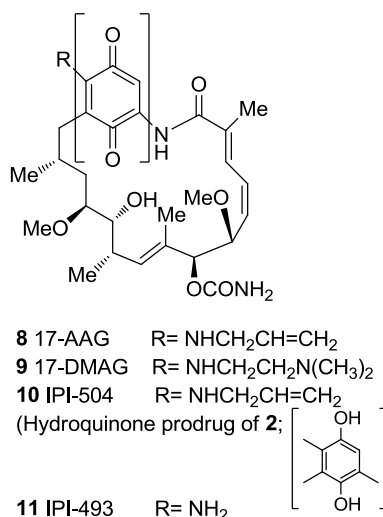
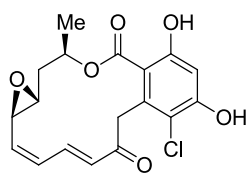


Figure 1.10 Chemical structure of geldanamycin derivatives.

The site of focus is the 17 position of the benzoquinone group to generate 17-allylamino-17-demethoxy geldanamycin (17-AAG, **8**). 17-AAG shows a better toxicity profile and was the first Hsp90 inhibitor to enter clinical trials and is now in phase II. This molecule has several limitations, such as poor solubility and limited bioavailability.⁵⁴ To overcome some of these issues two more water soluble GA derivatives, 17-DMAG (17-dimethylamino-ethyl-GA, **9**) and the hydroquinone of 17-AAG-prodrug (called IP-504, **10**) were synthesized, which are reported to be in phase-I/Ib and phase-I/II clinical trials, respectively. In fact, studies revealed that **10** can be isolated as the hydrochloride salt, an intravenously administered small molecule.⁶³ Protonation of the aniline nitrogen in 17-AAG hydroquinone decreases electron density in the aromatic ring, thus reducing the oxidative potential of the hydroquinone. Infinity is developing one drug candidates in its Hsp90 chaperone inhibitor program: IPI-493 (**11**), which is administered orally.⁶⁴

1.8.2 Radicicol and its derivatives

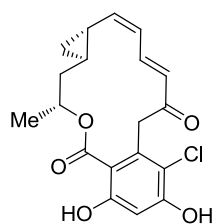


12 Radicicol

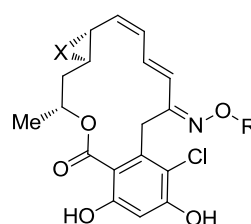
Figure 1.11 Chemical structure of radicicol.

Radicicol (**12**, in *Figure 1.11*) belongs to the macrocyclic lactone antibiotics originally extracted from the filtrate of fungus *Monosporium bonorden* and it binds human Hsp90 with nanomolar affinity *in vitro* ($K_d = 19$ nM).⁶⁵ Although radicicol is structurally dissimilar from benzoquinone ansamycins, it can also competitively bind to the N-terminal domain of Hsp90 to disrupt Hsp90 complex formation.⁶⁶ Radicicol showed more potent antitumor activity than geldenamycins *in vitro*, but weaker activity *in vivo*, which could be explained by the fact that the presence of epoxy and α , β , γ , δ -unsaturated carbonyl groups reduced the stability of radicicol. In the other side, structure–activity relationship analysis indicated that radicicol possesses phenolic ring structures that may be necessary for its function.⁶⁷

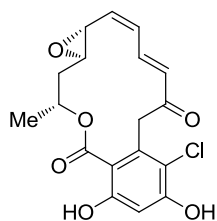
With the aim to improve the pharmacological properties of RD, several scaffold modifications have been analyzed.



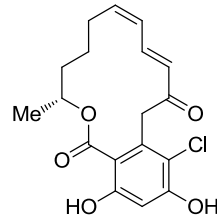
13 Cycloproparadicolo



14 Oxime-radicicol series



15 Pochonin A



16 Pochonin D

Figure 1.12 Chemical structure of radicicol derivatives.

Some analogues include cycloproparadicicol **13** and some radicicol oxime derivatives of general structure **14** (Figure 1.12) were designed to reduce the reactivity of the epoxide group. These results indicate that the oxime moiety plays a significant role in sustaining the stability and enhancing the biological activity of radicicoloxime analogue. All analogues show the propensity to adopt the bioactive conformation: among them Pochonin A (**15**) and D (**16**), two natural products, have an IC₅₀ value of 80 nM and 90 nM, respectively. In contrast to geldanamycin and its derivatives, radicicol has no hepatotoxicity, which implies that hepatotoxicity of benzoquinone ansamycins is not a common characteristic of all Hsp90inhibitors. Thus, radicicol and its analogues are promising drug candidates for further development as non-benzoquinone ansamycin Hsp90 inhibitors. Until now no compound of this class has yet entered clinical trials.^{68,69}

1.8.3 Purines-based derivatives

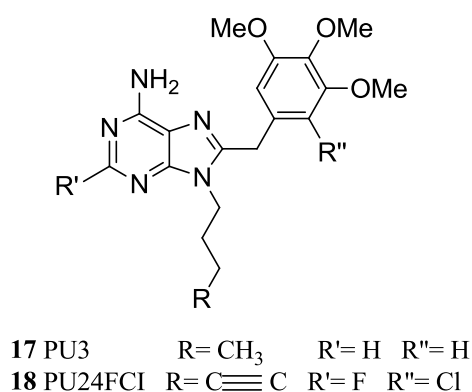


Figure 1.13 Chemical structure of PU3 and PU24FCI.

The purine scaffold is another important class of Hsp90 N-terminal domain inhibitors.⁷⁰ This class (PU-class) was empirically designed by Chiosis and coworkers following the idea to mimic the unique shape adopted by ATP when bound to the N-terminal nucleotide pocket of Hsp90: the adenine ring was envisioned to mimic the adenine ring of ATP, while the benzene moiety was decorated to capture the same network of hydrogen bonds in which the quinone ring of geldanamycin is involved.

The first synthesized derivative of this class was PU3 (**17**) with an affinity of 10-20 μM and antiproliferative activity against several cancer lines. The weakly active PU3 was an important starting point for the development of clinically useful Hsp90 inhibitors and the purine scaffold was adopted for further optimisation by several investigators. Further

efforts focused at improving the potency of this agent, have led to the synthesis of several compounds with improved activity in both biochemical and cellular assays.

Initial optimisation led to the identification of PU24FCl (**18**), a selective inhibitor of tumor Hsp90 that exhibits antitumor activities in both *in vitro* and *in vivo* models of cancer. The biological effects of PU24FCl are demonstrated in the 2-6 μM concentration range.⁷¹ The synthesis of subsequent structure-based optimization was resulted in the discovery of the potent, water-soluble inhibitor PU-H71 (**19** in *Figure 1.14*).

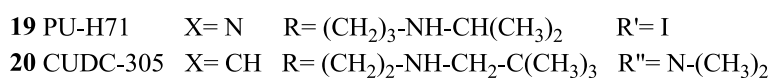
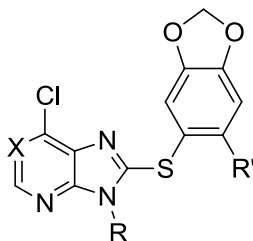


Figure 1.14 Chemical structure of PU-H71 and CUDC-305.

Until now PU-H71 remains the most active derivative in the PU series and it is scheduled to enter phase I clinical trial.

Recently Bao et al. described compound CUDC-305 (**20**) similar to arylsulfanyl adenine; this molecule has IC₅₀ of 100 nM and blocks proliferation of a panel of cancer cell lines; moreover, it has good pharmacological properties as oral bioavailability, blood-brain barrier penetration, and tumor retention.⁷²

A series of purine with improved physicochemical properties was discovered by Kasibhatla et al. by rearrangement of substituents around the purine ring. They shift the aryl binding moiety from the C-8 to the N-9 position and the NH₂ group from the 6 to the 2 position so as to re-establish the overall six-bond distance between the 6-NH₂ group and the aryl group.^{73,74}

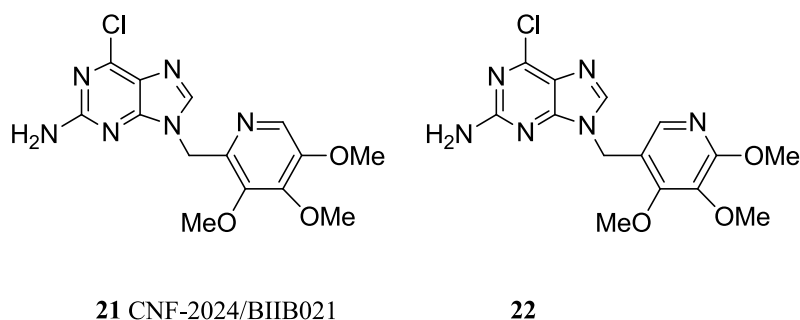
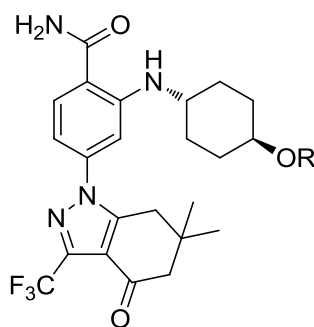


Figure 1.15 Chemical structure of CNF-2024/BIIB021 and derivatives.

Compounds of this structural series (in particular **21** and **22** in *Figure 1.15*) show significant binding selectivity, preferring interaction with the activated form of the Hsp90 complex, which is reflected in increased tumor cell retention and more effective tumor cell killing.^{75,76} CNF2024/BIIB021 (**21**) was advanced into phase I-II clinical trials.⁷⁷

1.8.4 *o*-Aminobenzoic acid derivatives and resorcinol derivatives



23 SNX-2112 R= H
24 SNX-5422 R= glycine ester mesylate

Figure 1.16 Chemical structure of SNX-2112 and SNX-5422.

New classes of Hsp90 inhibitors unrelated to any previously known scaffold were found through screening of focused compound libraries against sets of ATP-binding proteins. Huang and coworkers identified a novel class of indol-4-one and indazol-4-one derived 2-aminobenzamides that potently inhibit Hsp90. The crystal structure of the complexes between compound of this series and Hsp90 shows that these molecules mimic the carbamate/Asp93/water molecules interactions established by GA, as the benzamide group overlays the carbamate of GA and the rest of the molecule closely maps other parts of the ansamycin ring. The best compound of this series, SNX-2112 (**23**), show a high affinity ($K_d = 16$ nM) and its prodrug SNX-5422 (recently acquired by Pfizer PF-

04929113) (**24**) is orally bioavailable, efficacious in a broad range of cancer cell lines and entered phase I clinical trials.^{78,79}

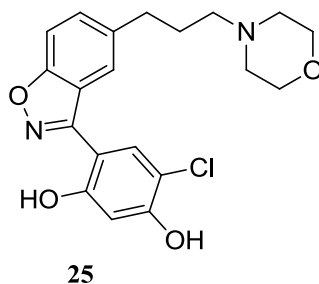


Figure 1.17 Chemical structure of benzisoxazole derivatives.

The benzisoxazole compound **25** identified (*Figure 1.17*), using high-throughput screening and optimisation, by Wyeth. It has high binding affinity ($IC_{50} = 0.03 \mu M$) and submicromolar IC_{50} values against a panel of cancer lines.

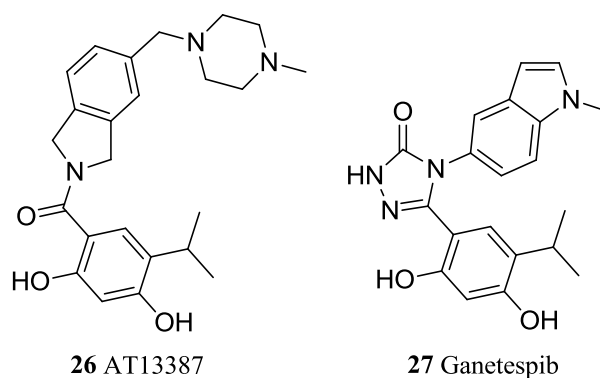


Figure 1.18 Chemical structure of resorcinols derivatives.

Other resorcinols, AT13387 (**26**) by Astex and ganetespiib (**27**) by Synta Pharmaceuticals Corp. (chemical structure not yet disclosed), entered recently into clinical trials.⁸¹

Other interesting molecules are AICAR (**28**), which destabilizes multiple client proteins in vivo and shows antiproliferative activity in multiple tumor cell lines, 2-naphthol compounds **29**, **30** and tetrahydrobenzopyrimidine molecule **31** with submicromolar inhibitory activity.⁷⁸

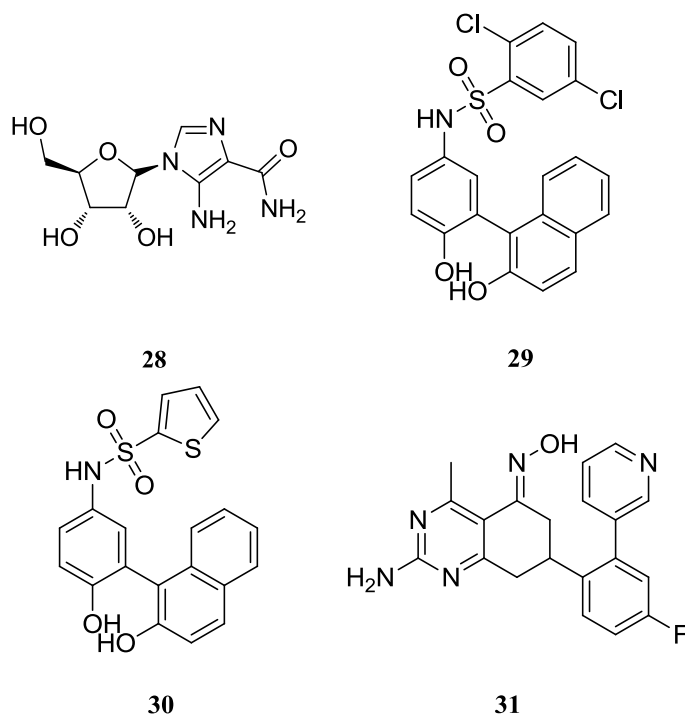
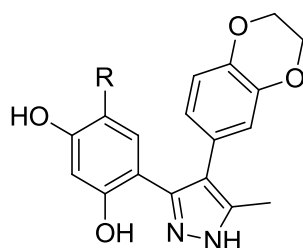


Figure 1.19 Chemical structure of other N-terminal domain inhibitors.

1.8.5 Pyrazoles and isoxazoles derivatives

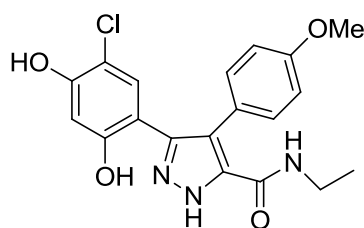


32 CCT018159 R=etile
33 CCT072440 R=cloro

Figure 1.20 Chemical structure of Pyrazole derivatives.

This class of synthetic Hsp90 inhibitors was identified by high-throughput screening of a library of 50,000 compounds.⁸¹ Wokman and co-workers identified CCT018159 (**32**) with an IC_{50} of 7.1 μ M in yeast ATPase assay and antiproliferative activity against HCT116 human colon cancer cells.⁸² The structure-based elaboration of this hit resulted in a series of active analogues. Further, replacement of the chlorine of the resorcinol ring in CCT018159 by an ethyl group in CCT072440 (**33**) results in an ATPase activity 2- to 3-fold more potent than **32** (Figure 1.20).⁸³

After extensive optimization, Vernalis found VER49009 (**34**) with in vitro potency comparable to 17-AAG (IC_{50} = 0.14 μ M).



34 VER49009

Figure 1.21 Chemical structure of VER49009.

Vernalis strategy to optimize the in vivo activity in diaripirazole series was focused on the structure-activity relationships (SAR) in three distinct areas of the molecule and was guided by structural information of ligands (such as VER-49009 in *Figure 1.21*) bound to the ATP binding site of Hsp90. Crystallographic data shows that this family of compounds binds to the ATP pocket in the N-terminal domain similar to RD.⁸⁴ The resorcinol groups are clearly central to the binding mode of the compound, particularly the 2'-hydroxyl, which makes a hydrogen bond to the residue Asp93, a residue, which has been previously identified to be critical for ATP binding. To evaluate the importance of the resorcinol OH moieties in the binding of this class of inhibitor, several O-methylated analogues of this class were synthesized. As demonstrated O-methylation caused a large drop in binding affinity compound, reduced potency and cellular activity and thus demonstrated no advantage over the free resorcinol.

Additional interactions between the adenine ring of ATP and protein residues of the binding pocket are bridged by several water molecules. Several of those water interacts with Asp93 and the pyrazole N2 of the inhibitor. This water is part of a network with Asp93 and two other waters that are seen in all reported crystal structures of Hsp90.⁸⁵ Beside the importance of the key interaction of the resorcinol with Asp93 no less important is the hydrogen bond from the 5-amide substituent to Gly97.⁸⁶ Crystallographic data shows that the amide group at C5 of the pyrazole ring forms a salt bridge to Lys58 as well as hydrogen bonds to two nearby water molecules (*Figure 1.22*).

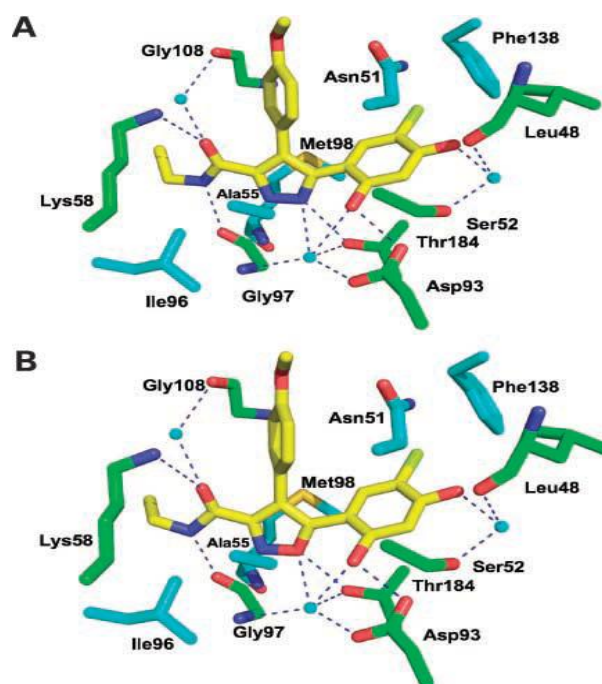


Figure 1.22 X-ray structure of VER-49009 (Figure A) and VER50589 (Figure B) bound to the ATP binding site of human Hsp90 α . H-bonds are shown as dotted blue line; green: protein residues involved in polar interactions; cyan: protein residues involved in non-polar interactions; blue ball: molecule of water.

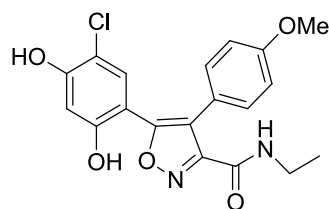
The high complementarities and tight packing between Hsp90 and the inhibitor in this area leave room only for small modifications of the inhibitor's core, but a wide range of substituents can be placed off of the pyrazole ring and the 5'-position of the resorcinol.⁸⁷ Vernalis focuses his work on three main areas:

- 1) modification of the central pyrazole heterocycle,
- 2) the optimization of the 5' substituent on the resorcinol ring,
- 3) incorporation of a solubilizing group on the 4-arylpyrazole substituents.

1) Modification of the central pyrazole heterocycle

As shown in Figure 22 A and B, examination of the binding for the pyrazole ring in ligands such as **34** demonstrated that the nitrogen adjacent to the resorcinol (N1) is involved in hydrogen bonding with the key Asp93/water network at the base of the pocket as an H-bond acceptor, but pyrazoles can exist in tautomeric forms, and when N1 is protonated, this represents a form which is unlikely to bind well to Hsp90. Further, the interaction between N2 and the amide backbone carbonyl of Gly97 is not in the ideal geometry. For this reason optimisations led to a series of isoxazole-resorcinol analogues **35** (Figure 1.23) eliminating the possibility of different tautomeric forms of the pyrazole ring

and pyrazole was substituted with an alternative hydrogen-bond acceptor such as oxygen of an isoxazole. Isoxazoles and pyrazoles differ in that the former does not bear hydrogen on a hetero atom and can therefore not be substituted. As a consequence, the isoxazole is also smaller in size and should still be accommodated in the binding site. In addition, there is no possibility of the existence of isomeric forms that can exist with the pyrazole.



35 VER50589

Figure 1.23 Chemical structure of VER50589.

The cytotoxic activity of VER-50589 was higher than VER-49009 on all cell lines tested, in *Table 1.4* we can observe the values of IG_{50} :

Tabella 1.4 Values of IG_{50} of VER-49009 and VER-50589 in different cells line.

Cell type	Cell line	IG_{50} (nmol/L)	
		VER-49009	VER-50589
Melanoma	SKMEL. 2	1.093± 111.2	62.0 ± 4.3
	SKMEL.5	163.3 ± 14.5	125 ± 22.6
Colon cancer	HCT116	357.0± 0.003	115± 0.005
	BEneg	372.5 ± 29.5	36.7 ± 2.7
	BE2	422.5 ± 46.2	35.0± 3.5
	HT29	4.600.0±611.0	32.7±0.3
Ovaric cancer	CH1	376.7±26.0	32.7±0.3
Brain cancer	MB-231	570.0±0.04	58.8±6.4
	BT20	550 ±0.09	59.0 ±12.7
Endothelial cell	HUVEC	444.0±91.9	19.0±2.4

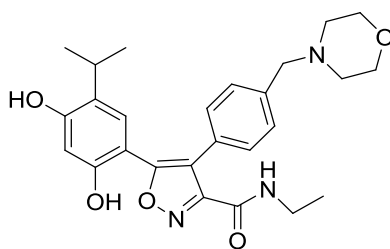
Unlike 17-AAG, but as with CCT018159, cellular potency of these analogues was independent of P-glycoprotein expression.⁸⁸ P-glycoprotein (P-gp) is a plasma membrane protein which acts as a localized drug transport mechanism, actively exporting drugs out of the cell. The effects of P-gp on the distribution, metabolism and excretion of drugs in the body is great. P-gp activity, for example, decreases the intracellular concentration of cancer drugs, enabling resistance to develop to them.

2) The optimization of the 5'substituent on the resorcinol ring

The substituents in this area have the potential to induce a conformational change in the protein by forming a helix between residues Ile104 and Ala111. In fact, there is considerable plasticity in this region of the structure, which is at the entrance to the ATP binding site. Some of the residues seen as important for binding to ligands are in this loop.⁸⁹ This structural change creates a lipophilic pocket in the ATP binding site of the Hsp90 protein. As previously demonstrated the removal of ethyl or chloro from this position resulted in a 20-fold decrease in binding affinity for ligands closely related to **34**. This loss in potency is rationalized by structural information showing that the ethyl and chloro protrudes into a hydrophobic pocket created by residues Phe138, Leu107, Val150, Met98, Val186, and Leu103. The size of the hydrophobic pocket is large enough to accommodate a bulkier substitution at the C5 position of the dihydroxyphenyl ring.⁹⁰ Replacement of the chlorine of the resorcinol ring in **34** or **35** by an isopropyl group results in an additional hydrophobic interaction with Leu107 in the flexible lipophilic pocket. Analogues with an 5' isopropyl group demonstrated excellent potency in cell growth inhibition assays.⁸⁷

3) Incorporation of a solubilizing group on the 4-arylpyrazole substituents.

Subsequently introduction of a solubilizing group led to a series of potent Hsp90 inhibitors with good pharmacokinetic properties. Further hydrophobic interactions are also seen with Thr109 and Gly135 when the methoxy group of VER-49009 or VER-50589 is replaced with the morpholino moiety of VER-52296, now acquired by Novartis NVP-AUY922 (*Figure 1.24*), which showed $GI_{50} = 9$ nM in antiproliferation assays against a panel of human cancer cell lines and has now entered phase II clinical trials.⁹¹



36 VER-52296\NVP-AUY922

Figure 1.24 Chemical structure of NVP-AUY922.

Table 1.5 shown a short summary of the characteristics of Hsp90 inhibitors described above.

Table 1.5 Hsp90-binding drugs: many classes of natural, semisynthetic and synthetic inhibitors of Hsp 90 have been discovered and some of them have been exploited in clinical trials for different types of tumours.

Binding site	Chemical class	Inhibitors	Properties
N-terminal ATP-binding pocket	Benzoquinone ansamycin	GA	Natural
		17AAG	Semisynthetic
		17DMGA	Semisynthetic
		IPI-504	Semisynthetic
N-terminal ATP-binding pocket	Macrolide	IPI-493	Semisynthetic
		Radicicol	Natural
		Cycloproparadicol	Semisynthetic
		Pochonin A	Semisynthetic
N-terminal ATP-binding pocket	Purine Scaffold	Pochonin D	Semisynthetic
		PU3	Synthetic
		PU24FC1	Synthetic
		PU-H71	Synthetic
		CUDC-305	Synthetic
N-terminal ATP-binding pocket	Pyrazole Isoxazole	CNF-2024/BIIB021	Synthetic
		CCT018159	Synthetic
		CCT072440	Synthetic
		VER49009	Synthetic
		VER50589	Synthetic
C-terminal	Coumarin	NVP-AUY922	Synthetic
		Novobiocin	Natural
		Coumermycin A1	Natural
		A4	Synthetic
		DHN2	Synthetic

Chapter 2

Aim of the thesis

As previously described, the 4,5-diaryl-isoxazole class represents the most investigated class of Hsp90 inhibitors. Compounds belonging to this class show biological activity in the micromolar range and high selectivity for tumor cells versus normal cells. However, to date, no Hsp90 inhibitors in clinical trials meet all of the requirements of safety and stability. Some of the drugs under clinical investigation have showed toxicity toward liver, eyes, stomach-intestine, and heart.^{92,93}

In this work, we identify NVP-AUY922, belonging to the class of 4,5-diaryl-isoxazoles and currently in Phase II clinical trials (*Figure 1.25*), as *lead compound*. When a molecule is identified as a "lead", the aim of the medicinal chemist is the optimization of the compound by modifying the structure to:

1. improve pharmacological properties (such as affinity and efficacy);
2. modify the physicochemical properties (such as solubility, permeability and chemical stability);
3. reduce, if necessary, any toxicity or side effects;
4. optimize pharmacokinetic characteristics (such as bioavailability, metabolic stability and duration of action).

Therefore, the aim of this work is the design and synthesis of more potent and selective Hsp90 inhibitors. It is important to remember that the project research has been developed in collaboration with pharmaceutical industry, Sigma Tau. Therefore the importance to make patentable the products synthesized.

Our attention was focused mainly on the C-4 position of the isoxazole scaffold, where we found, contrary to the literature, that a phenyl moiety at C-4 position is not a prerequisite for the activity on Hsp90.⁹⁴

In fact, during our preliminary studies we found that the derivative with a bromine in C-4 of the isoxazole maintain the binding activity (ability to bind Hsp90 (FP): $IC_{50} = 0,15 \mu M$ and inhibition of cell growth proliferation on NCI-H460: $IC_{50} = 460 \text{ } 3,8 \mu M$). Furthermore

we focused our work in a detailed structural investigation on a new class of 3,4-isoxazolidiamides (*Figure 2.1*) where we found that compounds with a nitrogen atom directly attached to the heterocycle ring possess *in vitro* Hsp90 inhibitory properties comparable to the 4,5-diaryl-isoxazole derivatives.

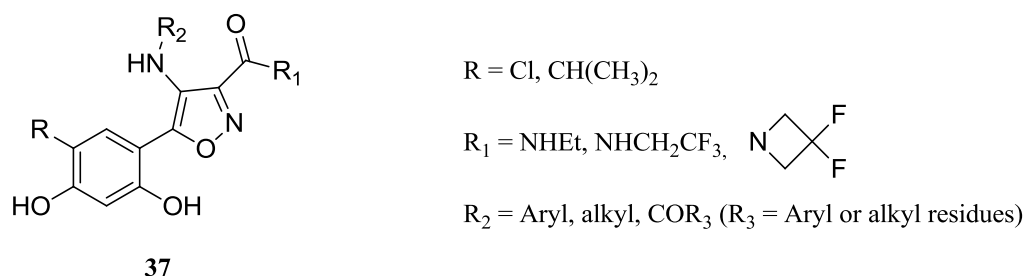


Figure 2.1 General structure of new Hsp90 inhibitors used in these study.

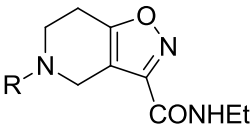
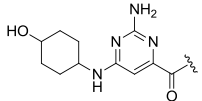
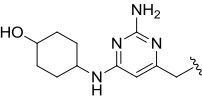
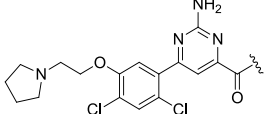
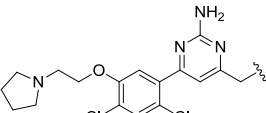
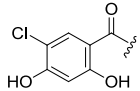
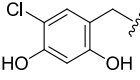
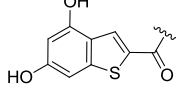
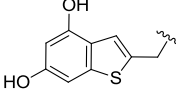
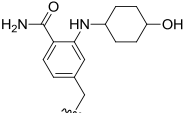
In particular:

- the feasibility of the project was initially investigated by preparing a small explorative series of C-4 amides bearing a chloro-resorcinol residue at the C-5 position. Meanwhile the amides at C-3 and C-4 of the isoxazole ring were varied as shown in *Figure 2.1*. The 5-chloro substitution was chosen at the beginning for its ease of synthesis. The synthetic route for these compounds allowed to obtain the final products faster and in a greater amount; moreover, 5-unsubstituted resorcinols are known to be less active with respect to the substituted ones;⁹⁵
- then, we moved to explore the potential of the new scaffold investigating a lot of additional substitution at the C-4 amide portion. Given that substitution of the chlorine atom at the resorcinol moiety with an isopropyl group was previously documented to improve cytotoxic activity of the 4,5-diaryl-isoxazole, such a type of substitution has been also utilized by us for the new compounds;
- furthermore, a C-4 amino series was synthesized to better substantiate our structure activity investigation. In fact, amide derivatives are more potent than the corresponding amine derivatives.

In continuation of our efforts in search of potential antitumor agents,⁹⁴ in order to obtain new Hsp90 inhibitors, different molecules have been specifically designed to interact with the whole binding pocket of Hsp90 (general scaffolds are shown in *Table 1.7*). In particular, docking experiments in collaboration with the pharmaceutical industry Sigma Tau, were used to “score” their potential complementarity to the binding site. The

results of these experiments are expressed in "**G-Score**", which is a measure of the free energy of the binding site-ligand complex. From the analysis of these sets of molecules compound **127** reported the highest value of G-score (*Table 2.1*).

Table 2.1 Data of G-score of structures proposed.

Compounds	R	GScore
		
123		-9.31
124		-8.4
125		-11.2
126		-10.74
127		-12.26
128		-11.2
129		-10.91
130		-10.41
131		-11.36

Based on the predicted activity, we planned to synthesize a series of derivatives of compound **127** as novel Hsp90 inhibitors.

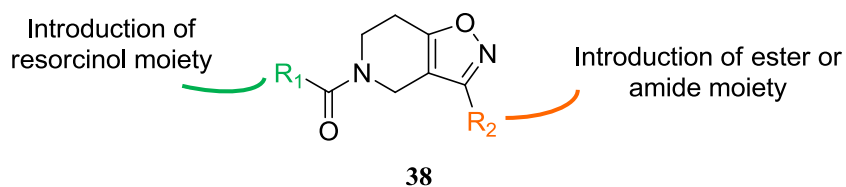


Figure 2.2 New 4,5,6,7-tetrahydro-isoxazolo-[4,5-c]pyridine scaffold.

As described in this chapter, compounds that contain an isoxazole nucleus (*Figure 1.18, 1.24 and 1.25*), have shown potent and selective inhibition of Hsp90.^{87,94,96,97} The presence of this heterocyclic moiety seem to play an important role in the interaction of this class of compounds with the ATP-binding site of Hsp90.⁹⁸ So we became interested in the synthesis of new hits containing the 4,5,6,7-tetrahydro-isoxazolo-[4,5-c]pyridine scaffold. In particular we focused on the synthesis of compounds bearing in N-5 resorcinol moiety and different ester/amide groups in C-3 due to their potential role in the interaction with the Hsp90 protein (*Figure 2.2*).

Chapter 3

Chemistry

Contents

3.1 Synthesis of 3,4-isoxazolidiamides scaffold

- 3.1.1 Synthesis of chloro-resorcinol derivatives
- 3.1.2 Modification at C-3
- 3.1.3 Synthesis of isopropyl-resorcinol derivatives
- 3.1.4 Modification at C-4
- 3.1.5 Synthesis of 4-aminoisoxazole

3.2 Attempts to synthesise 4,5,6,7-tetrahydro-isoxazole-[4,5-c]pyridine scaffold

3.3 Synthesis 4,5,6,7-tetrahydro-isoxazolo-[4,5-c]pyridine scaffold

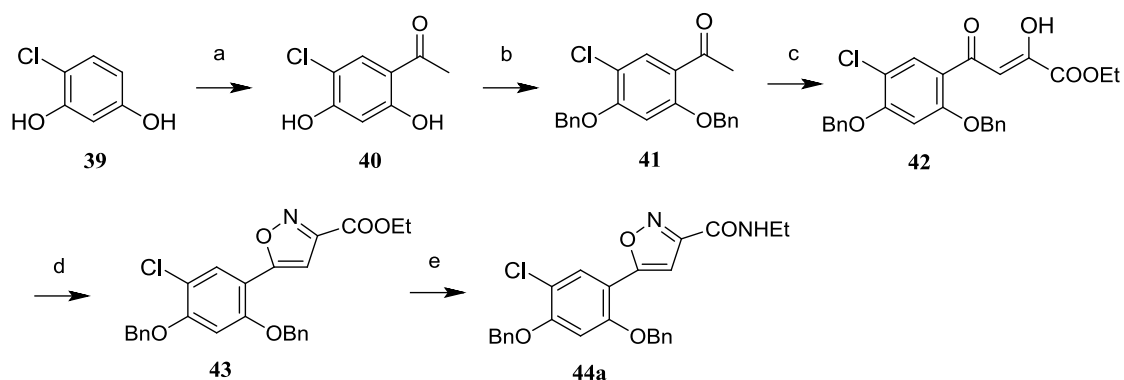
- 3.3.1 Synthesis of resorcinol acid
-

3.1 Synthesis of 3,4-isoxazolediamides scaffold

3.1.1 Synthesis of chloro-resorcinol derivatives

The route used for the synthesis of **44a** is shown in *Scheme 3.1*. Acetophenone **40** was obtained by regioselective Friedel-Crafts acylation of the commercially available 4-chlororesorcinol **39**. Both phenolic functions were protected with benzyl groups, generating **41** that was reacted with diethyl oxalate to afford keto-enol ester **42**. The isoxazole heterocycle **43** was obtained by reaction of **42** with hydroxylamina hydrochloride in ethanol. Finally, reaction of the ethyl ester moiety of **43** with ethylamine provided the desired ethylamide **44a**.

Scheme 3.1 Synthesis of chloro-resorcinol intermediate **44a**^a

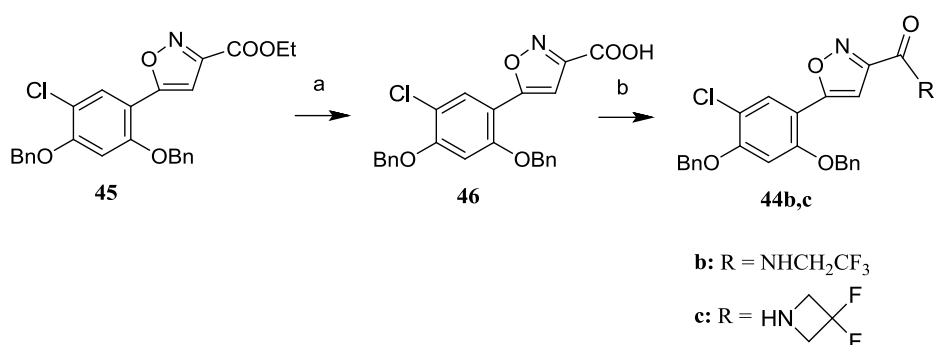


^aReagents and conditions: (a) AcOH , $\text{BF}_3 \cdot \text{xOEt}_2$; (b) BnBr , K_2CO_3 , MeCN; (c) $(\text{CO}_2\text{Et})_2$, EtO^-Na^+ , EtOH; (d) $\text{NH}_2\text{OH} \cdot \text{HCl}$, EtOH; (e) $\text{EtNH}_2/\text{MEOH}$, EtOH.

3.1.2 Modification at C-3

Compounds **44b,c** were prepared starting from the appropriate ester derivative with the following sequence of reactions (a) hydrolysis of ester moiety, (b) activation of resulting carboxylic acid, and (c) reaction with the proper commercially amines (*Scheme 3.2*).

Scheme 3.2 Synthesis of chloro-resorcinol intermediate **44b,c**^a



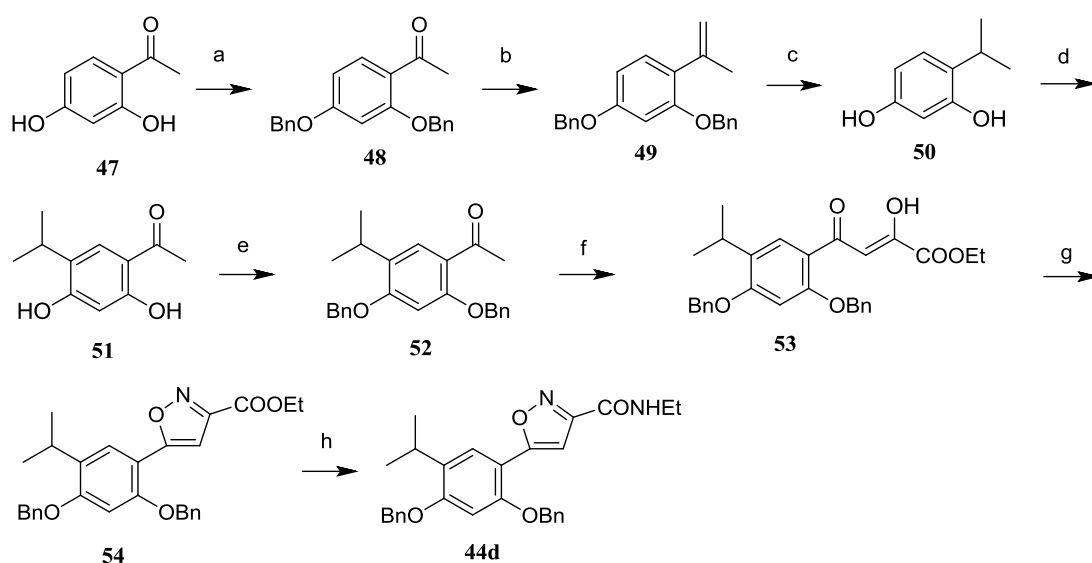
^a*Reagents and conditions:* (a) LiOH, H₂O, MeOH, 50-60°C; AcOH, BF₃·xOEt₂; (b) *i:* SOCl₂, 80°C; *ii:* NHR, TEA, 0°C.

3.1.3 Synthesis of isopropyl-resorcinol derivatives

For the synthesis of the isopropyl-substituted intermediate **44d** was used the same route outlined in *Scheme 3.3*

Starting from the commercially available 2,4-dihydroxyacetophenone, this was protected with benzyl groups to give compound **48**. A Wittig reaction, followed by hydrogenation generate compound **50**. The reduction of the styrene functionality in **50** caused concomitant debenzylation. So **51** was obtained by Friedel-Crafts acylation of the isopropyl derivatives **50**. The reaction occurs in a regioselective way only in presence of the free phenolic function. Then, the resorcinolic derivative was protected by the same route as that used for the intermediate **48**. The intermediate **53** was obtained by reaction **52** with diethyl oxalate that was reacted with hydroxylamina hydrochloride in ethanol to give **54**. Finally, reaction of the ethyl ester moiety of **54** with ethylamine provided the desired ethylamide **44d**.

Scheme 3.3 Synthesis of isopropyl-resorcinol intermediate **44d**^a

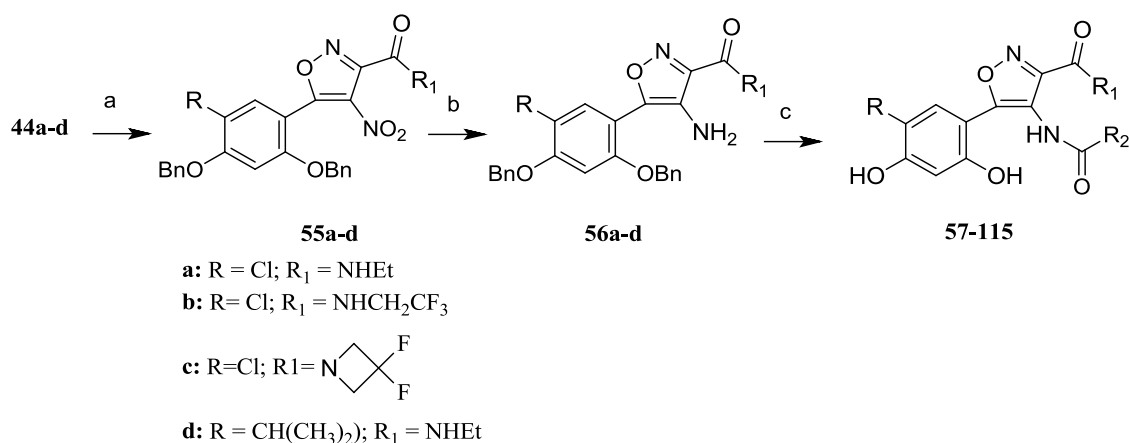


^aReagents and conditions: (a) BnBr, K₂CO₃, MeCN; (b) CH₃P⁺(Ph)₃Br⁻, NaH, toluene; (c) Pd/C, H₂; (d) AcOH, BF₃·OEt₂; (e) BnBr, K₂CO₃, MeCN; (f) (CO₂Et)₂, EtO⁻Na⁺, EtOH; (g) NH₂OH·HCl, EtOH; (h) EtNH₂/MeOH, EtOH.

3.1.4 Modification at C-4

The intermediates **44a-d** were used for the preparation of amides **57-116** (see *Tables 4.1, 4.2, 4.3*) as shown in *Scheme 3.4*. The 4-nitroisoxazoles **55a-d** were synthesized by chemoselective nitration of the isoxazoles **44a-d** using concentrated nitric acid and acetic anhydride. Reduction of the nitro compounds **55a-d** to give **56a-d** was done using zinc powder and ammonium chloride in a mixture of water and tetrahydrofuran as solvents. Reaction of the amines **56a-d** with the proper commercially available acyl chloride gave the corresponding dibenzylated amides that, after deprotection of phenolic groups with boron trichloride, furnished the desired amides **57-116**.

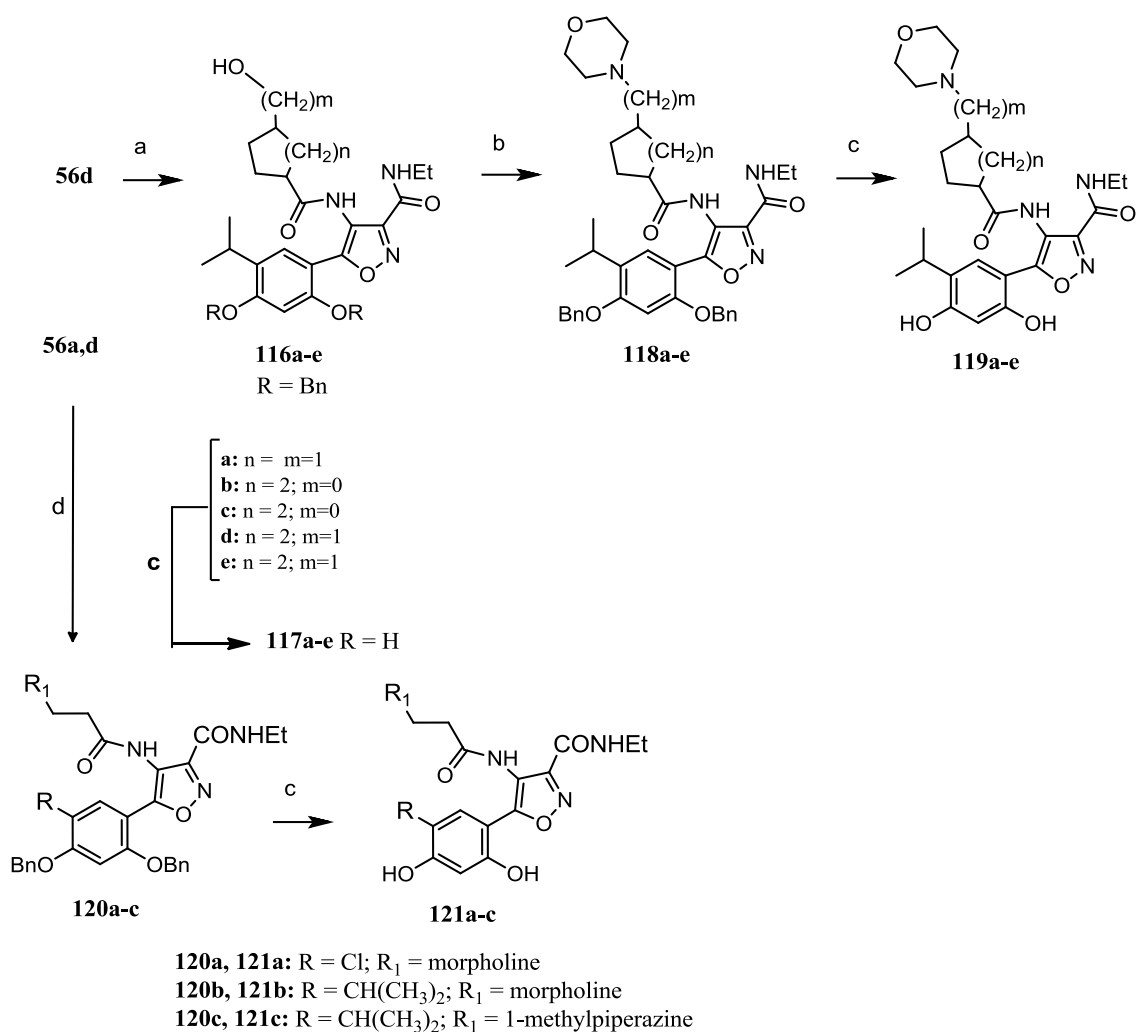
Scheme 3.4 Synthesis of 3,4-isoxazolidiamides inhibitors^a



^aReagents and conditions: (a) conc. HNO₃/Ac₂O; (b) Zn, H₂O/THF, NH₄Cl; (c) *i*: RCOCl, TEA, DCM; *ii*: BCl₃, DCM.

The morpholine derivatives **119a-e** and **121a,b** and the piperazine derivative **121c** were synthesized as reported in *Scheme 3.5*. The alcohols **116a-e** were simply prepared starting from the amine **56d** by reaction with the appropriate acyl chloride. The alcohols **116a-e** were then activated as mesylate derivatives by reaction with mesyl chloride in methylene chloride and then reacted with morpholine to give **118a-e**. Removal of benzylic protecting groups using boron trichloride furnished the final **119a-e** in good yields. Similarly, removal of benzylic groups from **116a-e** gave the deprotected derivatives **117a-e**. The derivatives **120a-c** were obtained by reaction of **56a,d** with acryloyl chloride, and the resulting acryloyl amides were then reacted through a Michael addition reaction with morpholine or 1-methylpiperazine. Removal of the benzylic protecting groups by means of boron trichloride yielded the desired compounds **121a-c**.

Scheme 3.5 Synthesis of morpholine and piperazine derivatives^a



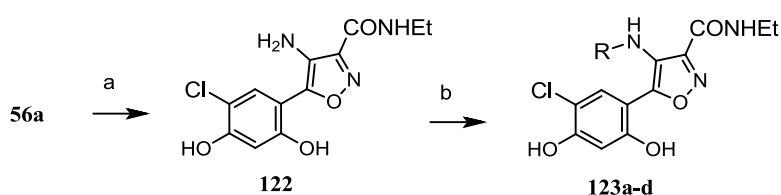
^aReagents and conditions: (a) *i*: acyl chloride, TEA, DCM; *ii*: BF₃·xEt₂O, DCM; (b) *i*: mesyl chloride, DIPEA, DCM; *ii*: morpholine, 70°C; (c) BCl₃, DCM, 0°C; (d) *i*: acryloyl chloride, TEA, DCM; *ii*: morpholine or 1-methylpiperazine, reflux

3.1.5 Generale procedure for preparation of 4-aminoisoxazole

The synthesis of amines **123a-d** is described in *Scheme 3.6*. In this case, the amine **56a** was first debenzylated using boron trichloride.

The reductive amination reaction of the resulting resorcinol derivative **122** by means of sodium cyanoborohydride and a proper aldehyde or ketone furnished the desired amines **123a-d** in moderate to good yields.

Scheme 3.6 Synthesis of amines-isoxazole derivatives **123a-d**^a



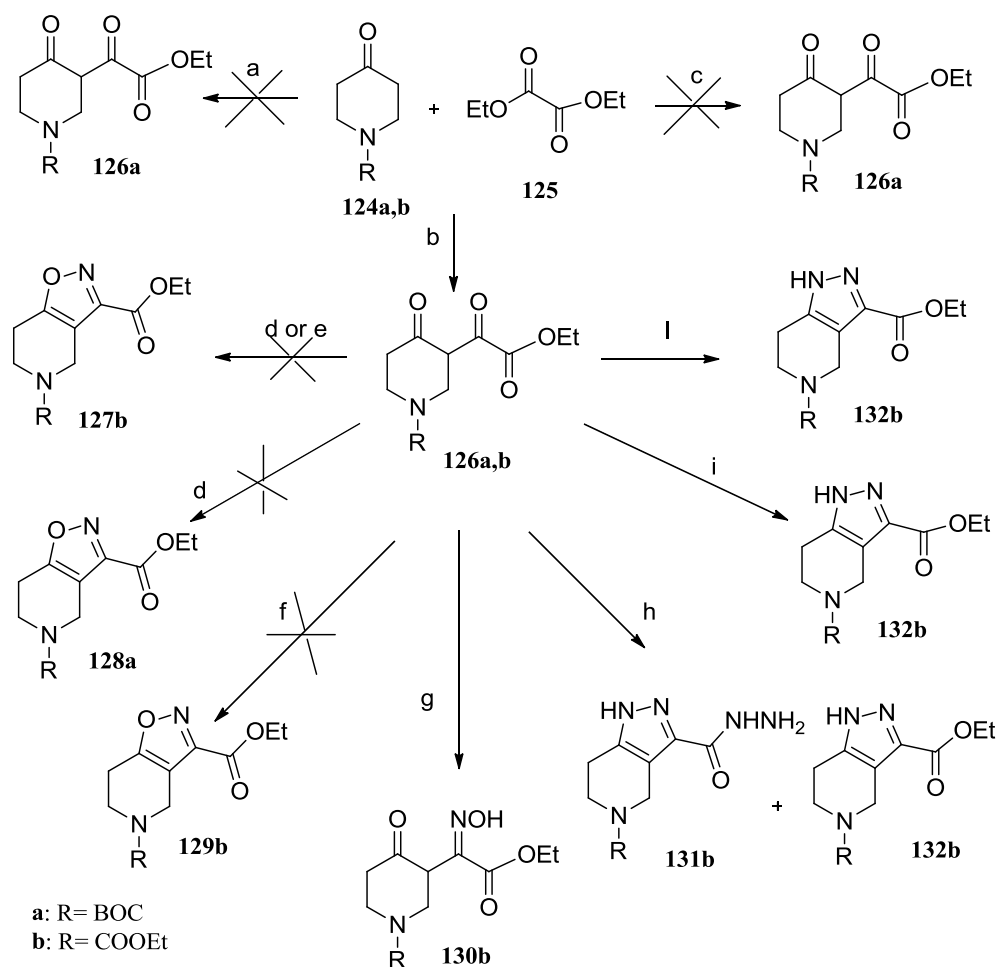
^a*Reagents and conditions:* (a) BCl₃, DCM, 0°C; (b) *i:* appropriate aldehyde or ketone, MeOH, AcOH 0.1%; *ii:* NaCNBH₃.

The reaction has been well described in literature until the formation of intermediates **44a** and **44d**. The chemoselective nitration in position 4 of the isoxazole, **55a-d**, was developed in my team's research, in addition to the synthesis of amide in position 3 of the isoxazole.

3.2 Attempts to synthesise 4,5,6,7-tetrahydro-isoxazole-[4,5-c]pyridine scaffold

Several efforts aimed at the synthesis of molecules with an 4,5,6,7-tetrahydro-isoxazolo-[4,5-c]pyridine scaffolds were reported in *Scheme 3.7*

Scheme 3.7 Attempts to synthesise 4,5,6,7-tetrahydro-isoxazole-[4,5-c]pyridine scaffold^a



^aReagents and conditions: (a) $Mg^{2+}EtO^-/THF$ dry; (b) $Na^+EtO^-/EtOH$ ass.; (c) $Li^+OEt^-/EtOH$ ass; (d) $NH_2OH \cdot HCl/EtOH$; (e) $NH_2OH \cdot HCl/H_2O/EtOH$; (f) $NH_2OH \cdot HCl/H_2O/EtOH/M.W.$; (g) $NH_2OH \cdot HCl/EtOH^+NaHCO_3/EtOH$; (h) $NH_2NH_2 \cdot H_2O/EtOH/R.T.$; (i) $NH_2NH_2 \cdot H_2O/CH_3COOH$; (l) $NH_2NH_2 \cdot HCl/EtOH/Rfx$.

The initial reaction between piperidone, protected with Boc or COOEt **124** and diethyl oxalate **125** to produce oxalil derivatives was performed using several conditions. At first, it was conducted with both magnesium and lithium ethoxide generated *in situ* but they did not work well. Therefore these conditions were optimized with sodium ethoxide to give **126a-b** in low yield (20%).

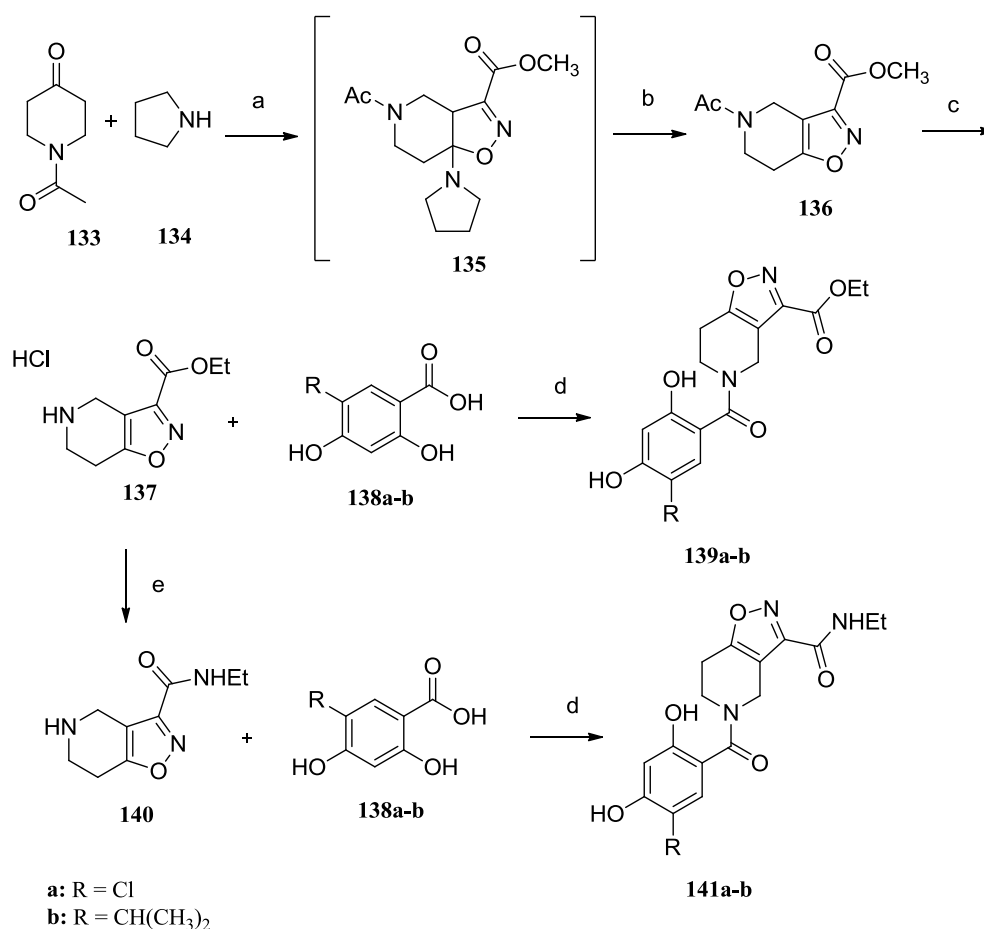
The attempts to build up the heterocycle condensed to the tetrahydropyridine were achieved by reaction of **126** with hydroxylamine hydrochloride in different condition of reaction, but unfortunately, all the attempts to the ring closure did not work at all.

Therefore, due to the difficulties encountered in obtaining isoxazoles derivatives, as shown in *Scheme 3.7*, we decided to built an heterocycle pyrazole by treatment of **126b** with hydrazina at room temperature in acid acetic or heating in EtOH to produce the derivative **132b** in a low yield in both conditions of reaction.

Hence, the low overall yield of the synthetic process to prepare **132b** prompted us to explore a new synthesis route of the pyrido-fused compound to obtained preferably an isoxazole ring because, as described before, an isoxazole instead of a pyrazole results more able to form hydrogen bond with the ribose binding pocket.

3.3 Synthesis 4,5,6,7-tetrahydro-isoxazlo-[4,5-c]pyridine scaffold

Scheme 3.8 Synthesis of 4,5,6,7-tetrahydro-isoxazole-[4,5-c]pyridine^a



^aReagents and conditions: (a) *i*: *p*-TSA, Toluene, Rfx.; *ii*: chlorohydroxyiminoacetic acid methyl ester, Et₃N, CH₂Cl₂; (b) TFA, CH₂Cl₂, Rfx; (c) HCl 32%, EtOH, Rfx; (d) TEA, EDCxCl, HOBT, DMF; (e) EtNH₂ in MeOH 2M, EtOH.

The new synthetic route (*Scheme 3.8*) starts from the commercially available acetylated piperidone **133**, which was condensed with pyrrolidine in presence of *p*-TSA as catalyst to obtain the corresponding enamine that was reacted with 2-chlorohydroxyiminoacetic acid methyl ester to give the intermediates **135** that was not isolated and directly reacted with TFA in DCM at reflux giving the derivative **136** in a 70% yield over two step. Deacetylation of compound **136** with 32% hydrochloric acid give the amine ethyl ester **137**. Then, the ethyl ester moiety was replaced with a ethylamide moiety to give **140**, since it seems that interactions with the receptor at this position seem to be relevant as according to previous experience of our group. The conversion of the ethyl ester moiety to the ethylamide was achieved by reaction with ethylamine in methanol

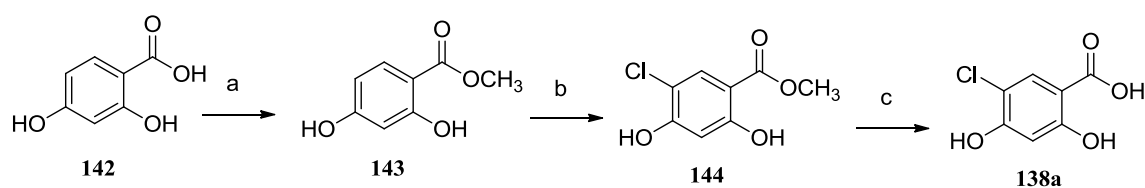
at reflux to give **140**. Reaction of the latter with the opportune carboxylic acid in the presence of HOBt and EDC in DMF gave in pretty good yield the desired **139a,b** and **141a,b**.

3.3.1 Synthesis of resorcinol acid

The synthesis of the carboxylic acid is shown in *Schemes 3.9* and *3.10*

The synthesis of chloro-resorcinol acid starts from the conversion of the 2,4-dihydroxybenzoic acid to the methyl 2,4-dihydroxybenzoate was achieved by reaction with H_2SO_4 in methanol at reflux. Chlorination of **143** with sulfuryl chloride furnished **144**, which was hydrolyzed to give acid **138a** in good yield.

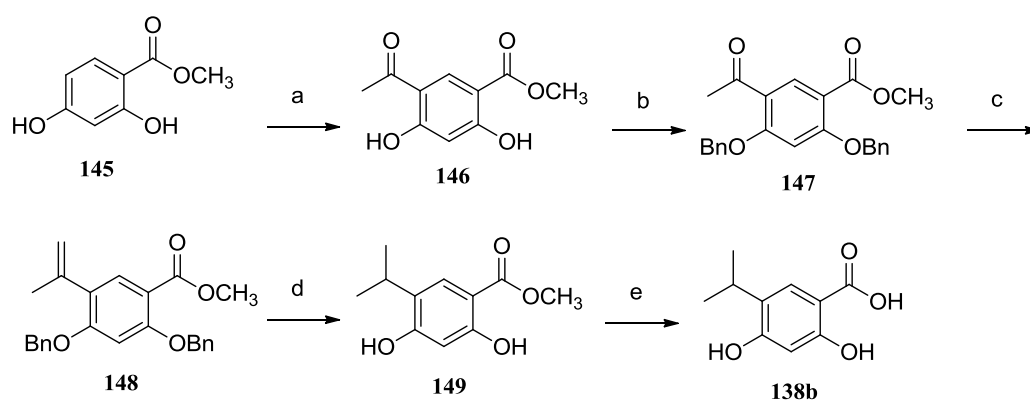
Scheme 3.9 Synthesis of chloro-resorcinol acid^a



^aReagents and conditions: (a) H_2SO_4 , MeOH, Rfx; (b) SO_2Cl_2 , DCM; (c) NaOH, $\text{H}_2\text{O}/\text{MeOH}$.

In *Scheme 3.10* the intermediate **146** was obtained by regioselective Friedel-Crafts acylation of the commercially available 2,4-dihydroxyacetophenone **145**. Then, both phenolic functions were protected with benzyl groups and a Wittig reaction generate compound **148**. The reduction of the styrene functionality in **148** caused concomitant debenzylation. Finally **149** was treated with NaOH to obtained the corresponding acid **138b**.

Scheme 3.10 Synthesis of isopropyl-resorcinol acid^a



^aReagents and conditions: (a) AcOH, $\text{BF}_3 \cdot \text{xOEt}_2$; (b) BnBr, K_2CO_3 , MeCN; (c) $\text{CH}_3\text{P}^+(\text{Ph})_3\text{Br}^-$, NaH, toluene; (d) Pd/C, H_2 ; (e) NaOH, $\text{H}_2\text{O}/\text{MeOH}$.

Chapter 4

Results and discussion

Contents

4.1 In vitro studies of 3,4-isoxazolidiamides scaffold

4.1.1 Analysis of the degradation of Hsp90 client proteins in A431 cells

4.2 In vivo studies of 3,4-isoxazolidiamides scaffold

4.3 In vitro studies of 4,5,6,7-tetrahydro-isoxazolo-[4,5-c]pyridine scaffold

4.1 In vitro study of 3,4-isoxazolidiamides scaffold

Then, in collaboration with the pharmaceutical industry Sigma Tau, we performed *in vitro* and *in vivo* study in order to obtain some SAR (Structure Activity Relationship) information on this new class of compounds.

Here we describe *in vitro* and *in vivo* biological profile of the most significant of these derivatives. Measurement of binding were done by a fluorescence polarization (FP) competitive binding assay, and inhibition of cell growth proliferation of the NCI-H460 tumor cell lung line was determinate.

The data of the compounds with a chlorine atom on resorcinol moiety are shown in *Table 4.1*. All the synthesized compounds, apart from the fluorinated derivative **67**, showed binding affinity in the range of 37-250 nM. Remarkable are results of the cell proliferation assay showed by compounds **61**, **63**, **65**, **121a** also showed cytotoxic activity in the submicromolar range (130-750 nM), resulting thus comparable with those previously reported for the 4,5-diarylisoxazoles **35** and **36**. The results offered by the alkylamides **63**, **65**, **121a** were quite surprisingly and unexpected, the drug design strategies on the 4,5-diarylisoxazoles series have indeed focused mainly on the C-aryl pendants. Instead, the fluorinated compound **66**, synthesized with the aim to reinforcing the H-bond with Lys58 and improve the metabolic stability, contrarily to our expectation, showed equivalent binding and cellular activity, thus demonstrating no advantage compared with the related ethylamide residue **58**. The other fluorinated derivative **67**, where the hydrogen on the C-3 amide was missing, resulted not active, reinforcing the importance of the presence of a hydrogen in this position for its H-bond capabilities and minimal steric hindrance.

The interesting activity showed both aryl and alkyl amides of the compounds bearing a chlorine at the C-5 position of the resorcinol residue gave therefore confirmation to the idea that manipulation around the C-4 region of the isoxazole scaffold may significantly alter the activity of the compounds providing an interesting opportunity for the construction of novel class of Hsp90 inhibitors.

The choose to introduction a second amide group was supported by docking study as shown in *Figure 4.1*. We hypothesized that the introduction of a second amide group at C-4, could play an additional role in the binding to the pocket of Hsp90 producing an extra interaction with Lys58, as well as a concomitant reorientation of the aromatic portion.

Interestingly, our modeling studies indicated also that the key interaction of the OH-resorcinol groups and the C-3 amide of the isoxazole ring still remain identical.⁸⁷ Thus, the

idea of an additional H-bond donor interaction in the site active, mediated by an amide moiety at position 4 of the isoxazole ring, was considered as the basic structural motif for the construction of a series of 3,4-isoxazolidiamides (see *Table 4.1*, *4.2* and *4.3*). The resorcinol portion and the C-3 amide moiety were maintained considering the privileged role offered by these group in the interaction with the Hsp90 protein in both radicicol and 4,5-diarylisoxazole. Docking investigation suggest also that the introduction of the 4-amide spacer give rise to two conflicting events: a positive H-bond interaction between carbonyl and Lys58 and a negative removal of the phenyl moiety which is put a part from the enzymatic pocket, this balance keeps the activity of NVP-AUY922 and of **91** almost comparable.

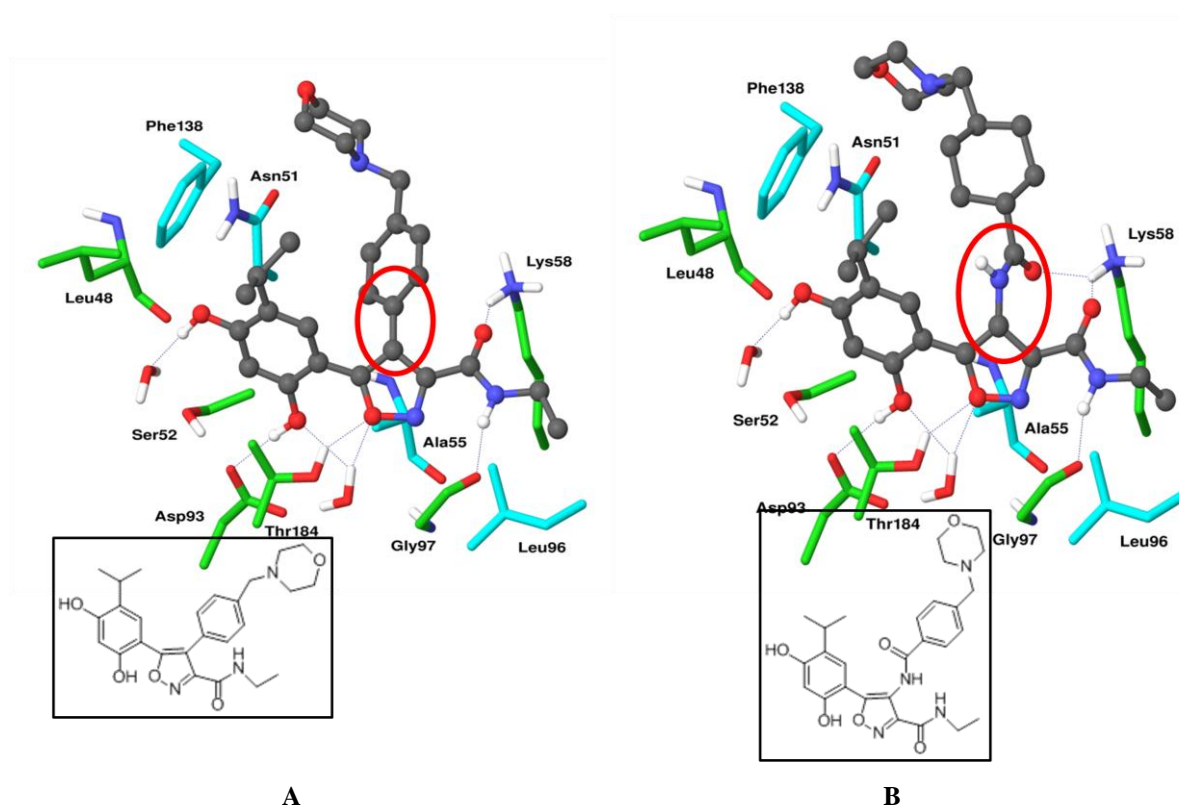


Figure 4.1 (A) **36** co-crystallized in Hsp90 active site (PDB code = 2vci). Color scheme is by atom type; grey: **36**, cyan: protein residues involved in non-polar interactions; green: protein residues involved in polar interactions. H-Bonds are shown as dotted line. (B) Docking pose of compound **91** in Hsp90 active site. Color scheme is by atom type; grey: **91**, cyan: protein residues involved in non-polar interactions; green: protein residues involved in polar interactions. H-Bonds are shown as dotted line.

Consequently, we explored the potential of the new scaffold investigating a lot of additional substitution at the C-4 amide portion. As can be seen from *Tables 4.2* and *4.3*,

and in agreement with finding previously described for 4,5-diarylisoaxazoles, compounds with a 5-chlorine substituent are significantly less active than derivatives containing the 5-isopropyl residue, the cell growth activity proving generally at the micromolar level. Therefore, to improve cytotoxicity,⁸⁷ a small library of isopropyl analogues bearing at C-4 of isoaxazole an alkyl, cicloalkyl, aryl and heteroaryl appendage were therefore synthesized. We carried out virtual docking experiments, using Hsp90-**36** X-ray complex structure and a virtual library of 3,4-isoxazolidiamides bearing diverse C-4 substituent. Such library was prepared by “reacting” the debenzylated intermediate **56d** with 350 commercially available acyl chlorides or carboxylic acids having molecular weight between 100 and 350. The resulting 3,4-isoxazolidiamides were filtered according to Rule of 5 < 2 (except **77-79** with two violations), subjected to a conformational analysis and then docked in the active site of the enzyme. Compound with scoring value higher than the simplest analogue (acetamide derivative, **68**) were selected for synthesis. Biological evaluation of a library of 60 isopropyl derivatives (*Tables 4.2 and 4.3*) showed binding affinity in the range of 1-260 nM. Remarkable compounds which combine notable binding properties with potent cell growth inhibitory activity (IC₅₀ values in the low nanomolar range) are **68, 69, 73, 85** (*Table 4.2*) in the class of alkyl and cycloalkyl derivatives; **88, 89, 91** in the class of phenyl derivatives; **97-100, 110, 113** and **114** in the class of heterocyclic derivatives (*Table 4.3*). Considerable are also the antiproliferative effects of compounds **70** and **72** were also noteworthy (16 and 42 nM respectively) notwithstanding a decrease of their binding activity.

Interestingly, replacement of phenyl ring with cycloalkyl residues increases the number of positive Van der Waals interactions while keeping the H-bond between Lys58 and C-4 amide. The strongest binding is found in 1,4-*trans*-cyclohexane (**119e**), since the *cis* conformation (**119d**) points the methylmorpholine to a region with poor van der Waals interactions.

These finding may give thus in part explanation of the potent binding activity of the alkyl amides. Replacement of the cyclohexane ring with a cyclopentane with *cis* stereochemistry as in compound **119a** does not modify the binding potency in respect to compound **119e**.

Interestingly, a pendant that can give water solubility, such as the morpholine derivatives **91, 115, 119a,d,e** and **121b** are well tolerated retaining good binding and cell growth inhibiting properties. On the contrary, the appendages such as **75, 76** carbamate **79**, piperidines **80, 81**, piperazines **90, 91** and pyrrolidine **93** fragments are detrimental proving much less potent as cell growth inhibitors.

Thus, focusing our attention on data of *Table 4.2* and *Table 4.3*, appear evident that only for few compounds there is a good correlation between cytotoxicity and binding properties. A large group of compounds (i.e. **74-84**, **86**, **87**, **90**, **92-96**, **102-105**, **107-109**, **111**, **112**, **115**, **117a-e** and **119b,c**) are characterized by an excellent binding profile but showed only poor cell proliferation inhibitory properties. Compounds **78-81**, **117b,c,e**, **119b** having binding potency at low nanomolar level, show antiproliferative effects only at micromolar level.

Interpretation of these results is not easy. As a tendency, the disparity in cell growth potency compared with binding activity is markedly higher in the subseries of alkyl amides. Such behavior can be accountable to permeability issues across cell membranes. A higher lipophilicity index (both aliphatic and aromatic substituent) may correlated with a higher cytotoxicity, indicating therefore that an increase of the lipophilic character could facilitate their cellular uptake. The limited permeability across cell membranes could be merely addressed to a large polar surface for some compounds (i.e., **77-81**, **86**, **96**, **102-104** and **115**) or to positively charged appendages at pH = 7.4 (i.e., **75**, **76**, **82** and **83**) as demonstrated by the LogD^{7.4}. Indeed, a lipophilicity index, calculated using ACD/Labs software, does correlate to a high cytotoxicity profile (**69**, **70**, **73**, **85**, **88**, **89**, **97**, **99** and **100**). Other factor may influence of course the activity of the compounds is the possibility of additional hydrogen bonds. Hydrogen bond donor groups are normally disadvantage versus hydrogen bond acceptors groups, giving additional explanation of the poor activity of compounds **117b**, **117c** vs **73** and **85** vs **86**.

In this context we attempted a correlation between binding and cytotoxicity. Some descriptors have been calculated for a group of 40 molecules showing a binding/cytotoxicity ratio at least less than 50 times. A multiple linear regression calculation identified two main variables that correlate cytotoxicity and binding:

- a) the pka of the 2-OH of resorcinol which takes consideration of the influence of the substituent C-5 of the resorcinol group (Cl or isopropyl), the positive coefficient indicating that 5-Cl-resorcinol derivatives are less cytotoxic;
- b) the aryl surface accessible by the solvent, a negative coefficient indicating that a lower aromatic character of the C-4 amide substituent is preferred.

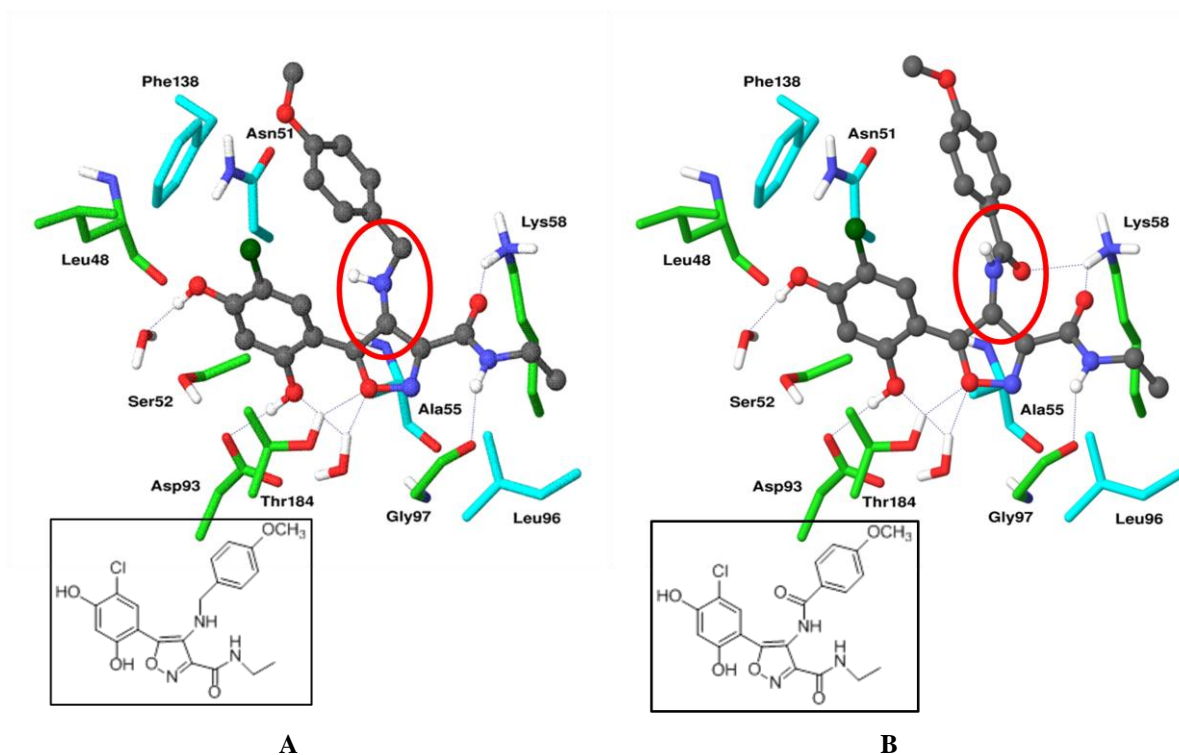


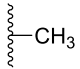
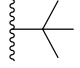
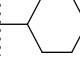
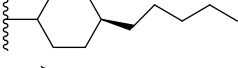
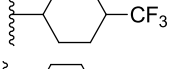
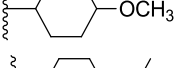
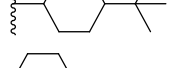
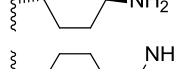
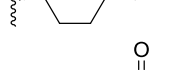
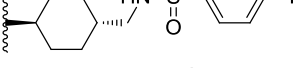
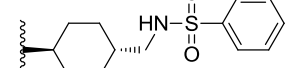
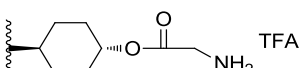
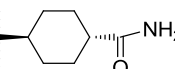
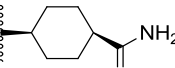
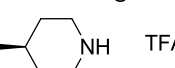
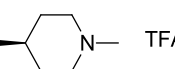
Figure 4.2 (A) **123b** co-crystallized in Hsp90 active site (PDB code = 2vci). Color scheme is by atom type; grey: **123b**, cyan: protein residues involved in non-polar interactions; green: protein residues involved in polar interactions. H-Bonds are shown as dotted line. (B) Docking pose of compound **58** in Hsp90 active site. Color scheme is by atom type; grey: **58**, cyan: protein residues involved in non-polar interactions; green: protein residues involved in polar interactions. H-Bonds are shown as dotted line.

Finally, C-4-aminomethyl derivatives **123a-d** (Table 4.4) were synthesized mainly with the aim to explore the importance of the C-4 amide carbonyl moiety and to add support the premise that the 3,4-diamides class of compound can interact with Hsp90 by means of an additional Lys58. Amines compounds **123a,b** (Table 4.4) showed a drop in binding affinity probably due to the lack of carbonyl interaction with Lys58. The cytotoxicity values were inconsistent when compared with the parent amides **61** and **58**. A loss of a putative interaction of C-4 amide carbonyl with Lys58 and a reorientation of aromatic group, as shown in the Figure 4.2 of compound **123b**, could explain in some way the decrease of binding affinity. Anyway, the loss of cytotoxic activity showed by all the C-4 amines **123a-d** allowed to consider this type of substitution of little interest for further investigations.

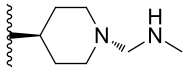
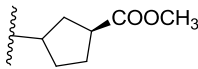
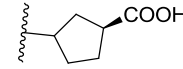
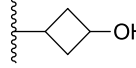
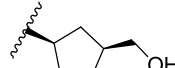
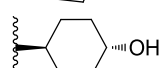
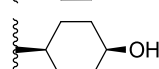
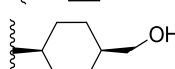
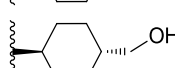
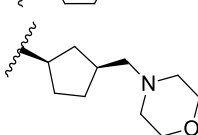
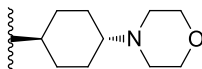
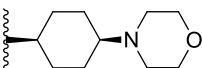
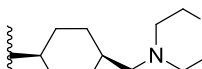
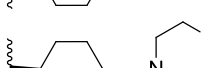
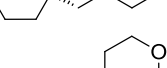
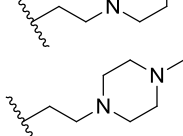
Table 4.1 Data for isoxazole-3,4-diamides. Binding on Hsp90 by a fluorescence polarization assay (FP Assay) and cytotoxicity on NCI-H460 non small cell lung carcinoma cells.

Compound	R	R ₁	NCI-H460 (IC ₅₀ ; μM)	Hsp90 (FP) (IC ₅₀ ; μM)
NVP-AUY922	-	-	0.024	0.061
57	CH ₃ CH ₂ -NH-		> 1	0.153
58	CH ₃ CH ₂ -NH-		> 1	0.184
59	CH ₃ CH ₂ -NH-		> 1	0.163
60	CH ₃ CH ₂ -NH-		> 1	0.130
61	CH ₃ CH ₂ -NH-		0.41	0.074
62	CH ₃ CH ₂ -NH-		> 1	0.037
63	CH ₃ CH ₂ -NH-		0.310	0.085
64	CH ₃ CH ₂ -NH-		> 1	0.167
65	CH ₃ CH ₂ -NH-		0.750	0.250
66	-CF ₃ CH ₂ -NH-		> 1	0.160
67			> 1	> 100
121a	CH ₃ CH ₂ -NH-		0.130	0.168

Table 4.2 Data for isoxazole-4-alkyl/cycloalkyl amides. Binding on Hsp90 (FP Assay) and cytotoxicity on NCI-H460 non small cell lung carcinoma cells.

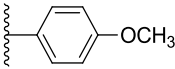
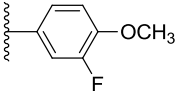
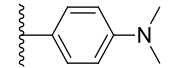
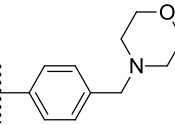
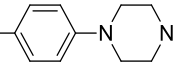
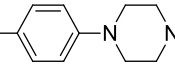
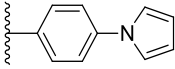
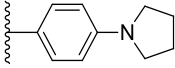
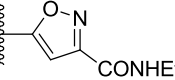
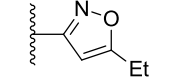
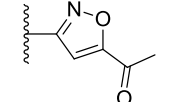
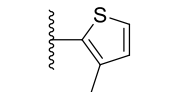
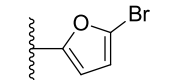
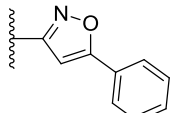
Compound	R ₁	NCI-H460 (IC ₅₀ ; μM)	Hsp90 (FP) (IC ₅₀ ; μM)
NVP-AUY922	-	0.024	0.061
68		0.081	0.055
69		0.024	0.041
70		0.016	0.190
71		> 1	0.260
72		0.042	0.240
73		0.013	0.024
74		0.200	0.300
75	 HCl	> 1	0.028
76	 HCl	> 1	0.040
77		0.640	0.0054
78		> 1	< 0.005 ^a
79	 TFA	> 1	< 0.005 ^a
80		> 1	< 0.005 ^a
81		0.990	< 0.005 ^a
82	 TFA	> 1	< 0.005 ^a
83	 TFA	> 1	0.024

Continued...

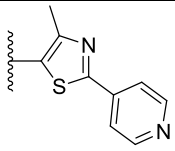
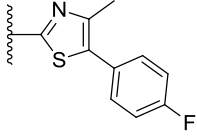
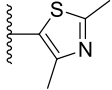
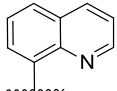
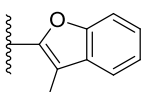
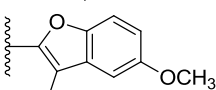
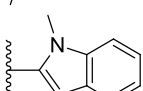
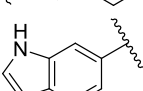
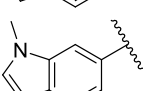
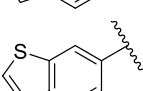
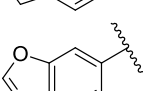
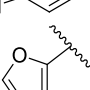
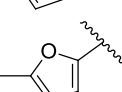
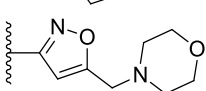
84		TFA	> 1	0.0086
85			0.022	0.005
86			> 1	0.039
87			0.920	0.014
117a			0.260	0.0126
117b			> 1	0.002
117c			0.500	0.0022
117d			0.870	0.015
117e			0.600	0.0012
119a			0.170	0.012
119b		HCl	0.680	0.0014
119c		TFA	0.610	0.0074
119d		HCl	0.140	0.196
119e		HCl	0.130	0.0088
121b			0.110	0.214
121c			> 1	0.120

^aFor detection limits of the assay, see Chiosis et al.⁹⁹

Table 4.3 Data for isoxazole-4-aryl/heteroaryl amides. Binding on Hsp90 (FP Assay) and cytotoxicity on NCI-H460 non small cell lung carcinoma cells.

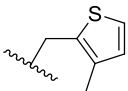
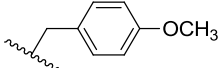
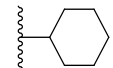
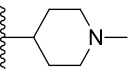
Compound	R ₁	NCI-H460 (IC ₅₀ ; μM)	Hsp90 (FP) (IC ₅₀ ; μM)
NVP-AUY922	-	0.024	0.061
88		0.017	0.026
89		0.055	0.034
90		0.240	0.034
91		0.095	0.071
92		> 1	0.024
93		> 1	0.032
94		> 1	0.032
95		0.810	0.022
96		> 1	0.024
97		0.022	0.020
98		0.082	0.019
99		0.017	0.084
100		0.019	0.022
101		> 1	0.25

Continued...

102		> 1	0.027
103		> 1	0.04
104		0.560	0.010
105		0.490	0.036
106		> 1	0.260
107		0.750	0.048
108		0.360	0.062
109		0.170	0.033
110		0.087	0.034
111		0.180	0.020
112		0.110	0.015
113		0.016	< 0.005a
114		0.022	< 0.005a
115		0.200	0.040

^aFor detection limits of the assay, see Chiosis et al.⁹⁹

Table 4.4 Data for 4-amino isoxazole. Binding on Hsp90 (FP Assay) and cytotoxicity on NCI-H460 non small cell lung carcinoma cells.

Compound	R	NCI-H460 (IC ₅₀ ; μM)	Hsp90 (FP) (IC ₅₀ ; μM)
NVP-AUY922	-	0.024	0.061
123a		> 1	0.230
123b		> 1	0.430
123c		> 1	0.620
123d		> 1	1.600

4.1.1 Analysis of the degradation of Hsp90 client proteins in A431 cells

To measure the activities of these compounds against Hsp90 in cells, a few selected compounds (**69**, **70**, **73**, **91**, **97** and **99**) were further tested for their effects in causing degradation of some typical Hsp90 client proteins in the A431 (human epidermoid carcinoma) cell line and in inducing Hsp70 gene expression. The effects on the expression of client proteins and Hsp70 induction are a mark of Hsp90 inhibition. The activity on the examined client proteins (Akt, Cdk4 and EGFR) and Hsp70 were evaluated by means of the classical Western Blotting analysis on total protein extracts of A431 cells, following 24h exposure to various concentrations of the test-compound. All tested compounds were effective, causing dramatic depletion of the examined client proteins and, as expected for the Hsp90 inhibitors, always inducing a very strong increase in the expression levels of the chaperone Hsp70 (*Figure 4.3*). The depletion was always dose dependent and was achieved with potency similar to that of the reference compound (17-DMAG). The only partial exception was represented by compound **97**, which caused a marked depletion of EGFR and Cdk4 client proteins but, at the same time, showed only a marginal effect on the expression of Hsp70. These results support therefore premises that the effects on cell

growth of the 3,4-isoxazolidiamides was a consequence of their Hsp90 chaperone inhibitory properties.

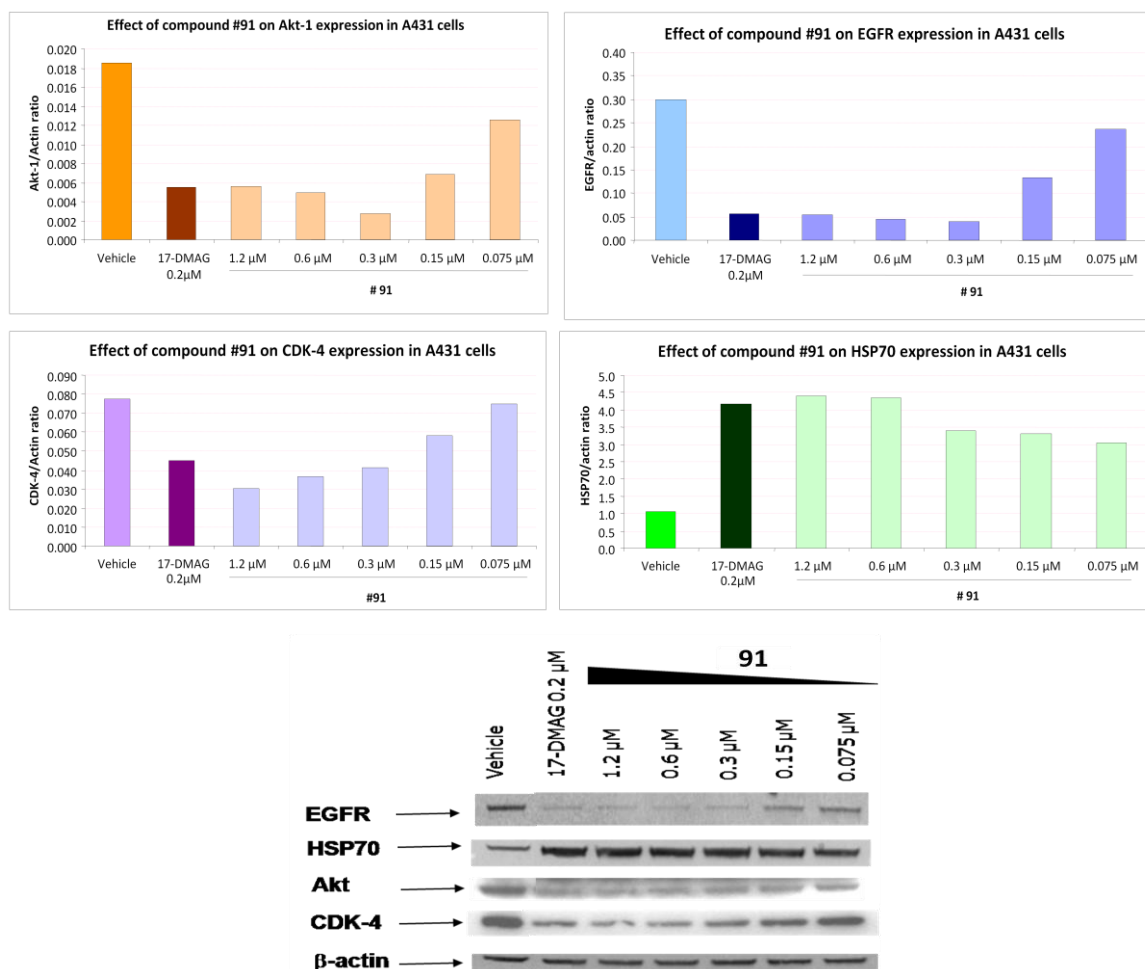
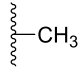
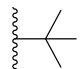
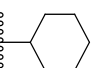
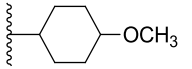
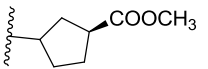
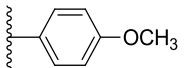
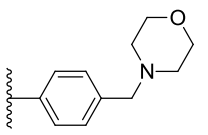
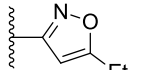
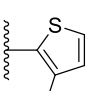
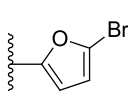
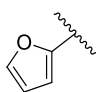
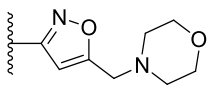


Figure 4.3 Analysis of Hsp90 client protein levels (EGFR, Akt, CDK-4) and Hsp70 in A431 tumor cells treated with compound 91. Total cellular extracts were obtained 24 h after treatment. Actin is shown as a control for protein loading. Results of densitometry analysis were reported as normalized (to β-actin) ratios.

4.2 In vivo study of 3,4-isoxazolidiamides scaffold

Finally, twelve compounds were selected for *in vivo* study against human epidermoid carcinoma A431 tumor xenografts (Table 4.5).

Table 4.5 Data of cytotoxicity on A431 epidermoid carcinoma cells of the compounds tested *in vivo*.

Compound	R	A431 (IC ₅₀ ; μM)
10	-	0.0019
27		0.088
28		0.030
29		0.013
32		0.011
44		0.014
47		0.011
50		0.020
56		0.013
58		0.026
59		0.011
72		0.011
74		0.050

All compounds were administered intraperitoneally once daily at their maximum tolerated doses (i.e., doses which produced a body weight loss of 7-8%) without any sign of toxicity.

Table 4.6 Antitumor activity of compounds **91** and **115** in comparison with NVP-AUY922 against A431 epidermoid carcinoma. (TVI = tumor volume inhibition; BWL = body weight loss).

Drug treatment	Dose/route (mg/kg)	TVI±SE (%)	BWL (%)
NVP-AUY922	60/ip	48±5	8
91	60/ip	48±4	7
115	60/ip	33±4	2

Compound **115** showed a comparable antitumor effect (tumor volume inhibition 48%) to that of the reference compound **36** (Table 4.6 and Figure 4.4).

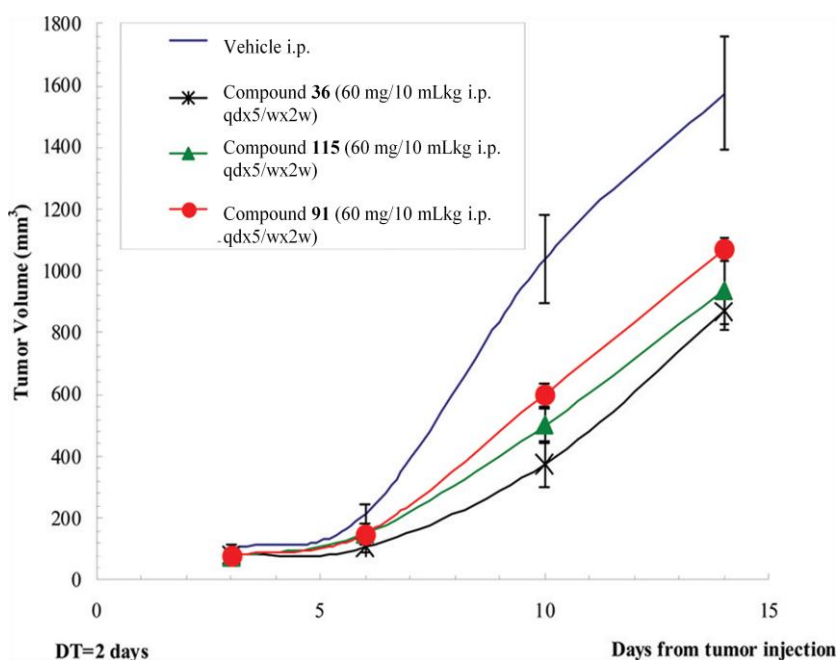


Figure 4.4 Antitumor activity of the compounds **91** and **115** in comparison with that of compound **36** (NVP-AUY922) against A431 epidermoid carcinoma xenografted in CD1 nude mice.

In contrast, compound **91**, structurally related to the reference compound **36** (NVP-AUY922), showed a reduced *in vivo* activity. The ability of **115** to effect *in vivo* the expression of typical Hsp90 client proteins was assessed in A431 tumor xenografts, 2 hours after the last treatment.

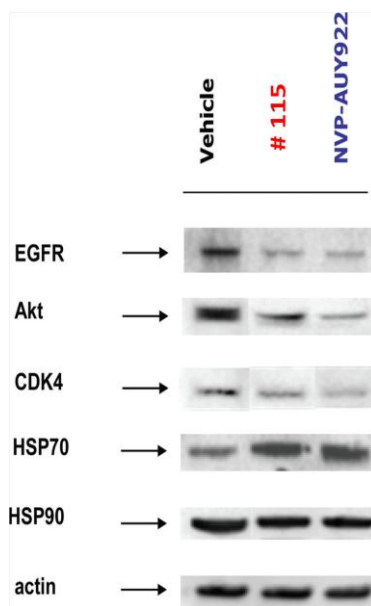


Figure 4.5 Analysis of Hsp90 client protein levels (EGFR, Akt, CDK-4, and Hsp70) in A431 tumor xenografts, following treatment with **115** and **36** (NVP-AUY922). Total proteins were purified 2 h after the last treatment. Actin is shown as a control for protein loading. A representative blot is shown.

As shown in *Figure 4.5*, **115** induced a strong degradation of three typical “client” proteins (Akt, Cdk4 and EGFR) and significantly increase the expression levels of Hsp70, with a potency comparable to that of the reference inhibitor **36** (NVP-AUY922). Thus, although *in vivo* activity of **115** is somehow moderate, the compound still shows a very good *in vivo* activity profile among those tested.

4.3 In vitro studies of 4,5,6,7-tetrahydro-isoxazolo-[4,5-c]pyridine scaffold

As previously described, the structure of the N-terminus of Hsp90 is characterized by a network of highly ordered water molecules at the base of the adenine binding pocket. On binding of ATP, the endogenous ligand forms hydrogen bonds with three of these conserved waters and one hydrogen bond with the protein residue Asp93.

The resorcinol portion was firstly introduced for its role in the interaction with the Hsp90 protein in both radicicol and 4,5-diarylisoxazole series of compounds.⁸⁷ In fact, the resorcinol moiety provides a key hydrogen bond network with conserved water molecules coordinated through Asp93 in the region that typically binds the adenine ring of ATP.

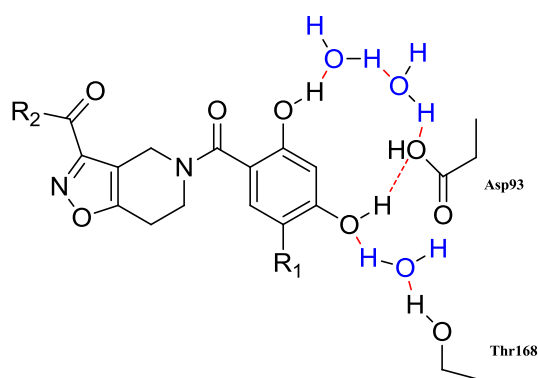


Figure 4.6 Interaction between Hsp90 and resorcinol moiety.

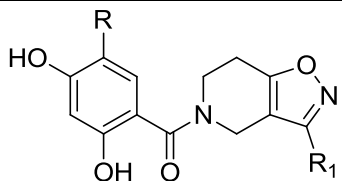
Initially, we used the resorcinolic acid with a chlorine atom as substituent at the 5-position to give compounds **139a** and **141a**. Then, the chlorine atom was replaced by an isopropyl group to understand if additional interactions with the ribose binding pocket were also possible. Studies of modeling has been demonstrated that an isopropyl group is able to efficiently fill a proximal hydrophobic cavity, bounded by the residues Leu107, Phe138, Val150, and Val186.

The introduction of a tertiary amide linker between the resorcinol and the isoxazole-pyrido-fused core is known in literature to induce an important twist in the conformation of the molecule, forcing the carbonyl out of the plane of the phenyl ring. This allows the carbonyl to efficiently form of a bidentate interaction between the carbonyl and a conserved water molecule and the side chain hydroxyl of Thr184.¹⁰⁰ The low energy twisted conformation of the tertiary amide also allows the tetrahydropyrido-isoxazole

group to form positive hydrophobic interactions with the backbones of Asp54 and Ala55 (not shown in the figure in *Figure 4.6*).

All the newly synthesised compounds were submitted to fluorescence polarization (FP) competitive binding assay, to evaluate their ability to bind Hsp90, and inhibition of cell growth proliferation of the NCI-H460 tumor cell line was determinate. Data are reported in *Table 4.7*.

Table 4.7 Data of binding on Hsp90 (FP Assay) and citotoxicity on NCI-H460 non small cell lung carcinoma cells.

Compound	R ₁	R ₂			Hsp90 (FP)
			NCI-H460 (IC ₅₀ ; μM)	(IC ₅₀ ; μM)	
139a	Cl	COOEt	>1	165	
141a	Cl	CONHEt	>1	110	
139b	<i>i</i> Pr	COOEt	0.87-0.91	34	
141b	<i>i</i> Pr	CONHEt	0.45-0.36	29.7	

Among the group of esters **139a** and **139b**, the isopropyl resorcinol derivative **139b** was the most potent compound having cellular activity at nanomolar level; whereas, compound **139a** despite retaining some binding ability, resulted deprived of cellular activity.

Among the group of the ethylamides **141a** and **141b**, compound **141b**, along with an important binding property, showed a notable antiproliferative activity. Otherwise, the chlororesorcinol derivative **141a** resulted deprived of cytotoxicity.

Additionally, cell viability, apoptosis analysis of cell cycle was determined for compounds **141a** and **141b** in comparison with 17-AAG. **141a** and **141b** elicited a concentration-dependent growth inhibitory effect in K562 cells (chronic myeloid leukemia cell line) with an IC₅₀ of 32.6 μM and 0.72 μM respectively after 72 hour drug exposure (*Table 4.8*).

Table 4.8 Cytotoxic and apoptotic effects of the Hsp90 inhibitors in K562 cells.^a

Compounds	IC₅₀ (μM)	IC₅₀ (μM)
17-AAG	0.15	3.1
141a	32.6	> 100
141b	0.72	5.4

^a The cells were exposed to the drugs for 72 hours. Cytotoxicity was evaluated by the Trypan blue dye exclusion test, while apoptosis was measured by fluorescence microscopy IC₅₀: growth inhibitory concentration inducing 50% apoptotic cell death.

Chapter 5

Conclusion

In summary, starting from a docking investigation on 4,5-diarylisoxazoles we postulated that the introduction of a second amide group at the C-4 position of the isoxazole ring could give an additional interaction with Lys58 providing the opportunity for the construction of a novel class of Hsp90 inhibitors. We have performed a detailed investigation and elaboration of the isoxazole scaffold leading to the discovery of a novel class of 3,4-isoxazolidiamides endowed with potent Hsp90 inhibitory activity. The C-4 amide appendage could be either an alkyl or aryl moiety. A group of amides showed affinity for the target comparable to that showed by 4,5-diaryl products **35** and **36**. Compounds of interest which combined potent binding and cell growth activity were obtained. The IC₅₀ values were in the low nanomolar range for the series of alkyl and cycloalkyldiamides (**68**, **69**, **73** and **85**), as well as in the series of the aryl and heteroaryl derivatives (**88**, **89**, **91**, **97-100**, **110**, **113** and **114**). The antiproliferative effects of compounds **70** and **72**, (16 and 42 nM respectively) were notable notwithstanding having rather moderate binding affinities. Quite surprisingly and unexpected, a large group of diamides show an important drop of cell proliferation inhibitory activity notwithstanding their potent binding affinity (1-9 nM).

The compound **91**, bearing an aryl amide C-4, decorated with an aminomethyl morpholine appendage, was found active in vivo and comparable with the reference (**36**).

Analysis of the degradation of the client proteins A431 cell proved unequivocally that the diamides were active in human cancer cell lines where they inhibit cell proliferation and exhibit a characteristic profile of depletion of oncogenic proteins and concomitant very strong increase in the expression levels of the chaperone Hsp70.

Thus, manipulation at the C-4 position of the isoxazole scaffold significantly altered the biological activity of the compounds. The active site residue Lys58, involved in H-bond with the C-3 carbonyl group of amide, suggested that the introduction of a second amide group at C-4 could play an important role in the interaction with the protein. Comparing

the binding geometry and data obtained in the amino series and in the amide series analogous we had to confirm this hypothesis. In fact derived amides are more potent than the corresponding amine derivatives.

Twelve compounds with a different range of in vitro profile were selected to be studied in vivo against human epidermoid carcinoma A431. The compound **115** revealed a comparable antitumor effect (tumor volume inhibition 48%) to that of the reference compound NVP-AUY922, **36** currently in Phase II clinical trials, belongs to this class of compounds.

The synthesis of new 4,5,6,7-tetrahydro-isoxazolo-[4,5-c]pyridine scaffold has been described.

A new synthetic route of these compounds has been developed to the preparation of a small family of potential Hsp90 inhibitors. The new derivatives has been tested for their affinity to Hsp90 and for their antiproliferative activity.

Among those prepared, all of derivatives proved to be able to bind to Hsp90 protein with IC₅₀ values in the low nanomolar range.

We can say that the activity increases when a isopropyl group is added on the resorcinol moiety (*e.g.* **139b** and **141b**) and it is interesting to note that, among the different side substituents of the isoxazole, the ethyl amide affords the best IC₅₀ value. Therefore, an additional halogen atom on the aromatic moiety improves the IC₅₀ (*e.g.* **141a** vs **141b**).

The compounds **141a-141b**, showed binding affinity at micromolar/nanomolar level and showed also cytotoxic activity in sub-micromolar range (130-750 nM).

Moreover, the first representative of 4,5,6,7-tetrahydro-isoxazolo-[4,5-c]pyridine scaffold **141b** have been identified.

The next study will focus on the identify original and patentable changes of the molecules such that maintain the values in the order of binding **141b** and improve the values of cytotoxicity.

New scaffolds, based on a computational approach, have been proposed and some examples have been synthesize. The biological evaluation of these last compounds is still on going.

Chapter 6

Experimental section

Contents

6.1 Biological section

6.2 Molecular modeling

6.3 Materials and methods

6.4 Experimental procedures

6.1 Biological section

Experiments were carried out at Sigma-Tau (Rome, Italy) to evaluate the antiproliferative activity of the neo-synthesized compounds.

Tumor Xenograft Model

Experiments were carried out using female athymic nude CD-1 mice, 8–11 weeks old (Harlan, Italy). Mice were maintained in laminar flow rooms with constant temperature and humidity. Experimental protocols were approved by the Ethic Committee for Animal Experimentation. A431 epidermoid carcinoma cells (3×10^6 /mouse) were inoculated subcutaneously (sc) in the right flank of CD1 nude mice. Drug treatments started 3 days after tumor injection according to the schedule qd \times 5/w \times 2w. To evaluate the antitumor activity, tumor diameters were measured biweekly with a Vernier caliper. The formula TV (mm³) = [length (mm) \times width (mm)²]/2 was used, where the width and the length are the shortest and the longest diameters of each tumor, respectively. When tumors reached a volume of 1 cm³, mice were sacrificed by cervical dislocation. Body weight was recorded every day throughout the study. Toxicity of the molecules was determined as follows: body weight loss percent (% BWL_{max}) = 100 - [(mean BW_x/mean BW₁) \times 100], where BW_x is the mean BW at the day of maximal loss during the treatment and BW₁ is the mean BW on the first day of treatment. Lethal toxicity was also evaluated. Doubling time (DT) of control tumors was also calculated. In order to assess the effect in vivo of **115**, compared to the reference compound **36** (NVP-AUY922), on the expression of typical Hsp90 client proteins, A431 tumor xenografts (3 samples/group) were excised 2 h after the last treatment and then total proteins were extracted through the homogenization of tumor samples in T-PER tissue protein extraction reagent (Pierce, Rockland, IL, U.S.), supplemented with 10 μ g/mL protease inhibitor cocktail (Sigma Chemical Co., St. Louis, MO, U.S.). Determination of the protein concentration and Western blotting analysis were finally performed as described in the section Client Protein Degradation Assay.

Cellular Sensitivity to Drugs

In non-small-cell lung carcinoma cells (NCI-H460) and in epidermoid carcinoma cells (A431), cellular sensitivity to drugs was evaluated by growth-inhibition assay after 72 h of drug exposure. Cells in the logarithmic phase of growth were seeded into 96-well plates, and 24 h after seeding, the drug was added to the medium. Cell survival was evaluated after 72 h of drug exposure by the sulforhodamine B test. IC₅₀ was calculated by the ALLFIT program and was defined as the drug concentration causing a 50% reduction of cell number compared to that of untreated control cells.

Binding on Hsp90 by a Fluorescence Polarization Assay.⁹⁹

GM-FITC, supplied by Invivogen (catalog no. 06C23-MT, CA, U.S.) was previously dissolved in DMSO to obtain 10 mM stock solutions and kept at -20 °C until use. Hsp90, purchased from Stressgen (catalog no. SPP-776, Victoria, BC, Canada), was previously dissolved in assay buffer (HFB) to form 2.2 μM stock solutions and kept at -80°C until use.

The compounds were previously dissolved in DMSO to obtain stock solutions and kept at -20 °C. On the day of the experiment, various concentration solutions were prepared by serial dilutions in assay buffer (HFB) containing 20 mM HEPES (K), pH 7.3, 50 mM KCl, 5 mM MgCl₂, 20 mM Na₂MoO₄, and 0.01% NP40. Before each use, 0.1 mg/mL bovine γ globulin and 2 mM DTT were freshly added. Fluorescence polarization (FP) was performed in Opti-Plate-96F well plates (Perkin-Elmer, Zaventem, Belgium) using a plate reader (Wallac Envision 2101 multilabel reader, Perkin-Elmer, Zaventem, Belgium). To evaluate the binding affinity of the molecules, an amount of 50 μL of the GM-FITC solution (5 nM) was added to 30 nM Hsp90 in the presence of 5 μL of the test compounds at increasing concentrations.

The plates were shaken at 4°C for 4 h, and the FP values in mP (millipolarization units) were recorded. The IC₅₀ values were calculated as the inhibitor concentration that displaced 50% of the tracer, each data point being the result of the average of triplicate wells, and were determined from a plot using nonlinear least-squares analysis. Curve fitting was performed using Prism GraphPad software program (GraphPad Software, Inc., San Diego, CA, U.S.).

Client Protein Degradation Assay

Client protein degradation was determined by Western blotting. Twenty-four hours after seeding on Petri dishes, A431 (human epidermoid carcinoma) cells were treated, for 24 h in complete medium, with various concentrations of test compounds depending on their relative potency. 17-DMAG (at 0.2 μM) was used as internal reference inhibitor. Following treatments, cells were rinsed twice with ice-cold PBS and lysed in RIPA buffer supplemented with protease and phosphatase inhibitors. After determination of the protein concentration by Bradford protein assay (Thermo Scientific, Rockford, IL, U.S.), equal amounts of cellular extracts were separated by SDS gel electrophoresis (SDS-PAGE), transferred onto nitrocellulose membranes, and probed with the following primary antibodies: anti-EGFR (Upstate Biotechnology, Millipore Corporate, Billerica, MA, U.S.), anti-Cdk4 (Santa Cruz Biotechnology Inc., CA, U.S.), anti-Akt (Cell Signaling Technology, Inc., MA, U.S.), anti-Hsp70 (BRM-22), and anti-actin (Sigma Chemical Co., St. Louis, MO, U.S.). Immunoreactive bands were revealed by horseradish peroxidase conjugated secondary antibodies, using an enhanced chemiluminescence detection reagent (ECL Plus, GE Healthcare Bio-Sciences, Uppsala, Sweden) and a specific image system (STORM 860; Molecular Dynamics, Sunnyvale, CA, U.S.). Protein loading equivalence was corrected in relation to the expression of β -actin. For quantification of signals, blots were subjected to densitometry analysis.

6.2 Molecular Modeling

Protein for docking were retrieved from PDB (code: 2VCI) and prepared with Protein Preparation Wizard implemented in Maestro, version 9.1 (www.schrodinger.com). Inhibitors molecules were enumerated using TSAR (www.accelrys.com) and then transformed in 3D by using LigPrep, version 2.2 (www.schrodinger.com). Tautomers, charged species and stereochemistry were taken into account. Conformers were generated using MacroModel version 9.8 with MCMM algorithm and an energetic window of 10 kcal/mol. Docking experiments were carried out with Glide, version 5.6. Re-scoring of best poses was carried out with Prime version 2.2, MMGBSA protocol (www.schrodinger.com).

6.3 Materials and methods

Reagents were purchased from commercial suppliers and used without further purification. ¹H-NMR spectra were recorded, unless otherwise indicated, in DMSO solution at 200 MHz on a Bruker AC-200, 300 MHz on a Varian Gemini-300, 400 MHz on a Varian Mercury Plus 400 and 500 MHz on a Varian Gemini-500 spectrometer, and peak positions are given in parts per million downfield from tetramethylsilane as the internal standard. *J* values are expressed in hertz. Electrospray mass spectra were recorded on a Waters Micromass ZQ-2000 instrument or a double-focusing Finnigan MAT 95 instrument with BE geometry. Thin layer chromatography (TLC) was carried out using Merck precoated silica gel F-254 plates. Flash chromatography was done using Merck silica gel 60 (0.063–0.200 mm). Solvents were dried according to standard procedures, and reactions requiring anhydrous conditions were performed under argon. Solutions containing the final products were dried with Na₂SO₄, filtered, and concentrated under reduced pressure using a rotatory evaporator. All the final products undergoing biological testing were analyzed in a Jasco HPLC system consisting of two PU-2080 pumps and an MD-2010 detector. A purity threshold of 98% was set up. Microanalysis of all new synthesized compounds indicated values were within ±0.4% of the calculated value.

6.4 Experimental procedures

Synthesis of Cl-resorcinol derivatives

1-(5-Chloro-2,4-dihydroxyphenyl)ethanone (**40**).

Acetic acid (17.5 mL) was added dropwise to a suspension of 4-chlorobenzene-1,3-diol **39** (20g, 0.138 mol) in BF_3OEt_2 (100 mL, 1.62 mol) under a nitrogen atmosphere. The reaction mixture was heated at 90 °C for 3.5 h and then allowed to cool to room temperature, causing a solid to precipitate. The mixture was poured into a 10% w/v aqueous sodium acetate solution (350 mL). This mixture was then stirred vigorously for 2.5 h to afford a lightbrown solid, which was filtered, washed with water, and air-dried overnight to afford the title compound **40** (31.11.3 g).

Yield 58%. ^1H NMR (400 MHz, DMSO) δ 2.70 (s, 3H), 6.62 (s, 1H), 8.03 (s, 1H), 11.45 (s, 1H), 12.35 (s, 1H); ^{13}C NMR (100.6 MHz, DMSO-*d*6) δ 27.0 (CH₃), 103.5 (CH), 111.4 (C), 113.6 (C), 132.6 (CH), 159.9 (CH), 162.1 (C), 202.1 (C); m/z 185 [M + H]⁺; IR: ν = 3257, 1608 cm⁻¹.

1-(2,4-Bis(benzyloxy)-5-chlorophenyl)ethanone (**41**).

Benzyl bromide (17.5 mL, 0.147 mol) was added to a mixture of 1-(5-chloro-2,4-dihydroxyphenyl)ethanone **40** (11 g, 0.059 mol) and potassium carbonate (20.34 g, 0.147 mol) in acetonitrile (180 mL). The mixture was heated at reflux for 6 h and then allowed to cool to ambient temperature and stirred overnight. The mixture was filtered, and the solids were washed with dichloromethane (3 × 50 mL). The combined organic filtrates were evaporated in vacuo to leave a pale-yellow solid, which was triturated with a mixture of hexane (175 mL)/EtOAc (7.5 mL) and filtered to give the title compound **41** (20.4 g) as an off-white solid.

Yield 58%. ^1H NMR (400 MHz, DMSO) δ 2.55 (s, 3H), 5.06 (s, 2H), 5.13 (s, 2H), 6.55 (s, 1H), 7.3-7.4 (m, 10H), 7.90 (s, 1H); IR: ν = 3035, 1660 cm⁻¹.

4-(2,4-Bis(benzyloxy)-5-chlorophenyl)-2-hydroxy-4-oxobut-2-enoic Acid Ethyl Ester (42).

Sodium metal (1.35 g, 58 mmol) was cut into small pieces, washed with hexane to remove mineral oil, and added to anhydrous EtOH (100 mL) under a nitrogen atmosphere over a period of 20 min. The reaction mixture was stirred for a further 10 min until all sodium had reacted. Compound **41** (10 g, 27.26 mmol) was added in portions over 5 min, and the resulting suspension was then stirred for a further 5 min. Diethyl oxalate (6 mL, 43 mmol) was added, resulting in a thicker yellow-colored precipitate. The reaction mixture was heated to reflux for 4 h, affording a dark-colored homogeneous solution, which, upon cooling, produced a solid mass to which acetic acid (6 mL) was added. The mixture was triturated to afford a yellow solid, which was filtered, washed sequentially with water, EtOH, and diethyl ether, and then dried in vacuo to afford the title compound **42** (12.4 g) as a yellow solid.

Yield 98%. ¹H NMR (400 MHz, CDCl₃) δ, 1.29 (t, 3H, *J* = 7.0 Hz), 4.28 (q, 2H, *J* = 7.0 Hz), 5.11 (s, 2H), 5.17 (s, 2H), 6.58 (s, 1H), 7.33–7.42 (m, 10H), 8.01 (s, 1H), 15.34 (brs, 1H).

5-(2,4-Bis(benzyloxy)-5-chlorophenyl)isoxazole-3-carboxylic Acid Ethyl Ester (43).

4-(2,4-Bis(benzyloxy)-5-chlorophenyl)-2-hydroxy-4-oxobut-2-enoic acid ethyl ester **42** (5.0 g, 10.7 mmol) was suspended in EtOH (100 mL), and hydroxylamine hydrochloride (0.89 g, 12.8 mmol) was added. The reaction mixture was heated to reflux for 3.5 h and then allowed to cool to ambient temperature. The resulting suspension was filtered, washed sequentially with EtOH (2 × 10 mL), water (2 × 10 mL), and EtOH (2 × 20 mL), and dried in vacuo to afford the title compound **43** (3.97 g) as a flocculent light-yellow solid.

Yield 80%. ¹H NMR (400 MHz, CDCl₃) δ 1.40 (s, 3H, *J* = 7.1 Hz), 4.42 (q, 2H, *J* = 7.1 Hz), 5.13 (s, 2H), 5.15 (s, 2H), 6.62 (s, 1H), 7.01 (s, 1H), 7.30-7.43 (m, 10H), 8.80 (s, 1H).

Generale procedure for preparation of 3-isoxazole fluoro amide 44b,c.

A mixture of ethyl 5-(2,4-bis(benzyloxy)-5-chlorophenyl)isoxazole-3-carboxylate **45** (200 mg, 0.43 mmol), methanol (10 mL), water (6-7 mL), and lithium hydroxide (16 mg, 0.65 mmol) was allowed to stand at 50-60 °C for 24 h. The solution was concentrated under vacuo to remove methanol, and the remaining aqueous solution was extracted with Et₂O (2 x 15 mL) to remove traces of unreacted starting material. The aqueous solution was

acidified with 1 M HCl and extracted with AcOEt (3 x 20 mL). The combined organic extracts were washed with saturated aqueous sodium chloride and dried over sodium sulfate. Removal of the solvent under reduced pressure afforded a residue, which was chromatographed on silica gel (DCM/methanol: 9/1).

5-[2,4-Bis(benzyloxy)-5-chlorophenyl]-isoxazole-3-carboxylic acid (46).

A solution of 5-[2,4-Bis(benzyloxy)-5-chlorophenyl]-isoxazole-3-carboxylic acid **46** in thionyl chloride was heated at 80 °C for 4h. The excess of thionyl chloride was removed under reduced pressure at room temperature, the residue obtained was diluted with DCM (10 mL) and the opportune amine fluorinate was added. To the mixture was cooled at 0 °C and TEA was added dropwise, the resulting solution was stirred at room temperature for 4h. The reaction was diluted with DCM (15 mL) and washed with 5% HCl (10 mL) and brine (10 mL). After evaporation of solvent in vacuo the crude residue was purified by flash chromatography on silica gel.

Yield 85%. White solid. ¹H NMR (200 MHz CDCl₃): 5.34 (s, 2H), 5.38 (s, 2H), 6.91, (s, 1H), 7.36-7.51 (m, 11H), 7.90 (s, 1H), 13.95, (br, 1H); *m/z* 436.2/438.4 [M+H]⁺.

5-[2,4-Bis-(benzyloxy)-5-chlorophenyl]-N-(2,2,2-trifluoroethyl)-isoxazole-3-carboxamide (44b). Yield 55%. White solid. ¹H NMR (400 MHz CDCl₃): 4.08-4.12 (m, 2H), 5.12 (s, 2H), 5.16 (s, 2H), 6.61, (s, 1H), 7.10-7.12 (m, 2H), 7.33-7.40 (m, 10H), 7.98 (s, 1H); *m/z* 517.5/519.3 [M+H]⁺.

5-(2,4-Bis-(benzyloxy)-5-chlorophenyl)-isoxazol-3-yl(3,3-difluoroazetid-1-yl)-methanone (44c). Yield 63%. White solid. ¹H NMR (200 MHz CDCl₃): 4.46-4.59 (m, 2H), 4.84-4.97 (m, 2H), 5.11 (s, 2H), 5.15 (s, 2H), 6.60, (s, 1H), 7.09 (s, 2H), 7.35-7.41 (m, 10H), 7.97 (s, 1H); *m/z* 511.4/513.5. [M+H]⁺.

Synthesis of isopropyl-resorcinol derivatives

1-(2,4-Bis(benzyloxyphenyl)ethanone (48).

Potassium carbonate (20.34 g, 0.147 mol) was added to a solution of 2,4-dihydroxyacetophenone **47** (9 g, 0.059 mol) in acetonitrile (180 mL), and the suspension was stirred at room temperature. Benzyl bromide (17.5 mL, 0.147 mol) was added dropwise over 10 min and the mixture heated at reflux for 6 h. The mixture was cooled, the

solvents were evaporated in vacuo to afford a slurry, which was partitioned between water (250 mL) and DCM (3 x 50 mL), and the phases were separated. The aqueous layer was further extracted with dichloromethane (250 mL), and the organic extracts were combined, dried over Na₂SO₄, and evaporated in vacuo. The product was triturated with hexane/AcOEt (175/7.5 mL), filtered, washed with cold hexane, and dried in vacuo to give the title compound **48** (18.4 g), as a white powder.

Yield 94%. ¹H NMR (400 MHz, CDCl₃) δ 2.55 (s, 3H), 5.08 (s, 2H), 5.11 (s, 2H), 6.63–6.60 (m, 2H), 7.44–7.35 (m, 10H), 7.85 (d, 1H, *J* = 9.3 Hz); *m/z* 333[M + H]⁺.

2,4-Bis(benzyloxy)-1-isopropenylbenzene (49).

To a suspension of methyltriphenylphosphonium bromide (27.5 g, 0.077 mol) and 1-(2,4-bis(benzyloxy)phenyl)ethanone **48** (18.4 g, 0.059 mol) in PhMe (100 mL) was added NaH portion wise. When the addition was complete, the mixture was heated at 100°C for 3 h under a nitrogen atmosphere. The mixture was allowed to cool to room temperature and MeOH (20 mL) was added. The mixture was filtered through a pad of Celite, the filtered was washed with H₂O (50 mL x 2), dried over Na₂SO₄ and the resulting solution was evaporated in vacuo. Hexane was added to the resulting oil, and the mixture was heated to reflux at 60°C for 30 min, then filtered and evaporated in vacuo to give a colorless oil **49** (16 g).

Yield 82%. ¹H NMR (400 MHz, CDCl₃) δ 2.12 (s, 3H), 5.03 (s, 2H), 5.05 (s, 2H), 5.07 (brs, 2H), 6.54 (dd, 1H, *J* = 8.3 Hz, 2.5 Hz), 6.59 (d, 1H, *J* = 2.5 Hz), 7.14 (d, 1H, *J* = 8.3 Hz), 7.29–7.44 (m, 10H); *m/z* 331 [M+H]⁺.

4-Isopropylbenzene-1,3-diol (50).

Compound **49** (37.15 g, 0.113 mol) was dissolved in EtOH (300 mL) and carefully added to 10% palladium on carbon, which had been pre-wetted with water under a nitrogen atmosphere. Hydrogen was introduced to the flask, and the mixture was allowed to shake under a positive hydrogen atmosphere for 16 h. The catalyst was filtered from the reaction mixture, and the filtrate solvents were removed in vacuo to give the title compound **50** (12.05 g) as a white crystalline solid.

Yield 70%. ^1H NMR (400 MHz, CDCl_3) δ 1.22 (d, 6H, $J = 7.1$ Hz), 3.09 (sept, 1H, $J = 7.1$ Hz), 4.63 (brs, 1H), 4.74 (brs, 1H), 6.29 (d, 1H, $J = 2.5$ Hz), 6.38 (dd, 1H, $J = 8.3, 2.5$ Hz), 7.03 (d, 1H, $J = 8.3$ Hz); m/z 153.1 $[\text{M} + \text{H}]^+$;

1-(2,4-Dihydroxy-5-isopropylphenyl)ethanone (51).

4-Isopropylbenzene-1,3-diol **50** (12.05 g, 0.079 mol) was dissolved in $\text{BF}_3 \cdot \text{OEt}_2$ (60 mL, 0.486 mol) and acetic acid (9 mL, 0.157 mol) was added. The solution was heated for 16 h at 90 °C, allowed to cool to room temperature, added dropwise to 10% $\text{NaOAc}(\text{aq})$ solution (200 mL), and allowed to stand for 2.5 h before being extracted with EtOAc (2×400 mL). The organic phases were combined and washed with saturated $\text{NaHCO}_3(\text{aq})$, dried over Na_2SO_4 and filtered, and the filtrate solvents were removed in vacuo. The residual oil was triturated with cold hexane to afford the title compound **51** (13.57 g) as an off-white solid.

Yield 88%. ^1H NMR (400 MHz, CDCl_3) δ 1.25 (d, 6H, $J = 6.8$ Hz), 2.57 (s, 3H), 3.13 (sept, 1H, $J = 6.8$ Hz), 5.64 (s, 1H), 6.30 (s, 1H), 7.50 (s, 1H), 12.56 (s, 1H); m/z 195.1 $[\text{M} + \text{H}]^+$.

1-(2,4-Bis(benzyloxy)-5-isopropylphenyl)ethanone (52).

1-(2,4-Dihydroxy-5-isopropylphenyl)ethanone **51** (13.57 g, 0.070 mol) was dissolved in CH_3CN (120 mL), and potassium carbonate (21.27 g, 0.154 mol) and benzyl bromide (18.3 mL, 0.154 mol) were added. The resulting suspension was heated under a nitrogen atmosphere for 16 h. The solution was cooled to room temperature with stirring overnight, and the solvent was removed in vacuo. The mixture was poured into H_2O (1000 mL) and then extracted with DCM (2×300 mL). The organic phases were combined and washed with saturated $\text{NaCl}(\text{aq})$ solution (3×300 mL), dried over Na_2SO_4 and filtered. The filtrate solvents were removed in vacuo to give a solid, which was purified by trituration with diethyl ether/hexane (1:1) to give the title compound **52** (23.10 g) as a colorless solid.

Yield 88%. ^1H NMR (400 MHz, CDCl_3) δ 1.22 (d, 6H, $J = 6.9$ Hz), 2.56 (s, 3H), 3.28 (sept, 1H, $J = 6.9$ Hz), 5.08 (s, 2H), 5.10 (s, 2H), 6.51 (s, 1H), 7.31–7.44 (m, 10H), 7.76 (s, 1H); m/z 375.2 $[\text{M} + \text{H}]^+$;

4-(2,4-Bis(benzyloxy)-5-isopropylphenyl)-2-hydroxy-4-oxobut-2-enoic Acid Ethyl Ester (53).

Sodium metal (1.2 g, 0.052 mol) was cut into small pieces, washed with hexane to remove mineral oil, and added to anhydrous EtOH (100 mL) under a nitrogen atmosphere over a period of 20 min. The reaction mixture was stirred for a further 10 min until all sodium had reacted. Compound **52** (9.2 g, 0.026 mol) was added in portions over 5 min, and the resulting suspension was then stirred for a further 5 min, then diethyl oxalate (6 mL, 43 mmol) was added. The reaction mixture was heated to reflux for 4 h, then was allowed to cool to room temperature and acetic acid (6 mL) was added. The mixture was stirred for 1 h. The solvent was removed in vacuo and the resulting gum was triturated with hexane to afford a yellow solid, which was filtered to afford the title compound **53** (12.4 g) as a yellow solid.

Yield 98%. ¹H NMR (400 MHz, CDCl₃) δ 1.23 (d, 6H, *J* = 6.8 Hz), 1.28 (t, 3H, *J* = 7.1 Hz), 3.29 (sept, 1H, *J* = 6.8 Hz), 4.28 (q, 2H, *J* = 7.1 Hz), 5.11 (s, 2H), 5.14 (s, 2H), 6.53 (s, 1H), 7.32–7.46 (m, 11H), 7.87 (s, 1H); *m/z* 475 [M + H]⁺.

5-(2,4-Bis(benzyloxy)-5-isopropylphenyl)isoxazole-3-carboxylic Acid Ethyl Ester (54).

Compound **53** (14.94 g, 31.5 mmol) was dissolved in EtOH (150 mL), hydroxylamine hydrochloride (2.63 g, 37.8 mmol) was added, and the solution was heated to reflux for 4 h under a nitrogen atmosphere. The reaction mixture was cooled to room temperature. The precipitate was triturated with an EtOH/water mix, filtered, and dried to afford the title compound **54** (13.5 g) as a yellow solid.

Yield 91%. ¹H NMR (400 MHz, CDCl₃) δ 1.26 (d, 6H, *J* = 6.8 Hz), 1.41 (t, 3H, *J* = 7.1 Hz), 3.34 (sept, 1H, *J* = 6.8 Hz), 4.42 (q, 2H, *J* = 7.1 Hz), 5.07 (s, 2H), 5.16 (s, 2H), 6.57 (s, 1H), 7.00 (s, 1H), 7.32–7.43 (m, 10H), 7.83 (s, 1H); *m/z* 472 [M + H]⁺.

Generale procedure for preparation of 3-isoxazole ethylamide 44a,d.

The appropriate ester derivative (13.57 g, 28.8 mmol) was suspended in ethylamine in MeOH solution (2.0 M, 140 mL, 280 mmol) and heated to 90 °C for 1 h to afford a homogeneous solution. The solution was allowed to cool to room temperature, and a colorless solid precipitated. The solid was collected by filtration, washed with cold MeOH, and dried in vacuo as a colorless solid.

5-(2,4-Bis(benzyloxy)-5-chlorophenyl)isoxazole-3-carboxylic Acid Ethylamide (44a).

Yield 85%. ¹H NMR (400 MHz, CDCl₃) δ 1.25 (s, 3H, *J* = 7.4 Hz), 3.47 (dq, 2H, *J* = 7.3, 5.2 Hz), 5.10 (s, 2H), 5.16 (s, 2H), 6.59 (s, 1H), 6.82 (brt, 1H, *J* = 5.2 Hz) 7.08 (s, 1H), 7.30-7.43 (m, 10H), 7.96 (s, 1H).

5-(2,4-Bis(benzyloxy)-5-isopropylphenyl)isoxazole-3-carboxylic Acid Ethylamide

(44d). Yield 83%. ¹H NMR (400 MHz, CDCl₃) δ 1.25 (d, 6H, *J* = 6.8 Hz), 1.26 (t, 3H, *J* = 7.0 Hz), 3.33 (sept, 1H, *J* = 6.9 Hz), 3.49 (m, 2H), 5.03 (s, 2H), 5.17 (s, 2H), 6.55 (s, 1H), 6.81 (brt, 1H, *J* = 5.7 Hz), 7.07 (s, 1H), 7.30-7.42 (m, 10H), 7.78 (s, 1H).

Generale procedure for preparation of 4-nitroisoxazole 55a-d.

A suspension of adequate isoxazole derivative **44a-d** (2.2 mmol) in Ac₂O (20 mL) was cooled to 0 °C, and concentrated HNO₃ (0.26 mL, 4.3 mmol) was added dropwise under stirring, the temperature being maintained between 0 and 5 °C. After the addition was complete, the mixture was stirred for 70 h at 5–10 °C and then poured into ice and extracted with DCM (3 × 40 mL). The extract was dried and concentrated under vacuo. The yellow solid obtained was triturated with Et₂O and filtered to give the desired nitro compound **55a-d**.

5-[2,4-Bis(benzyloxy)-5-chlorophenyl]-4-nitroisoxazole-3-carboxylic Acid Ethylamide

(55a). Yield 73%. Yellow solid. ¹H NMR (200 MHz CDCl₃) δ: 1.26 (t, *J* = 7.4 Hz, 3H), 3.46–3.55 (m, 2H), 5.0 (s, 2H), 5.10 (s, 2H), 6.57 (m, 2H), 7.23–7.29 (m, 2H), 7.32–7.37 (m, 8H), 7.66 (s, 1H). *m/z* 508.5/510.4 [M + H]⁺.

5-[2,4-Bis(benzyloxy)-5-chlorophenyl]-N-(2,2,2-trifluoroethyl)-4-nitroisoxazole-3-

carboxamide (55b). Yellow solid. ¹H NMR (400 MHz CDCl₃) δ: 4.07–4.15 (m, 2H), 5.01 (s, 2H), 5.10 (s, 2H), 6.59, (s, 1H), 6.93, (br, 1H), 7.22–7.27 (m, 2H), 7.32–7.40 (m, 8H), 7.68 (s, 1H). *m/z* 562.5/564.4 [M + H]⁺.

5-[2,4-Bis(benzyloxy)-5-chlorophenyl]-4-nitroisoxazol-3-yl)-(3,3-difluoroazetid-1-

yl)methanone (55c). Yellow solid. ¹H NMR (400 MHz CDCl₃) δ: 4.52–4.58 (m, 4H), 4.99 (s, 2H), 5.14 (s, 2H), 6.62, (s, 1H), 7.25–7.27, (m, 2H), 7.35–7.41 (m, 8H), 7.66 (s, 1H). *m/z* 556.5/558.4 [M + H]⁺.

5-[2,4-Bis(benzyloxy)-5-isopropylphenyl]-4-nitroisoxazole-3-carboxylic Acid

Ethylamide (55d). Yellow solid. ¹H NMR (200 MHz CDCl₃) δ : 1.22–1.26 (m, 9H), 3.24–3.38 (m, 1H), 3.43–3.57 (m, 2H), 5.02 (s, 4H), 6.54 (s, 1H), 6.59 (br, 1H), 7.30–7.39 (m, 10H), 7.46 (s, 1H). *m/z* 516.5 [M + H]⁺.

General procedure to obtain the 4-aminoisoxazoles 56a-d.

A solution of the appropriate nitro derivative **55a-d** (1.97 mmol) in THF (7 mL) was added to a solution of NH₄Cl (2.7 g, 50 mmol) in water (15 mL). Zinc dust (4 g, 61 mmol) was then added portionwise over 15 min with stirring at 0 °C. After 30 min at 0 °C, the mixture was filtered and the resulting cake was rinsed with MeOH. The combined filtrate was evaporated in vacuo to give the desired amino compounds **56a-d**.

4-Amino-5-[2,4-bis(benzyloxy)-5-chlorophenyl]isoxazole-3-carboxylic Acid

Ethylamide (56a). Yield 82%. Yellow solid. ¹H NMR (200 MHz CDCl₃) δ : 1.24 (t, *J* = 7.2 Hz, 3H), 3.38–3.53 (m, 2H), 5.02 (s, 2H), 5.15 (s, 2H), 6.64 (s, 1H), 6.79 (br, 1H), 7.35–7.42 (m, 10H), 7.64 (s, 1H). *m/z* 478.3/480.4 [M + H]⁺.

5-[2,4-Bis(benzyloxy)-5-chlorophenyl]-4-amino-N-(2,2,2-trifluoroethyl)isoxazole-3-

carboxamide (56b). Yield 77%. Yellow solid. ¹H NMR (200 MHz CDCl₃) δ : 3.97–4.14 (m, 2H), 4.35 (br, 2H), 5.04 (s, 2H), 5.16 (s, 2H), 6.65 (s, 1H), 7.08 (br, 1H), 7.31–7.44 (m, 10H), 7.65 (s, 1H). *m/z* 532.3/534.3 [M + H]⁺.

5-[2,4-Bis(benzyloxy)-5-chlorophenyl]-4-aminoisoxazol-3-yl)-(3,3-difluoroazetid-1-

yl)methanone (56c). Yield 65%. Yellow solid. ¹H NMR (200 MHz CDCl₃) δ : 4.43–4.55 (m, 4H), 4.83–4.95 (m, 2H), 5.03 (s, 2H), 5.15 (s, 2H), 6.64 (s, 1H), 7.29–7.43 (m, 10H), 7.64 (s, 1H). *m/z* 526.4/528.5 [M + H]⁺.

4-Amino-5-[2,4-bis(benzyloxy)-5-isopropylphenyl]-isoxazole-3-carboxylic Acid

Ethylamide (56d). Yield 72%. Yellow solid. ¹H NMR (200 MHz CDCl₃) δ : 1.21–1.28 (m, 9H), 3.28–3.38 (m, 1H), 3.39–3.53 (m, 2H), 4.38 (br, 2H), 5.05 (s, 2H), 5.08 (s, 2H), 6.61 (s, 1H), 6.83 (br, 1H), 7.33–7.42 (m, 10H), 7.45 (s, 1H). *m/z* 486.6 [M + H]⁺.

General procedure for preparation of 4-isoxazole amides 57-115.

A solution of the appropriate amine **56a–d** (1.45 mmol) and TEA (1.74 mmol, 0.24 mL) in DCM was added dropwise to a solution of the corresponding acyl chloride (1.45 mmol). The mixture was stirred for 5 h, diluted with DCM, and washed with 1 N HCl. The organic extract was dried and filtered. Solvents were removed in vacuo to give the crude residue that was used without further purification. The amide thus obtained (0.35 mmol) was dissolved in DCM (10 mL) and was cooled under an inert atmosphere at 0 °C, and BCl₃ 1M in DCM (1.05 mmol, 1.05 mL) was added dropwise. The mixture was stirred at 0 °C for 20 min. The cooling bath was then removed and the mixture left for a further 50 min at room temperature. The mixture was cooled again and then quenched by cautious addition of saturated aqueous NaHCO₃ solution (20 mL). The DCM was removed in vacuo, and water (20 mL) was added. The mixture was then extracted with EtOAc (200 mL). The organic layers were washed with water (2 × 30 mL), saturated aqueous NaCl solution (50 mL) and then dried over Na₂SO₄. Crude products were purified by flash chromatography on silica gel (yield, 35–60%).

4-(4-Bromobenzoylamino)-5-(5-chloro-2,4-dihydroxyphenyl)isoxazole-3-carboxylic acid ethylamide (57). Yellow solid. ¹H NMR (200 MHz CD₃OD) δ: 1.22 (t, *J* = 7.4 Hz, 3H), 3.33-3.41 (m, 2H), 6.54 (s, 1H), 7.49 (s, 1H), 7.67 (d, *J* = 8.8 Hz, 2H), 7.80 (d, *J* = 8.8 Hz, 2H), 10.81 (br, 1H); *m/z* 480.1/482.2/483.5 [M+H]⁺. Anal. (C₁₉H₁₅BrClN₃O₅) C, H, Cl, N.

5-(5-Chloro-2,4-dihydroxy-phenyl)-4-(4-methoxybenzoylamino)isoxazole-3-carboxylic acid ethylamide (58). Light-yellow solid. ¹H NMR (400 MHz) δ: 1.06 (t, *J* = 6.8 Hz, 3H), 3.19-3.24 (m, 3H), 3.82 (s, 3H), 6.64 (s, 1H), 7.04 (d, *J* = 8.8 Hz, 2H), 7.43 (s, 1H), 7.87 (d, *J* = 8.8 Hz, 2H), 8.71 (t, *J* = 5.6 Hz, 1H), 9.62 (s, 1H), 10.48 (br, 1H), 10.68 (s, 1H). *m/z* 432.1/434.1 [M+H]⁺. Anal. (C₂₀H₁₈ClN₃O₆) C, H, Cl, N.

5-(5-Chloro-2,4-dihydroxyphenyl)-4-(3,4-dimethoxybenzoylamino)isoxazole-3-carboxylic acid ethylamide (59). White solid. ¹H NMR (400 MHz) δ: 1.06 (t, *J* = 6.8 Hz, 3H), 3.18-3.22 (m, 3H), 3.79 (s, 3H), 3.81 (s, 3H), 6.63 (s, 1H), 7.05 (d, *J* = 8.8 Hz, 1H), 7.41 (s, 1H), 7.43 (d, *J* = 1.6 Hz, 1H), 7.52 (dd, *J* = 8.8 Hz, *J* = 1.6 Hz, 1H), 8.69 (t, *J* = 6.0 Hz, 1H), 9.59 (s, 1H), 10.44 (br, 1H), 10.66 (s, 1H); *m/z* 462.4/464.5 [M+H]⁺. Anal. (C₂₁H₂₀ClN₃O₇) C, H, Cl, N.

5-(5-Chloro-2,4-dihydroxyphenyl)-4-(3,4,5-trimethoxybenzoylamino)isoxazole-3-carboxylic acid ethylamide (60).

White solid. ^1H NMR (400 MHz) δ : 1.08 (t, $J = 6.8$ Hz, 3H), 3.19-3.23 (m, 2H), 3.71 (s, 3H), 3.83 (s, 6H), 6.64 (s, 1H), 7.23 (s, 2H), 7.43 (s, 1H), 8.72 (t, $J = 5.6$ Hz, 1H), 9.70 (br, 1H), 10.45 (s, 1H), 10.70 (s, 1H); m/z 492.4/494.4 $[\text{M}+\text{H}]^+$. Anal. ($\text{C}_{22}\text{H}_{22}\text{ClN}_3\text{O}_8$) C, H, Cl, N.

5-(5-Chloro-2,4-dihydroxyphenyl)-4-[(3-methylthiophene-2-carbonyl)amino]

isoxazole-3-carboxylic Acid Ethylamide (61). Light-yellow solid. ^1H NMR (400 MHz) δ : 1.09 (t, $J = 6.8$ Hz, 3H), 2.43 (s, 3H), 3.20-3.2 (m, 2H), 6.65 (s, 1H), 7.01 (d, $J = 5.2$ Hz, 1H), 7.44 (s, 1H), 7.66 (d, $J = 5.2$ Hz, 1H), 8.58 (t, $J = 5.6$ Hz, 1H), 9.29 (br, 1H), 10.70 (s, 2H). m/z 422.1/424.1 $[\text{M} + \text{H}]^+$. Anal. ($\text{C}_{18}\text{H}_{16}\text{ClN}_3\text{O}_5\text{S}$) C, H, Cl, N, S.

4-Acetylamino-5-(5-chloro-2,4-dihydroxyphenyl)isoxazole-3-carboxylic acid

ethylamide (62). White solid. ^1H NMR (400 MHz, CD_3OD) δ : 1.21 (t, $J = 6.8$ Hz, 3H), 2.07 (s, 3H), 3.39 (q, $J = 6.8$ Hz, 2H), 6.55 (s, 1H), 7.40 (s, 1H); m/z 340.0/341.9 $[\text{M}+\text{H}]^+$. Anal. ($\text{C}_{14}\text{H}_{14}\text{ClN}_3\text{O}_5$) C, H, Cl, N.

5-(5-Chloro-2,4-dihydroxyphenyl)-4-(2,2-dimethylpropionylamino)isoxazole-3-

carboxylic Acid Ethylamide (63). White solid. ^1H NMR (400 MHz) δ : 1.06 (t, $J = 7.2$ Hz, 3H) 1.14 (s, 9H), 3.19-3.24 (m, 2H), 6.66 (s, 1H), 7.34 (s, 1H), 8.58 (t, $J = 5.6$ Hz, 1H), 8.83 (s, 1H), 10.50 (br, 1H), 10.70 (s, 1H). m/z 382.2/384.2 $[\text{M} + \text{H}]^+$. Anal. ($\text{C}_{17}\text{H}_{20}\text{ClN}_3\text{O}_5$) C, H, Cl, N.

4-Acryloylamino-5-(5-chloro-2,4-dihydroxyphenyl)isoxazole-3-carboxylic acid

ethylamide (64). White solid. ^1H NMR (400 MHz, CD_3OD) δ : 1.22 (t, $J = 7.6$ Hz, 3H) 3.23-3.41 (m, 2H), 5.76 (dd, $J = 10.4$ Hz, $J = 1.6$ Hz, 1H), 6.26 (dd, $J = 16.8$ Hz, $J = 1.6$ Hz, 1H), 6.39 (dd, $J = 16.8$ Hz, $J = 10.4$ Hz, 1H), 6.56 (s, 1H), 7.42 (s, 1H); m/z 352.1/354.6. $[\text{M}+\text{H}]^+$. Anal. ($\text{C}_{15}\text{H}_{14}\text{ClN}_3\text{O}_5$) C, H, Cl, N.

4-[(Adamantane-1-carbonyl)amino]-5-(5-chloro-2,4-dihydroxyphenyl)isoxazole-3-

carboxylic Acid Ethylamide (65). White solid. ^1H NMR (400 MHz) δ : 1.09 (t, $J = 7.2$ Hz, 3H), 1.65-1.69 (m, 6H), 1.81-1.82 (m, 6H), 1.99 (s, 3H), 3.18-3.24 (m, 2H), 6.67 (s, 1H), 7.34 (s, 1H), 8.74 (t, $J = 5.6$ Hz, 1H), 10.55 (br, 2H). m/z 460.2/462.3 $[\text{M} + \text{H}]^+$. Anal. ($\text{C}_{23}\text{H}_{26}\text{ClN}_3\text{O}_5$) C, H, Cl, N.

4-(4-Methoxybenzamido)-5-(5-chloro-2,4-dihydroxyphenyl)-N-(2,2,2-trifluoroethyl) isoxazole-3-carboxamide (66). White solid. ¹H NMR (400 MHz) δ : 3.82 (s, 3H), 3.99-4.04 (m, 2H), 6.62 (s, 1H), 7.02 (d, $J = 8.8$ Hz, 2H), 7.43 (s, 1H), 7.86 (d, $J = 8.8$ Hz, 2H), 9.36-9.39 (m, 1H), 9.80 (br, 1H), 10.66 (br, 2H); m/z 486.3/488.1 [M+H]⁺. Anal. (C₂₀H₁₅ClF₃N₃O₆) C, H, Cl, N.

4-(4-Methoxybenzamido)-5-(5-chloro-2,4-dihydroxyphenyl)isoxazol-3-yl-(3,3-difluoroazetid-1-yl)methanone (67). White solid. ¹H NMR (400 MHz), δ : 3.82 (s, 3H), 4.46-4.52 (m, 2H), 4.74- 4.80 (m, 2H), 6.66 (s, 1H), 7.02 (d, $J = 8.8$ Hz, 2H), 7.47 (s, 1H), 7.86 (d, $J = 8.8$ Hz, 2H), 9.88 (br, 1H), 10.72 (br, 1H), 10.66 (br, 2H); m/z 480.1/482.2 [M+H]⁺. Anal. (C₂₁H₁₆ClF₂N₃O₆) C, H, Cl, N.

4-Acetylamino-5-(2,4-dihydroxy-5-isopropylphenyl)-isoxazole-3-carboxylic Acid Ethylamide (68). White solid. ¹H NMR (400 MHz) δ : 1.07–1.12 (m, 9H), 3.06–3.13 (m, 1H), 3.21-3.26 (m, 2H), 6.49 (s, 1H), 7.11 (s, 1H), 8.55 (t, $J = 6.0$ Hz, 1H), 9.15 (br, 1H), 9.81 (s, 1H), 9.90 (br, 1H). m/z 348.5 [M + H]⁺. Anal. (C₁₇H₂₁N₃O₅) C, H, N.

5-(2,4-Dihydroxy-5-isopropylphenyl)-4-(2,2-dimethylpropionylamino)isoxazole-3-carboxylic Acid Ethylamide (69). White solid. ¹H NMR (400 MHz CD₃OD) δ : 1.18-1.24 (m, 18H), 3.17–3.24 (m, 1H), 3.48 (q, $J = 6.8$ Hz, 2H), 6.47 (s, 1H), 7.27 (s, 1H). m/z 390.5 [M + H]⁺. Anal. (C₂₀H₂₇N₃O₅) C, H, N.

4-(Cyclohexanecarbonylamino)-5-(2,4-dihydroxy-5-isopropylphenyl)isoxazole-3-carboxylic Acid Ethylamide (70). ¹H NMR (300 MHz) δ : 1.06 (t, $J = 5.1$ Hz, 3H), 1.08 (d, $J = 7.2$ Hz, 6H), 1.10–1.36 (m, 5H), 1.57-1.77 (m, 5H), 2.23 (m, 1H), 3.06 (m, 1H), 3.19 (m, 2H), 6.47 (s, 1H), 7.09 (s, 1H), 8.46 (t, $J = 6.3$ Hz, NH), 8.97 (s, OH), 9.77 (s, NH), 9.89 (s, OH). m/z 438.0 [M + Na]⁺. Anal. (C₂₂H₂₉N₃O₅) C, H, N.

5-(2,4-Dihydroxy-5-isopropylphenyl)-4-[(*trans*-4-pentylcyclohexanecarbonyl)amino]isoxazole-3-carboxylic acid ethylamide (71). ¹H NMR (300 MHz) δ : 0.87-1.02 (m, 5H), 1.18-1.51 (m, 20H), 1.82-1.86 (m, 2H), 1.94-1.97 (m, 2H), 2.25 (m, 1H), 3.19 (m, 1H), 3.37 (m, 2H), 6.44 (s, 1H), 7.24 (s, 1H); m/z 486.3 [M+H]⁺. Anal. (C₂₇H₃₉N₃O₅) C, H, N.

5-(2,4-Dihydroxy-5-isopropylphenyl)-4-[(4-trifluoromethylcyclohexanecarbonyl)amino]isoxazole-3-carboxylic acid ethylamide (72). ¹H NMR (300 MHz) δ : 1.22 (t, $J = 5.2$ Hz, 3H), 1.19 (d, $J = 7.1$ Hz, 6H), 1.65-1.75 (m, 6H), 2.09-2.13 (m, 3H), 2.64 (m, 1H), 3.19 (m, 1H), 3.37 (m, 2H), 6.44 (s, 1H), 7.24 (s, 1H); m/z 484.2 [M+H]⁺. Anal. (C₂₃H₂₈F₃N₃O₅) C, H, N.

5-(2,4-Dihydroxy-5-isopropylphenyl)-4-[(*cis*-4-methoxycyclohexanecarbonyl)amino]isoxazole-3-carboxylic Acid Ethylamide (73). ¹H NMR (300 MHz) δ : 1.07 (t, $J = 5.2$ Hz, 3H), 1.09 (d, $J = 7.3$ Hz, 6H), 1.37 (m, 2H), 1.49 (m, 2H), 1.61 (m, 2H), 1.80 (m, 2H), 2.26 (m, 1H), 3.06 (m, 1H), 3.14 (s, 3H), 3.16 (m, 2H), 3.29 (bs, 1H), 6.47 (s, 1H), 7.09 (s, 1H), 8.47 (t, $J = 6.2$ Hz, 1H), 8.9 (s, 1H), 9.76 (s, 1H), 9.85 (s, 1H). m/z 468.3 [M + Na]⁺. Anal. (C₂₃H₃₁N₃O₆) C, H, N.

4-[(4-*tert*-Butylcyclohexanecarbonyl)amino]-5-(2,4-dihydroxy-5-isopropylphenyl)isoxazole-3-carboxylic acid ethylamide (74). Obtained as mixture *cis:trans* ¹H NMR (300 MHz) δ : 0.73 (s, 6H), 0.8 (s, 3H), 0.93 (m, 2H), 1.07 (t, $J = 5.1$ Hz, 3H), 1.09 (d, $J = 7.3$ Hz, 6H), 1.18-1.41 (m, 4H), 1.73-1.89 (m, 2H), 2.05 (m, 2H), 3.06 (m, 1H), 3.21 (m, 2H), 6.46 (s, 1H), 6.47 (s, 1H), 7.09 (s, 1H), 7.11 (s, H), 8.48 (t, $J = 6.1$ Hz , NH), 9.76 (s, NH); m/z 472.3 [M+H]⁺. Anal. (C₂₆H₃₇N₃O₅) C, H, N.

4-[(*trans*-4-Aminocyclohexanecarbonyl)amino]-5-(2,4-dihydroxy-5-isopropylphenyl)isoxazole-3-carboxylic acid ethylamide hydrochloride (75). The N-Fmoc-amine was deprotected with piperidine in DCM. Addition of HCl in dioxane gave the titled compound. ¹H NMR (300 MHz) δ : 1.19 (d, $J = 7.1$ Hz, 6H), 1.22 (t, $J = 5.0$ Hz, 3H), 1.43-1.83 (m, 4H), 2.06-2.12 (m, 3H), 3.14 (m, 2H), 3.19 (m, H), 3.38 (m, 2H), 4.4 (sb, 1H), 6.44 (s, 1H), 7.23 (s, H), 8.54 (t, $J = 6.1$ Hz , NH); m/z 431.2 [M+H]⁺. Anal. (C₂₂H₃₀N₄O₅ HCl) C, H, N.

4-[(*trans*-4-Aminomethylcyclohexanecarbonyl)amino]-5-(2,4-dihydroxy-5-isopropylphenyl)isoxazole-3-carboxylic acid ethylamide hydrochloride (76). The N-Fmocamine was deprotected as reported for compound **75**. Addition of HCl in dioxane gave the titled compound. ¹H NMR (300 MHz) δ : 1.19 (d, $J = 7.1$ Hz, 6H), 1.21 (m, 2H), 1.22 (t, $J = 5.0$ Hz, 3H), 1.49-1.57 (m, 3H), 1.91 (m, 2H), 2.03 (m, 2H), 2.33 (m, 1H), 2.79 (d, $J = 8.1$ Hz, 2H), 3.19 (m, 1H), 3.37 (m, 2H), 6.43 (s, 1H), 7.23 (s, 1H); m/z 445.2 [M+H]⁺. Anal. (C₂₃H₃₂N₄O₅ HCl) C, H, N.

5-(2,4-Dihydroxy-5-isopropylphenyl)-4-{*trans*-4-[(4-fluorobenzenesulfonylamino)methyl]cyclohexanecarbonyl}aminoisoxazole-3-carboxylic acid ethylamide (77).

¹H NMR (300 MHz) δ : 0.83 (m, 2H), 1.07 (t, $J = 7.3$ Hz, 3H), 1.08 (d, $J = 7.0$ Hz, 6H), 1.16-1.28 (m, 3H), 1.66-1.78 (m, 4H), 2.14 (m, 1H), 2.56 (t, $J = 6.4$ Hz, 2H), 3.05 (m, 1H), 3.18 (m, 2H), 6.46 (s, 1H), 7.07 (s, 1H), 7.41 (t, $J = 8.8$ Hz, 2H), 7.6 (t, $J = 6.4$ Hz, 1H), 7.82 (dd, $J = 5.2$ Hz, $J = 8.8$ Hz, 2H), 8.46 (t, $J = 5.8$ Hz, 1H), 9.0 (s, 1H), 9.77 (s, 1H), 9.9 (s, 1H); m/z 602.5 [M+H]⁺. Anal. (C₂₉H₃₅FN₄O₇S) C, H, N.

4-{[4-*trans*-(Benzenesulfonylamino)methyl]cyclohexanecarbonyl}amino}-5-(2,4-dihydroxy-5-isopropylphenyl)isoxazole-3-carboxylic acid ethylamide (78).

¹H-NMR (300 MHz) δ : 0.85-1.06 (m, 2H), 1.19 (d, $J = 6.9$ Hz, 6H), 1.21 (t, $J = 7.2$ Hz, 3H), 1.31-1.50 (m, 3H), 1.75-2.01 (m, 2H), 2.25 (tt, $J = 12.2$ Hz, $J = 3.3$ Hz, 1H), 2.69 (d, $J = 6.8$ Hz, 2H), 3.19 (hept, $J = 6.9$ Hz, 1H), 3.37 (quint., $J = 7.2$ Hz, 2H), 6.44 (s, 1H), 7.24 (s, 1H), 7.53-7.65 (m, 3H), 7.83-7.86 (m, 2H); m/z 583.0 [M-H]⁻. Anal. (C₂₉H₃₆N₄O₇S) C, H, N.

Amino-acetic acid 4-*trans*-[5-(2,4-dihydroxy-5-isopropylphenyl)-3-ethylcarbamoyl]isoxazol-4-ylcarbamoyl]cyclohexyl ester trifluoroacetate (79). The N-Fmoc-amine was deprotected as reported for compound **75**. Preparative HPLC purification with H₂O/CH₃CN (0.1% TFA) gave the titled compound. ¹H-NMR (300 MHz) δ : 0.86-0.94 (m, 2H), 1.24 (d, $J = 6.9$ Hz, 6H), 1.27 (t, $J = 7.3$ Hz, 3H), 1.26-1.41 (m, 2H), 1.71-1.79 (m, 3H), 1.94-2.04 (m, 2H), 3.34 (hept., $J = 7.0$ Hz, 1H), 3.47 (quint., $J = 7.3$ Hz, 2H), 3.78-3.82 (m, 1H), 4.65-4.81 (m, 2H), 6.61 (s, 1H), 7.10 (s, 1H), 8.31 (bs, 3H), 8.50 (t, $J = 5.5$ Hz, 1H), 9.05 (s, 1H), 9.90 (s, 1H), 10.0 (s, 1H); m/z 487.3 [M-H]⁻. Anal. (C₂₄H₃₂N₄O₇.CF₃COOH) C, H, N.

Cyclohexane-*trans*-1,4-dicarboxylic acid 1-amide 4-[[5-(2,4-dihydroxy-5-isopropylphenyl)-3-ethylcarbamoyl]isoxazol-4-yl]amide} (80). ¹H NMR (500 MHz) δ : 1.08 (t, $J = 7.2$ Hz, 3H), 1.11 (d, $J = 6.9$ Hz, 6H), 1.28-1.36 (m, 4H), 1.77-1.84 (m, 4H), 2.04 (bs, 1H), 2.22 (bs, 1H), 3.08 (m, 1H), 3.20 (m, 2H), 6.50 (s, 1H), 6.65 (s, 1H), 7.10 (s, 1H), 7.18 (s, 1H), 8.49 (t, $J = 5.6$ Hz, 1H), 9.06 (s, 1H), 9.81 (s, 1H), 9.9 (s, 1H); m/z 459.4 [M+H]⁺. Anal. (C₂₃H₃₀N₄O₆) C, H, N.

Cyclohexane-*cis*-1,4-dicarboxylic acid 1-amide 4-{{5-(2,4-dihydroxy-5-isopropylphenyl)-3-ethylcarbamoylisoxazol-4-yl}amide} (81). ¹H NMR (300 MHz) δ : 1.08 (t, $J = 7.0$ Hz, 3H), 1.11 (d, $J = 6.9$ Hz, 6H), 1.42-1.54 (m, 4H), 1.75-1.84 (m, 4H), 2.15 (m, 1H), 2.36 (m, 1H), 3.08 (m, 1H), 3.20 (m, 2H), 6.49 (s, 1H), 6.69 (s, 1H), 7.12 (s, 1H), 7.12 (s, 1H), 8.5 (t, $J = 5.6$ Hz, 1H), 8.97 (s, 1H), 9.79 (s, 1H), 10.04 (s, 1H); m/z 459.4 [M+H]⁺. Anal. (C₂₃H₃₀N₄O₆) C, H, N.

Piperidine-4-carboxylic acid [5-(2,4-dihydroxy-5-isopropylphenyl)-3-ethylcarbamoylisoxazol-4-yl]amide trifluoroacetate (82). ¹H NMR (300 MHz) δ : 1.07 (t, $J = 5.1$ Hz, 3H), 1.09 (d, $J = 7.2$ Hz, 6H), 1.72-1.77 (m, 2H), 1.86-1.92 (m, 2H), 2.58 (m, 1H), 2.8-2.3 (m, 2H), 3.07 (m, 1H), 3.19 (m, 2H), 3.22-3.3 (m, 2H), 6.48 (s, 1H), 7.09 (s, 1H), 8.2-8.3 (bm, 1H), 8.58 (bm, 1H), 8.58 (t, $J = 6.2$ Hz, 1H), 9.22 (s, 1H), 9.83 (s, 1H), 9.91 (s, 1H); m/z 417.2 [M+H]⁺. Anal. (C₂₁H₂₈N₄O₅ CF₃COOH) C, H, N.

1-Methylpiperidine-4-carboxylic acid [5-(2,4-dihydroxy-5-isopropylphenyl)-3-ethylcarbamoylisoxazol-4-yl]amide trifluoroacetate (83). Major isomer (80%) ¹H NMR (300 MHz) δ : 1.07 (t, $J = 7.2$ Hz, 3H), 1.09 (d, $J = 6.9$ Hz, 6H), 1.69-1.78 (m, 2H), 1.92-1.97 (m, 2H), 2.5 (m, 1H), 2.73 (d, $J = 4.4$ Hz, 3H), 2.93 (m, 2H), 3.06 (m, 1H), 3.2 (m, 2H), 3.42-3.46 (m, 2H), 6.47 (s, 1H), 7.07 (s, 1H), 8.57 (t, $J = 5.7$ Hz, 1H), 9.27 (s, 1H), 9.28 (bs, 1H), 9.83 (s, 1H), 9.88 (s, 1H); 431.1 m/z [M+H]⁺. Minor isomer (20%) ¹H NMR (300 MHz) δ : 1.07 (t, $J = 7.2$ Hz, 3H), 1.09 (d, $J = 6.9$ Hz, 6H), 1.69-1.78 (m, 2H), 1.92-1.97 (m, 2H), 2.5 (m, 1H), 2.73 (d, $J = 4.4$ Hz, 3H), 2.93 (m, 2H), 3.06 (m, 1H), 3.2 (m, 2H), 3.3-3.4 (m, 2H), 6.47 (s, 1H), 7.1 (s, 1H), 8.62 (t, $J = 5.7$ Hz, 1H), 9.28 (s, 1H), 9.4-9.5 (bs, 1H), 9.88 (s, 1H), 9.89 (s, 1H); m/z 431.1 [M+H]⁺. Anal. (C₂₂H₃₀N₄O₅ CF₃COOH) C, H, N.

5-(2,4-Dihydroxy-5-isopropylphenyl)-4-[(*trans*-4-methylaminomethylcyclohexane carbonyl)amino]isoxazole-3-carboxylic acid ethylamide trifluoroacetate (84). ¹H NMR (300 MHz) δ : 0.9-1.1 (m, 2H), 1.08 (t, $J = 5.1$ Hz, 3H), 1.1 (d, $J = 7.2$ Hz, 6H), 1.25-1.4 (m, 2H), 1.5-1.7 (m, 1H), 1.7-1.9 (m, 4H), 2.28 (m, 1H), 2.53 (t, $J = 6.1$ Hz, 3H), 2.78 (m, 2H), 3.08 (m, 1H), 3.21 (m, 2H), 6.49 (s, 1H), 7.1 (s, 1H), 8.2-8.4 (bm, 2H), 8.52 (t, $J = 6.1$ Hz, 1H), 9.05 (s, 1H), 9.83 (s, 1H), 9.89 (s, 1H); m/z 459.3 [M+H]⁺. Anal. (C₂₄H₃₄N₄O₅ CF₃COOH) C, H, N.

(1S,3R)-3-[5-(2,4-Dihydroxy-5-isopropylphenyl)-3-ethylcarbamoylisoxazol-4-yl carbamoyl]cyclopentanecarboxylic Acid Methyl Ester (85). ¹H NMR (300 MHz) δ : 1.06 (t, $J = 7.0$ Hz, 3H), 1.08 (d, $J = 6.7$ Hz, 6H), 1.76-1.90 (m, 4H), 2.03-2.12 (m, 2H), 2.75-2.79 (m, 2H), 3.06 (hept, $J = 7.0$ Hz, 1H), 3.19 (q, $J = 7.0$ Hz, 2H), 3.56 (s, 3H), 6.48 (s, 1H), 7.08 (s, 1H), 8.49 (t, $J = 5.5$ Hz, 1H), 9.12 (bs, 1H), 9.78 (bs, 2H). m/z 459.9 [M + H]⁺. Anal. (C₂₃H₂₉N₃O₇) C, H, N.

1S,3R)-3-[5-(2,4-Dihydroxy-5-isopropylphenyl)-3-ethylcarbamoylisoxazol-4-yl carbamoyl]cyclopentanecarboxylic acid (86). This compound was made with the general procedure used for compound 5-[2,4-Bis(benzyloxy)-5-chlorophenyl]-isoxazole-3-carboxylic acid ¹H NMR (300 MHz) δ : 1.07 (t, $J = 7.3$ Hz, 3H), 1.09 (d, $J = 7.0$, 6H), 1.71-1.89 (m., 5H), 2.01-2.11 (m, 1H), 2.48-2.78 (m, 2H), 3.06 (hept., $J = 7.0$ Hz, 2H), 3.20 (quint., $J = 6.4$ Hz, 2H), 6.48 (s, 1H), 7.09 (s, 1H), 8.48 (t, $J = 5.5$ Hz, 1H), 9.1-10.1 (bs, 4H); m/z 444.7 [M-H]⁻. Anal. (C₂₂H₂₇N₃O₇) C, H, N.

5-(2,4-Dihydroxy-5-isopropylphenyl)-4-[(3-hydroxycyclobutanecarbonyl)amino]isoxazole-3-carboxylic acid ethylamide (87). Obtained as 1:1 *cis/trans* mixture. ¹H NMR (300 MHz) δ : 1.06 (t, $J = 7.3$ Hz, 3H), 1.09 (d, $J = 6.7$ Hz, 6H), 1.93-2.04 (m, 2H), 2.26-2.38 (m, 2H), 2.47-2.53 (m, 4H), 2.88-2.94 (m, 1H), 3.02-3.12 (m, 1H), 3.16-3.25 (m, 1H), 3.93 (quint., $J = 7.3$ Hz, 1H), 4.21 (quint., $J = 6.7$ Hz, 1H), 6.48 (s, 1H), 7.10 (s, 1H), 8.51 (t, 1H), 8.99 (s, 1H), 9.79 (s, 1H), 9.87 (s, 1H). m/z 404.7 [M+H]⁺. Anal. (C₂₀H₂₅N₃O₆) C, H, N.

5-(2,4-Dihydroxy-5-isopropylphenyl)-4-(4-methoxybenzoylamino)isoxazole-3-carboxylic Acid Ethylamide (88). White solid. ¹H NMR (400 MHz) δ : 1.04-1.28 (m, 9H), 3.03-3.08 (m, 1H), 3.19-3.23 (m, 2H), 3.82 (s, 3H), 6.47 (s, 1H), 7.02 (d, $J = 8.8$ Hz, 2H), 7.23 (s, 1H), 7.87 (d, $J = 8.8$ Hz, 2H), 8.61 (t, $J = 5.6$ Hz, 1H), 9.56 (br, 1H), 9.82 (s, 1H), 10.08 (br, 1H). m/z 440.4 [M + H]⁺. Anal. (C₂₃H₂₅N₃O₆) C, H, N.

5-(2,4-Dihydroxy-5-isopropylphenyl)-4-(3-fluoro-4-methoxybenzoylamino)isoxazole-3-carboxylic acid ethylamide (89). ¹H NMR (300 MHz) δ : 1.03 (d, $J = 6.9$ Hz, 6H), 1.06 (t, $J = 7.2$, 3H), 3.04 (hept., $J = 7.0$ Hz, 1H), 3.19 (quint., $J = 7.2$ Hz, 2H), 3.89 (s, 3H), 6.46 (s, 1H), 7.19 (s, 1H), 7.25 (t, $J = 8.9$ Hz, 1H), 7.69-7.75 (m, 2H), 8.59 (t, $J = 5.7$ Hz, 1H), 9.66 (bs, 1H), 9.79 (s, 1H), 9.99 (bs, 1H); m/z 457.95 [M+H]⁺. Anal. (C₂₃H₂₄FN₃O₆) C, H, N.

5-(2,4-Dihydroxy-5-isopropylphenyl)-4-(4-dimethylaminobenzoylamino)isoxazole-3-carboxylic acid ethylamide (90). ¹H NMR (300 MHz) δ : 1.04 (d, $J = 7.0$ Hz, 6H), 1.05 (t, $J = 7.3$ Hz, 3H), 2.96 (s, 6H), 3.04 (hept., $J = 6.9$ Hz, 1H), 3.19 (quint., $J = 6.4$ Hz, 2H), 6.48 (s, 1H), 6.69 (d, $J = 8.8$ Hz, 2H), 7.21 (s, 1H), 7.73 (d, $J = 8.8$ Hz, 2H), 7.93 (s, 1H), 8.53 (t, $J = 5.7$ Hz, 1H), 9.31 (bs, 1H), 9.78 (bs, 1H); m/z 453.3 [M+H]⁺. Anal. (C₂₄H₂₈N₄O₅) C, H, N.

5-(2,4-Dihydroxy-5-isopropylphenyl)-4-(4-morpholin-4-ylmethylbenzoylamino)isoxazole-3-carboxylic Acid Ethylamide (91). ¹H NMR (300 MHz) δ : 1.04 (d, $J = 7.2$ Hz, 6H), 1.07 (t, $J = 7.0$ Hz, 3H), 3.18–3.22 (m, 4H), 3.02–3.09 (m, 3H), 3.78 (m, 2H), 3.89 (m, 2H), 4.38 (bs, 2H), 6.52 (s, 1H), 7.21 (s, 1H), 7.73 (d, $J = 7.3$ Hz, 2H), 7.96 (d, $J = 7.3$ Hz, 2H), 8.64 (t, $J = 5.8$ Hz, 1H), 9.76 (s, 1H), 9.86 (s, 1H), 10.13 (s, 1H), 11.2 (s, 1H). m/z 530.8 [M + Na]⁺. Anal. (C₂₇H₃₂N₄O₆ HCl) C, H, N.

5-(2,4-Dihydroxy-5-isopropylphenyl)-4-[4-(4-methylpiperazin-1-yl)benzoylamino]isoxazole-3-carboxylic acid ethylamide trifluoroacetate (92) ¹H NMR (300 MHz) δ : 1.03 (d, $J = 6.7$ Hz, 6H), 1.05 (t, $J = 7.2$ Hz, 3H), 2.84 (s, 3H), 2.99–3.23 (m, 7H), 3.5–3.6 (m, 2H), 4–4.04 (m, 2H), 6.47 (s, 1H), 7.05 (d, $J = 9.0$ Hz, 1H), 7.22 (s, 1H), 7.81 (d, $J = 9.0$ Hz, 1H), 8.58 (t, $J = 5.8$ Hz, 1H), 9.43 (s, 1H), 9.81 (s, 1H), 9.92 (s, 1H), 10.05 (s, 1H); m/z 508.6 [M+H]⁺. Anal. (C₂₇H₃₃N₅O₅ CF₃COOH) C, H, N.

5-(2,4-Dihydroxy-5-isopropylphenyl)-4-(4-piperazin-1-ylbenzoylamino)isoxazole-3-carboxylic acid ethylamide (93). ¹H-NMR (300 MHz, DMSO+TFA) δ : 1.03 (d, $J = 7.0$ Hz, 6H); 1.05 (t, $J = 7.0$ Hz, 3H); 3.01 (hept., $J = 7.0$ Hz, 1H); 3.15–3.35 (m, 6H); 3.46–3.55 (m, 4H); 6.47 (s, 1H); 7.03 (d, $J = 8.9$ Hz, 2H); 7.22 (s, 1H); 7.80 (d, $J = 8.9$ Hz, 2H); 8.57 (t, $J = 5.8$ Hz, 1H); 8.80 (bs, 2H); 9.43 (s, 1H); 10.05 (bs, 1H); m/z 494.9 [M+H]⁺. Anal. (C₂₆H₃₁N₅O₅ CF₃COOH) C, H, N.

5-(2,4-Dihydroxy-5-isopropylphenyl)-4-(4-pyrrolidin-1-ylbenzoylamino)isoxazole-3-carboxylic acid ethylamide (94). ¹H-NMR (300 MHz) δ : 1.04 (d, $J = 7.0$ Hz, 6H), 1.09 (t, $J = 7.0$ Hz, 3H), 3.04 (hept., $J = 7.3$ Hz, 1H), 3.16–3.29 (m, 2H), 6.29 (t, $J = 2.1$ Hz, 2H), 6.46 (s, 1H), 7.21 (s, 1H), 7.49 (t, $J = 2.1$ Hz, 2H), 7.71 (d, $J = 8.9$ Hz, 2H), 7.97 (d, $J = 8.9$ Hz, 2H), 8.61 (t, $J = 5.8$ Hz, 1H), 9.78 (bs, 3H); m/z 473.3 [M-H]⁻. Anal. (C₂₆H₂₆N₄O₅) C, H, N.

5-(2,4-Dihydroxy-5-isopropylphenyl)-4-(4-pyrrolidin-1-yl-benzoylamino)isoxazole-3-carboxylic acid ethylamide (95). $^1\text{H-NMR}$ (300 MHz) δ : 1.06 (t, $J = 7.3$ Hz, 3H), 1.08 (d, $J = 7.0$ Hz, 6H), 1.88-1.95 (m, 4H), 3.05 (hept., $J = 7.0$ Hz, 1H), 3.12-3.29 (m, 6H), 6.42 (d, $J = 8.6$ Hz, 2H), 6.52 (s, 1H), 7.20 (s, 1H), 7.70 (d, $J = 8.6$ Hz, 2H); 8.50 (t, $J = 5.5$ Hz, 1H), 10.2 (bs, 3H). m/z 477.3 $[\text{M-H}]^-$. Anal. ($\text{C}_{26}\text{H}_{30}\text{N}_4\text{O}_5$) C, H, N.

N5-[3-(Ethylcarbamoyl)-5-(2,4-dihydroxy-5-isopropylphenyl)isoxazol-4-yl]-N3-ethylisoxazole-3,5-dicarboxamide (96). White solid. $^1\text{H NMR}$ (400 MHz) δ : 1.05-1.12 (m, 12H), 3.04-3.08 (m, 1H), 3.19-3.28 (m, 4H), 3.31 (s, 1H), 6.47 (s, 1H), 7.18 (s, 1H), 7.44 (s, 1H), 8.71 (t, $J = 5.6$ Hz, 1H), 8.95 (t, $J = 5.6$ Hz, 1H), 9.88 (s, 1H), 10.08(s, 1H); m/z 472.3 $[\text{M+H}]^+$. Anal. ($\text{C}_{22}\text{H}_{25}\text{N}_5\text{O}_7$) C, H, N.

5-(2,4-Dihydroxy-5-isopropylphenyl)-4-(5-ethylisoxazole-3-carbonyl)aminoisoxazole-3-carboxylic Acid Ethylamide (97). White solid. $^1\text{H NMR}$ (400 MHz CD_3OD) δ : 1.18–1.31 (m, 12H), 2.80–2.86 (m, 2H), 3.16–3.22 (m, 1H), 3.39 (q, $J = 7.2$ Hz, 2H), 6.47 (s, 1H), 6.48 (s, 1H), 7.33 (s, 1H). m/z 429.0 $[\text{M} + \text{H}]^+$. Anal. ($\text{C}_{21}\text{H}_{24}\text{N}_4\text{O}_6$) C, H, N.

4-(5-Acetylisoxazole-3-carbonyl)amino-5-(2,4-dihydroxy-5-isopropylphenyl)isoxazole-3-carboxylic acid ethylamide (98). White solid. $^1\text{H NMR}$ (400 MHz CD_3OD) δ : 1.19-1.26 (m, 9H), 2.62 (s, 3H), 3.16-3.25 (m, 1H), 3.39 (q, $J = 7.6$ Hz, 2H), 6.48 (s, 1H), 7.32 (s, 1H), 7.41 (s, 1H); m/z 443.0 $[\text{M+H}]^+$. Anal. ($\text{C}_{21}\text{H}_{22}\text{N}_4\text{O}_7$) C, H, N.

5-(2,4-Dihydroxy-5-isopropylphenyl)-4-[(3-methylthiophene-2-carbonyl)amino]isoxazole-3-carboxylic Acid Ethylamide (99). White solid. $^1\text{H NMR}$ (400 MHz) δ : 1.07–1.11 (m, 9H), 2.44 (s, 3H), 3.05–3.11 (m, 1H), 3.19–3.25 (m, 2H), 6.52 (s, 1H), 7.01 (d, $J = 5.2$ Hz, 1H), 7.22 (s, 1H), 7.66 (d, $J = 5.2$ Hz, 1H), 8.66 (t, $J = 5.6$ Hz, 1H), 9.12 (s, 1H), 9.89 (s, 1H), 10.22 (br, 1H). m/z 430.6 $[\text{M} + \text{H}]^+$. Anal. ($\text{C}_{21}\text{H}_{23}\text{N}_3\text{O}_5\text{S}$) C, H, N, S.

4-[(5-Bromofuran-2-carbonyl)amino]-5-(2,4-dihydroxy-5-isopropylphenyl)isoxazole-3-carboxylic Acid Ethylamide (100). $^1\text{H NMR}$ (300 MHz) δ : 1.05 (d, $J = 7.0$ Hz, 6H), 1.07 (t, $J = 7.6$ Hz, 3H), 3.05 (hept, $J = 6.7$ Hz, 1H), 3.21 (quint, $J = 7.6$ Hz, 2H), 6.47 (s, 1H), 6.78 (d, $J = 3.7$ Hz, 1H), 7.17 (s, 1H), 7.24 (d, $J = 3.7$ Hz, 1H), 8.62 (t, $J = 5.7$ Hz, 1H), 9.75 (bs, 1H), 9.81 (s, 1H), 10.08 (bs, 1H). m/z 477.3/479.3 $[\text{M} - \text{H}]^-$. Anal. ($\text{C}_{20}\text{H}_{20}\text{BrN}_3\text{O}_6$) C, H, N.

5-(2,4-Dihydroxy-5-isopropylphenyl)-4-[(5-phenylisoxazole-3-carbonyl)amino]-isoxazole-3-carboxylic acid ethylamide (101). ¹H NMR (300 MHz) δ : 1.09 (t, $J = 7.0$ Hz, 3H), 1.10 (d, $J = 6.7$ Hz, 6H), 3.08 (hept., $J = 6.7$ Hz, 1H), 3.23 (quint., $J = 7.0$ Hz, 2H), 6.53 (s, 1H), 7.23 (s, 1H), 7.45 (s, 1H), 7.53-7.57 (m, 3H), 7.92-7.96 (m, 2H), 8.69 (t, $J = 5.8$ Hz, 1H), 9.90 (s, 2H), 10.54 (bs, 1H), m/z 475.5 [M-H]⁻. Anal. (C₂₅H₂₄N₄O₆) C, H, N.

5-(2,4-Dihydroxy-5-isopropylphenyl)-4-[(4-methyl-2-pyridin-4-ylthiazole-5-carbonyl)amino]isoxazole-3-carboxylic acid ethylamide (102). ¹H NMR (300 MHz) δ : 1.08 (t, $J = 7.0$ Hz, 3H), 1.09 (d, $J = 6.9$ Hz, 6H), 2.68 (s, 3H), 3.07 (hept., $J = 6.6$ Hz, 1H), 3.22 (quint., $J = 6.9$ Hz, 2H), 6.68 (s, 1H), 7.18 (s, 1H), 8.16 (d, $J = 6.0$ Hz, 2H), 8.71 (t, $J = 5.5$ Hz, 1H), 8.85 (d, $J = 6.0$ Hz, 2H), 9.73 (s, 1H), 10.06 (bs, 1H), 10.46 (bs, 1H); m/z 506.9 [M-H]⁻. Anal. (C₂₅H₂₅N₅O₅ HCl) C, H, N.

5-[2,4-Dihydroxy-5-(prop-2-yl)phenyl]-N-ethyl-4-[[5-(4-fluorophenyl)-4-methyl-1,3-thiazol-2-yl]carbonyl]amino]isoxazole-3-carboxamide (103). ¹H NMR (300 MHz) δ : 1.08 (t, $J = 7.3$ Hz, 3H), 1.09 (d, $J = 7.0$ Hz, 6H), 2.61 (s, 3H), 3.07 (m, 1H), 3.22 (m, 2H), 6.5 (s, 1H), 7.20 (s, 1H), 7.34 (t, $J = 8.5$ Hz, 2H), 7.96 (dd, $J = 8.5$ Hz, $J = 5.5$ Hz, 2H), 8.65 (t, $J = 5.6$ Hz, NH), 9.5 (s, 1H), 9.83 (s, 1H), 10.2 (s, 1H); m/z 525.6 [M+H]⁺. Anal. (C₂₆H₂₅FN₄O₅S) C, H, N.

5-(2,4-Dihydroxy-5-isopropylphenyl)-4-[(2,4-dimethylthiazole-5-carbonyl)amino]isoxazole-3-carboxylic acid ethylamide (104). ¹H-NMR (300 MHz) δ : 1.05 (t, $J = 7.6$ Hz, 3H), 1.08 (d, $J = 7.4$ Hz, 6H), 2.51 (s., 3H), 2.60 (s, 3H), 3.07 (hept., $J = 6.7$ Hz, 1H), 3.21 (quint., $J = 7.0$ Hz, 2H), 6.50 (s, 1H), 7.18 (s, 1H), 8.62 (t, $J = 5.8$ Hz, 1H), 9.29 (bs, 1H), 9.85 (s, 1H), 10.23 (bs, 1H); m/z 443.6 [M-H]⁻. Anal. (C₂₁H₂₄N₄O₅S) C, H, N.

Quinoline-8-carboxylic acid [5-(2,4-dihydroxy-5-isopropylphenyl)-3-ethylcarbamoyl isoxazol-4-yl]amide (105). ¹H NMR (300 MHz) δ : 1.06 (d, $J = 6.9$ Hz, 6H), 1.08 (t, $J = 7.1$ Hz, 3H), 3.05 (m, 1H), 3.21 (m, 2H), 6.53 (s, 1H), 7.16 (s, 1H), 7.71-7.78 (m, 2H), 8.24 (m, 1H), 8.57-8.65 (m, 2H, 1H), 9.13 (dd, $J = 1.8$ Hz, $J = 4.1$ Hz, 1H), 9.8 (s, 1H), 10.12 (s, 1H), 12.78 (s, 1H); m/z 461.7 [M+H]⁺. Anal. (C₂₅H₂₄N₄O₅) C, H, N.

5-(2,4-Dihydroxy-5-isopropylphenyl)-4-[(3-methylbenzofuran-2-carbonyl)-amino]isoxazole-3-carboxylic acid ethylamide (106). ¹H NMR (300 MHz) δ : 1.07 (d, $J = 5.2$ Hz, 6H); 1.08 (t, $J = 7.5$, 3H); 2.49 (s., 3H); 3.05 (hept., $J = 6.6$ Hz, 1H); 3.23 (quint., $J = 7.2$ Hz, 2H); 6.50 (s, 1H); 7.23 (s, 1H); 7.34 (t, $J = 7.8$ Hz, 1H); 7.49 (t, $J = 7.3$ Hz; 1H); 7.54 (d, $J = 13.9$ Hz, 1H); 7.74 (d, $J = 7.8$ Hz, 1H); 8.65 (t, $J = 6.0$ Hz, 1H); 9.75 (bs, 1H); 9.84 (s, 1H); 10.25 (bs, 1H); m/z 464.2 [M+H]⁺. Anal. (C₂₅H₂₅N₃O₆) C, H, N.

5-(2,4-Dihydroxy-5-isopropylphenyl)-4-[(5-methoxy-2-methylbenzofuran-3-carbonyl)amino]isoxazole-3-carboxylic acid ethylamide (107). ¹H-NMR (300 MHz) δ : 1.08 (t, $J = 7.2$ Hz, 3H); 1.09 (d, $J = 6.9$ Hz, 6H); 2.60 (s, 3H); 3.07 (hept., $J = 6.9$ Hz, 1H); 3.23 (quint., $J = 7.0$ Hz, 2H); 3.77 (s, 3H); 6.48 (s, 1H); 6.88 (dd, $J = 8.9$ Hz, $J = 2.6$ Hz, 1H); 7.22 (s, 1H); 7.28 (s, 1H); 7.45 (d, $J = 8.9$ Hz, 1H); 8.68 (t, $J = 5.7$ Hz, 1H); 9.16 (bs, 1H); 9.82 (s, 1H); 10.11 (bs, 1H); m/z 494.3 [M+H]⁺. Anal. (C₂₆H₂₇N₃O₇) C, H, N.

1-Methyl-1H-indole-2-carboxylic acid [5-(2,4-dihydroxy-5-isopropylphenyl)-3-ethylcarbamoylisoxazol-4-yl]amide (108). ¹H NMR (300 MHz) δ : 1.07 (d, $J = 7.1$ Hz, 6H), 1.09 (t, $J = 5.6$ Hz, 3H), 3.06 (m, 1H), 3.22 (m, 2H), 3.93 (s, 3H), 6.5 (s, 1H), 7.1 (m, 1H), 7.18 (s, 1H), 7.24 (s, 1H), 7.29 (m, 1H), 7.52 (d, $J = 8.2$ Hz, 1H), 7.65 (d, $J = 8.2$ Hz, 1H), 8.63 (t, $J = 5.2$ Hz, 1H), 9.63 (s, 1H), 9.83 (s, 1H), 10.15 (s, 1H); m/z 463.7 [M+H]⁺. Anal. (C₂₅H₂₆N₄O₅) C, H, N.

1H-Indole-6-carboxylic acid [5-(2,4-dihydroxy-5-isopropylphenyl)-3-ethylcarbamoyl isoxazol-4-yl]amide (109). ¹H NMR (300 MHz) δ : 1.04 (d, $J = 6.9$ Hz, 6H), 1.07 (t, $J = 7.2$ Hz, 3H), 3.04 (m, 1H), 3.21 (m, 2H), 6.48 (s, 2H), 7.25 (s, 1H), 7.52-7.59 (m, 3H), 7.99 (s, H), 8.59 (t, $J = 7$ Hz, 1H), 9.52 (s, 1H), 9.78 (s, 1H), 10.07 (s, 1H), 11.43 (s, 1H); m/z [M+H]⁺ 449.2. Anal. (C₂₄H₂₄N₄O₅) C, H, N.

1-Methyl-1H-indole-6-carboxylic acid [5-(2,4-dihydroxy-5-isopropylphenyl)-3-ethylcarbamoylisoxazol-4-yl]amide (110). ¹H NMR (300 MHz) δ : 1.04 (d, $J = 6.9$ Hz, 6H), 1.07 (t, $J = 7.2$ Hz, 3H), 3.04 (m, 1H), 3.21 (m, 2H), 3.84 (s, 3H), 6.48 (d, $J = 3.2$ Hz, 1H), 6.48 (s, 1H), 7.26 (s, 1H), 7.50 (d, $J = 3.1$ Hz, 1H), 7.55-7.62 (m, 2H), 8.05 (s, 1H), 8.59 (t, $J = 5.6$ Hz, 1H), 9.56 (s, 1H), 9.79 (s, 1H), 10.09 (s, 1H); m/z 485.2 [M+Na]⁺. Anal. (C₂₅H₂₆N₄O₅) C, H, N.

4-[(Benzo[thiophene-6-carbonyl)amino]-5-(2,4-dihydroxy-5-isopropylphenyl)-isoxazole-3-carboxylic acid ethylamide (111). ¹H NMR (300 MHz) δ : 1.04 (d, $J = 6.9$ Hz, 6H), 1.07 (t, $J = 7.2$ Hz, 3H), 3.04 (m, 1H), 3.21 (m, 2H), 6.47 (s, 1H), 7.24 (s, 1H), 7.53 (d, $J = 5.5$ Hz, 1H), 7.87 (d, $J = 8.4$ Hz, 1H), 7.95 (d, $J = 5.5$ Hz, 1H), 7.96 (d, $J = 8.4$ Hz, 1H), 8.54 (s, 1H), 8.61 (t, $J = 7.1$ Hz, 1H), 9.79 (bs, 2H), 10.1 (s, 1H); m/z 465.9 [M+H]⁺. Anal. (C₂₄H₂₃N₃O₅S) C, H, N.

Benzo[oxazole-5-carboxylic acid [5-(2,4-dihydroxy-5-isopropylphenyl)-3-ethylcarbamoylisoxazol-4-yl]amide (112) ¹H NMR (300 MHz) δ : 1.03 (d, $J = 6.9$ Hz, 6H), 1.06 (t, $J = 7.3$ Hz, 3H), 3.04 (m, 1H), 3.21 (m, 2H), 6.46 (s, 1H), 7.23 (s, 1H), 7.87 (d, $J = 8.4$ Hz, 1H), 7.98 (d, $J = 8.4$ Hz, 1H), 8.33 (s, 1H), 8.62 (t, $J = 5.6$ Hz, 1H), 8.85 (s, 1H), 9.77 (s, 1H), 10 (bs, 2H); m/z 451.2 [M+H]⁺. Anal. (C₂₃H₂₂N₄O₆) C, H, N.

5-(2,4-Dihydroxy-5-isopropylphenyl)-4-[(furan-2-carbonyl)-amino]isoxazole-3-carboxylic Acid Ethylamide (113). ¹H NMR (300 MHz) δ : 1.06 (d, $J = 7.0$ Hz, 6H), 1.08 (t, $J = 7.5$ Hz, 3H), 3.06 (m, 1H), 3.21 (m, 2H), 6.49 (s, 1H), 6.65 (dd, $J = 1.6$ Hz, $J = 3.5$ Hz, 1H), 7.19 (s, 1H), 7.2 (d, $J = 3.5$ Hz, 1H), 7.88 (d, $J = 1.6$ Hz, 1H), 8.62 (t, $J = 5.4$ Hz, 1H), 9.5 (s, 1H), 9.83 (s, 1H), 10.2 (s, 1H). m/z 400.3 [M + H]⁺. Anal. (C₂₀H₂₁N₃O₆) C, H, N.

5-(2,4-Dihydroxy-5-isopropylphenyl)-4-[(5-methylfuran-2-carbonyl)amino]isoxazole-3-carboxylic acid ethylamide (114). ¹H NMR (300 MHz) δ : 1.06 (d, $J = 6.9$ Hz, 6H), 1.07 (t, $J = 7.2$ Hz, 3H), 2.33 (s, 3H), 3.06 (m, 1H), 3.20 (m, 2H), 6.27 (d, $J = 3.3$ Hz, 1H), 6.49 (s, 1H), 7.08 (d, $J = 3.3$ Hz, 1H), 7.19 (s, 1H), 8.6 (t, $J = 5.7$ Hz, 1H), 9.4 (s, 1H), 9.82 (s, 1H), 10.25 (s, 1H); m/z 414.4 [M+H]⁺. Anal. (C₂₁H₂₃N₃O₆) C, H, N.

5-(2,4-Dihydroxy-5-isopropylphenyl)-4-(5-morpholinomethyl)isoxazole-3-carbonyl amino]isoxazole-3-carboxylic Acid Ethylamide (115). ¹H NMR (400 MHz CD₃OD), δ : 1.18–1.26 (m, 9H), 2.52–2.54 (m, 4H), 3.17–3.25 (m, 1H), 3.39 (q, $J = 7.2$ Hz, 2H), 3.68–3.70 (m, 4H), 3.78 (s, 1H), 6.47 (s, 1H), 6.72 (s, 1H), 7.34 (s, 1H). m/z 499.9 [M + H]⁺. Anal. (C₂₄H₂₉N₅O₇) C, H, N.

General procedure for preparation of 116a-e derivatives.

The coupling step of the opportune acyl chloride to **56d** followed the procedure described for the compounds **57-115**. To a solution of opportune silylated acid **116a-e** (2 mmol) in DCM (15 mL), cooled in a ice bath, was added dropwise $\text{BF}_3 \cdot \text{Et}_2\text{O}$ (3.6mL/mmol). The reaction mixture was quenched with sat. NaHCO_3 aq. The organic layer was separated, dried and the solvent was removed under reduced pressure. The residue obtained was purified by flash chromatography with DCM/ CH_3OH . (yield: 85-90%).

***cis*-5-[2,4-Bis(benzyloxy)-5-isopropylphenyl]-4-[(3-hydroxymethyl-cyclopentane carbonyl)-amino]-isoxazole-3-carboxylic acid ethylamide (116a).** ^1H NMR (300 MHz) δ : 1.06 (t, $J = 7.2$ Hz, 3H), 1.09 (d, $J = 7.0$ Hz, 6H), 1.28-1.38 (m, 2H), 1.57-1.75 (m, 3H), 1.83-2.0 (m, 2H), 2.71 (m, 1H), 3.06 (m, 1H), 3.15-3.28 (m, 4H), 5.20 (s, 2H), 5.22 (s, 2H), 6.47 (s, 1H), 7.09 (s, 1H), 7.3-7.5 (m, 10H), 8.46 (t, $J = 5.6$ Hz, 1H), 9.1 (s, 1H); m/z $[\text{M}+\text{H}]^+$ 612.7.

5-[2,4-Bis(benzyloxy)-5-isopropylphenyl]-4-[(4-*trans*-hydroxy-cyclohexanecarbonyl)-amino]-isoxazole-3-carboxylic acid ethylamide (116b). ^1H -NMR (300 MHz, CD_3OD) δ : 1.20 (d, $J = 6.9$ Hz, 6H), 1.22 (t, $J = 7.2$ Hz, 3H), 1.22-1.37 (m, 2H), 1.44-1.60 (m, 2H), 1.99 (bm, 4H), 2.28 (tt, $J = 12.0$ Hz, $J = 3.4$ Hz, 1H), 3.20 (hept., $J = 6.9$ Hz, 1H), 3.38 (q, $J = 7.2$ Hz, 2H), 3.52 (tt, $J = 10.6$ Hz, $J = 4.1$ Hz, 1H), 5.20 (s, 2H), 5.22 (s, 2H), 6.44 (s, 1H); 7.24 (s, 1H); 7.3-7.5 (m, 10H); m/z 610.7 $[\text{MH}]^-$.

5-[2,4-Bis(benzyloxy)-5-isopropylphenyl]-4-[(4-*cis*-hydroxy-cyclohexanecarbonyl)-amino]-isoxazole-3-carboxylic acid ethylamide (116c). ^1H -NMR (300 MHz) δ : 1.07 (t, $J = 7.3$ Hz, 3H), 1.09 (d, $J = 6.7$ Hz, 6H), 1.35-1.49 (m, 4H), 1.58-1.82 (m, 4H), 2.24 (m, 1H), 3.06 (hept., $J = 7.0$ Hz, 1H), 3.19 (quint., $J = 7.1$ Hz, 2H), 3.73 (bs, 1H), 5.20 (s, 2H), 5.22 (s, 2H), 6.48 (s, 1H); 7.10 (s, 1H); 7.3-7.5 (m, 10H), 8.47 (t, $J = 5.8$ Hz, 1H), 8.92 (s, 1H); m/z $[\text{M}-\text{H}]^- = 610.7$.

5-[2,4-Bis(benzyloxy)-5-isopropylphenyl]-4-[(4-*cis*-hydroxymethyl-cyclohexane carbonyl)-amino]-isoxazole-3-carboxylic acid ethylamide (116d). ^1H -NMR (300 MHz) δ : 1.07 (t, $J = 7.1$ Hz, 3H), 1.09 (d, $J = 6.9$ Hz, 6H), 1.37-1.56 (m, 5H), 1.63-1.77 (m, 4H), 2.38 (m, 1H), 3.07 (hept, $J = 6.9$ Hz, 1H), 3.14-3.29 (m, 4H), 4.36 (t, $J = 5.3$ Hz, 1H), 5.20 (s, 2H), 5.22 (s, 2H), 6.49 (s, 1H), 7.11 (s, 1H), 7.3-7.5 (m, 10H), 8.50 (t, $J = 5.8$ Hz, 1H), 8.94 (s, 1H); m/z 624.6 $[\text{M}-\text{H}]^-$.

***trans*-5-[2,4-Bis(benzyloxy)-5-isopropylphenyl]-4-[(4-hydroxymethyl-cyclohexyl carbonyl)-amino]-isoxazole-3-carboxylic acid ethylamide (116e).** ¹H NMR (300 MHz) δ : 0.81-0.92 (m, 2H), 1.06 (t, $J = 7.1$ Hz, 3H), 1.09 (d, $J = 6.9$ Hz, 6H), 1.22-1.35 (m, 3H), 1.72-1.82 (m, 4H), 2.17 (m, 1H), 3.06 (m, 1H), 3.15-3.24 (m, 4H), 4.33 (t, $J = 5.2$ Hz, 1H), 5.20 (s, 2H), 5.22 (s, 2H), 6.48 (s, 1H), 7.09 (s, 1H), 7.3-7.5 (m, 10H), 8.46 (t, $J = 5.7$ Hz, 1H), 9.00 (s, 1H); m/z 626.9 [M+H]⁺.

General procedure for preparation of morpholino derivatives 118a-e.

To a solution of the appropriate alcohol **116a-e** (1 mmol) in DCM (10 mL) dry, was added mesylchloride (1.2 mmol, 0.093 mL) and DIPEA at 0 °C. The reaction was stirred at r.t. for 2h, diluted with DCM (20 mL), and washed with 1N HCl(aq). The organic layer was dried and the solvent removed under reduced pressure to give a crude residue that was used without further purification. To the crude mesylate previous obtained was added morpholine (3 mL) and the reaction mixture was stirred at 70 °C for 6h. After dilution with DCM, the solution was washed with H₂O (3 x 15 mL), brine (15 mL) and dried. The crude product obtained after evaporation of the solvent was purified by flash chromatography with Hex/EtOAc 4:6 to 2:8. (yield: 50-65%)

***cis*-5-[2,4-Bis(benzyloxy)-5-isopropylphenyl]-4-[(3-morpholin-4-yl-methyl-cyclopentane carbonyl)-amino]-isoxazole-3-carboxylic acid ethylamide trifluoroacetate (118a).** ¹H NMR (500 MHz) δ : 1.09 (t, $J = 7.0$ Hz, 3H), 1.1 (d, $J = 6.7$ Hz, 6H), 1.35 (m, 1H), 1.50 (dt, $J = 12.5$ Hz, $J = 9.1$ Hz, $J = 9.1$ Hz, 1H), 1.81-1.86 (m, 3H), 2.02 (dt, $J = 12.5$ Hz, $J = 7.6$ Hz, $J = 7.6$ Hz, 1H), 2.32 (m, 1H), 2.83 (m, 1H), 3.02-3.11 (m, 3H), 3.15 (m, 2H), 3.21 (m, 2H), 3.43 (d, $J = 12.2$ Hz, 2H), 3.69 (t, $J = 11.9$ Hz, 2H), 3.95 (dd, $J = 12.5$ Hz, $J = 2.1$ Hz, 2H), 5.20 (s, 2H), 5.22 (s, 2H), 6.51 (s, 1H), 7.11 (s, 1H), 7.3-7.5 (m, 10H), 8.54 (t, $J = 5.6$ Hz, 1H), 9.12 (s, 1H), 9.57 (bm, 1H); m/z 681.5 [M+H]⁺.

5-[2,4-Bis(benzyloxy)-5-isopropylphenyl]-4-[(*trans*-4-morpholin-4-yl-cyclohexane carbonyl)-amino]-isoxazole-3-carboxylic acid ethylamide hydrochloride (118b).

¹H NMR (300 MHz) δ : 1.08 (d, $J = 6.9$ Hz, 6H), 1.08 (t, $J = 7.1$ Hz, 3H), 1.35-1.43 (m, 4H), 1.88-1.95 (m, 2H), 2.14-2.24 (m, 3H), 3-3.4 (m, 8H), 3.76-3.84 (m, 2H), 3.9-4 (m, 2H), 5.20 (s, 2H), 5.22 (s, 2H), 6.51 (s, 1H), 7.08 (s, 1H), 7.3-7.5 (m, 10H), 8.52 (t, $J = 5.6$ Hz, NH), 9.12 (s, 1H), 10.6-10.7 (bm, 1H); m/z 681.5 [M+H]⁺.

5-[2,4-Bis(benzyloxy)-5-isopropylphenyl]-4-[(*cis*-4-morpholin-4-yl-cyclohexane carbonyl)-amino]-isoxazole-3-carboxylic acid ethylamide trifluoroacetate (118c).

¹H NMR (300 MHz) δ : 1.08 (t, $J = 7.1$ Hz, 3H), 1.1 (d, $J = 6.9$ Hz, 6H), 1.53-1.57 (m, 2H), 1.78-1.89 (m, 4H), 2.03-2.13 (m, 2H), 2.56 (m, 1/2 Wh=12.5Hz, 1H), 3.03-3.33 (m, 8H), 3.69-3.77 (m, 2H), 3.92-3.96 (m, 2H), 5.20 (s, 2H), 5.22 (s, 2H), 6.51 (s, 1H), 7.12 (s, 1H), 7.3-7.5 (m, 10H), 8.58 (t, $J = 5.6$ Hz, 1H), 9.09 (s, 1H), 9.9 (bs, 1H); m/z 681.5 [M+H]⁺.

5-[2,4-Bis(benzyloxy)-5-isopropylphenyl]-4-[(4-*cis*-morpholinylmethyl-cyclohexane carbonyl)-amino]-isoxazole-3-carboxylic acid ethylamide (118d). ¹H NMR (300 MHz) δ : 1.07 (t, $J = 7.6$ Hz, 3H), 1.08 (d, $J = 7.3$ Hz, 6H), 1.52 (bs, 6H), 1.72 (m, 2H), 1.98 (bs, 1H), 2.40 (bs, 1H), 3.01 (m, 5H), 3.19 (q, $J = 7.0$ Hz, 2H), 3.40 (d, $J = 11.9$ Hz, 2H), 3.78 (t, $J = 11.3$ Hz, 2H), 3.90 (d, $J = 11.9$ Hz, 2H), 5.20 (s, 2H), 5.22 (s, 2H), 6.53 (s, 1H), 7.11 (s, 1H), 7.3-7.5 (m, 10H), 8.51 (t, $J = 5.2$ Hz, 1H), 8.99 (s, 1H), 9.84 (s, 1H); m/z 694.5 [M-H]⁻.

5-[2,4-Bis(benzyloxy)-5-isopropylphenyl]-4-[(4-*trans*-morpholin-4-yl-methylcyclohexanecarbonyl)-amino]-isoxazole-3-carboxylic acid ethylamide hydrochloride (118e). ¹H NMR (300 MHz) δ : 0.95-1.1 (m, 11H), 1.30-1.42 (m, 2H), 1.7-1.88 (m, 5H), 2.22 (m, 1H), 2.92-3.11 (m, 5H), 3.19 (m, 2H), 3.40 (d, $J = 12.5$ Hz, 2H), 3.78 (t, $J = 11.6$ Hz, 2H), 3.90 (d, $J = 9.8$ Hz, 2H), 5.20 (s, 2H), 5.22 (s, 2H), 6.51 (s, 1H), 7.09 (s, 1H), 7.3-7.5 (m, 10H), 8.50 (t, $J = 5.7$ Hz, 1H), 9.04 (s, 1H), 10.12 (bs, 1H); m/z 695.9 [M+H]⁺.

General procedure for the synthesis of compounds 120a-c.

The coupling step of acryloyl chloride to **56a** or **56d** was made using the procedure described above. A solution of appropriate acryloyl derivative, (0.32 mmol) and morpholine or methyl piperazine (1.5 mL) was heated under reflux for 1 h. Solvents were removed under reduced pressure, and the residue was purified by chromatography on silica gel (eluent: ethyl acetate-methanol).

5-(2,4-Bis-benzyloxy-5-chloro-phenyl)-4-(3-morpholin-4-yl-propionylamino)-isoxazole-3-carboxylic acid ethylamide (120a). ¹H NMR (200 MHz CDCl₃) δ : 1.25 (t, $J = 7.4$ Hz, 3H), 2.24-2.34 (m, 4H), 2.41-2.45 (m, 2H), 3.38-3.50 (m, 2H), 3.64-3.72 (m, 4H), 4.97 (s, 2H), 5.12 (s, 2H), 6.58 (s, 1H), 6.86 (br, 1H), 7.28-7.42 (m, 10H), 7.62 (s, 1H), 9.95 (m, 1H), m/z 619.6/621.5 [M+H]⁺.

5-[2,4-Bis-(benzyloxy)-5-isopropyl-phenyl]-4-(3-morpholin-4-yl-propionylamino)-isoxazole-3-carboxylic acid ethylamide (120b). ¹H NMR (200 MHz CDCl₃) δ: 1.18-1.25 (m, 9H), 2.22-2.27 (m, 2H), 2.36-2.44 (m, 2H), 2.88-2.86 (m, 4H), 3.20-3.48 (m, 3H), 3.62-3.66 (m, 4H), 4.97 (s, 2H), 5.02 (m, 2H), 6.52 (s, 1H), 6.88 (br, 1H), 7.24-7.37 (m, 10H), 7.42 (s, 1H), 10.66 (s, 1H); *m/z* 627.4 [M+H]⁺.

5-[2,4-Bis(benzyloxy)-5-isopropylphenyl]-4-[3-(4-methylpiperazin-1-yl)-propionylamino]-isoxazole-3-carboxylic acid ethylamide (120c). ¹H NMR (400 MHz CDCl₃) δ: 1.22-1.28 (m, 9H), 2.23 (s, 3H), 2.28 (t, *J* = 6.8 Hz, 2H), 2.29-2.38 (m, 8H), 3.32 (hept, *J* = 6.9 Hz, 1H), 3.45-3.50 (m, 2H), 5.02 (s, 2H), 5.04 (s, 2H), 6.55 (s, 1H), 6.84 (br, 1H), 7.30-7.40 (m, 10H), 7.44 (s, 1H), 9.68 (m, 1H); *m/z* 640.7 [M+H]⁺.

General procedure to remove the benzyl group

The deprotection of phenol group was made using the procedure described for compounds **57-115**. The HCl salt was made by trituration with 1.0 M HCl in ether solution.

***cis*-5-(2,4-Dihydroxy-5-isopropyl-phenyl)-4-[(3-hydroxymethyl-cyclopentanecarbonyl)-amino]-isoxazole-3-carboxylic acid ethylamide (117a).** ¹H NMR (300 MHz) δ: 1.06 (t, *J* = 7.2 Hz, 3H), 1.09 (d, *J* = 7.0 Hz, 6H), 1.28-1.38 (m, 2H), 1.57-1.75 (m, 3H), 1.83-2.0 (m, 2H), 2.71 (m, 1H), 3.06 (m, 1H), 3.15-3.28 (m, 4H), 6.47 (s, 1H), 7.09 (s, 1H), 8.46 (t, *J* = 5.6 Hz, 1H), 9.1 (s, 1H), 9.77 (bs, 2H); *m/z* 432.4 [M+H]⁺. Anal. (C₂₂H₂₉N₃O₆) C, H, N.

5-(2,4-Dihydroxy-5-isopropyl-phenyl)-4-[(4-*trans*-hydroxy-cyclohexanecarbonyl)-amino]-isoxazole-3-carboxylic acid ethylamide (117b). ¹H NMR (300 MHz, CD₃OD) δ: 1.20 (d, *J* = 6.9 Hz, 6H), 1.22 (t, *J* = 7.2 Hz, 3H), 1.22-1.37 (m, 2H), 1.44-1.60 (m, 2H), 1.99 (bm, 4H), 2.28 (tt, *J* = 12.0 Hz, *J* = 3.4 Hz, 1H), 3.20 (hept., *J* = 6.9 Hz, 1H), 3.38 (q, *J* = 7.2 Hz, 2H), 3.52 (tt, *J* = 10.6 Hz, *J* = 4.1 Hz, 1H), 6.44 (s, 1H), 7.24 (s, 1H); *m/z* 430.4 [M-H]⁻. Anal. (C₂₂H₂₉N₃O₆) C, H, N.

5-(2,4-Dihydroxy-5-isopropyl-phenyl)-4-[(4-*cis*-hydroxy-cyclohexanecarbonyl)-amino]-isoxazole-3-carboxylic acid ethylamide (117c). ¹H-NMR (300 MHz) δ: 1.07 (t, *J* = 7.3 Hz, 3H), 1.09 (d, *J* = 6.7 Hz, 6H), 1.35-1.49 (m, 4H), 1.58-1.82 (m, 4H), 2.24 (m, 1H), 3.06 (hept., *J* = 7.0 Hz, 1H), 3.19 (quint., *J* = 7.1 Hz, 2H), 3.73 (bs, 1H), 6.48 (s, 1H), 7.10 (s, 1H), 8.47 (t, *J* = 5.8 Hz, 1H), 8.92 (s, 1H), 9.78 (s, 1H), 9.90 (s, 1H); *m/z* 430.1 [M-H]⁻. Anal. (C₂₂H₂₉N₃O₆) C, H, N.

5-(2,4-Dihydroxy-5-isopropyl-phenyl)-4-[(4-*cis*-hydroxymethyl-cyclohexanecarbonyl)-amino]-isoxazole-3-carboxylic acid ethylamide (117d). ¹H NMR (300 MHz) δ : 1.07 (t, $J = 7.1$ Hz, 3H), 1.09 (d, $J = 6.9$ Hz, 6H), 1.37-1.56 (m, 5H), 1.63-1.77 (m, 4H), 2.38 (m, 1H), 3.07 (hept, $J = 6.9$ Hz, 1H), 3.14-3.29 (m, 4H), 4.36 (t, $J = 5.3$ Hz, 1H), 6.49 (s, 1H), 7.11 (s, 1H), 8.50 (t, $J = 5.8$ Hz, 1H), 8.94 (s, 1H), 9.81 (s, 1H), 9.95 (bs, 1H); m/z 444.3 [M-H]⁻. Anal. (C₂₃H₃₁N₃O₆) C, H, N.

***trans*-5-(2,4-Dihydroxy-5-isopropyl-phenyl)-4-[(4-hydroxymethyl-cyclohexyl carbonyl)-amino]-isoxazole-3-carboxylic acid ethylamide (117e).** ¹H NMR (300 MHz) δ : 0.81-0.92 (m, 2H), 1.06 (t, $J = 7.1$ Hz, 3H), 1.09 (d, $J = 6.9$ Hz, 6H), 1.22-1.35 (m, 3H), 1.72-1.82 (m, 4H), 2.17 (m, 1H), 3.06 (m, 1H), 3.15-3.24 (m, 4H), 4.33 (t, $J = 5.2$ Hz, OH), 6.48 (s, 1H), 7.09 (s, 1H), 8.46 (t, $J = 5.7$ Hz, 1H), 9.00 (s, 1H), 9.78 (bs, 2H); m/z 446.6 [M+H]⁺. Anal. (C₂₃H₃₁N₃O₆) C, H, N.

***cis*-5-(2,4-Dihydroxy-5-isopropyl-phenyl)-4-[(3-morpholin-4-yl-methylcyclopentane carbonyl)-amino]-isoxazole-3-carboxylic acid ethylamide trifluoroacetate (119a).** ¹H NMR (500 MHz) δ : 1.09 (t, $J = 7.0$ Hz, 3H), 1.1 (d, $J = 6.7$ Hz, 6H), 1.35 (m, 1H), 1.50 (dt, $J = 12.5$ Hz, $J = 9.1$ Hz, $J = 9.1$ Hz, 1H), 1.81-1.86 (m, 3H), 2.02 (dt, $J = 12.5$ Hz, $J = 7.6$ Hz, $J = 7.6$ Hz, 1H), 2.32 (m, 1H), 2.83 (m, 1H), 3.02-3.11 (m, 3H), 3.15 (m, 2H), 3.21 (m, 2H), 3.43 (d, $J = 12.2$ Hz, 2H), 3.69 (t, $J = 11.9$ Hz, 2H), 3.95 (dd, $J = 12.5$ Hz, $J = 2.1$ Hz, 2H), 6.51 (s, 1H), 7.11 (s, 1H), 8.54 (t, $J = 5.6$ Hz, 1H), 9.12 (s, 1H), 9.57 (bm, 1H), 9.84 (s, 1H), 9.93 (s, 1H); m/z 501.2 [M+H]⁺. Anal. (C₂₆H₃₆N₄O₆ CF₃COOH) C, H, N.

5-(2,4-Dihydroxy-5-isopropyl-phenyl)-4-[(*trans*-4-morpholin-4-yl-cyclohexane carbonyl)-amino]-isoxazole-3-carboxylic acid ethylamide hydrochloride (119b). ¹H NMR (300 MHz) δ : 1.08 (d, $J = 6.9$ Hz, 6H), 1.08 (t, $J = 7.1$ Hz, 3H), 1.35-1.43 (m, 4H), 1.88-1.95 (m, 2H), 2.14-2.24 (m, 3H), 3-3.4 (m, 8H), 3.76-3.84 (m, 2H), 3.9-4 (m, 2H), 6.51 (s, 1H), 7.08 (s, 1H), 8.52 (t, $J = 5.6$ Hz, 1H), 9.12 (s, 1H), 9.82 (s, 1H), 9.89 (s, 1H), 10.6-10.7 (bm, 1H); m/z 501.2 [M+H]⁺. Anal. (C₂₆H₃₆N₄O₆ HCl) C, H, N.

5-(2,4-Dihydroxy-5-isopropyl-phenyl)-4-[(*cis*-4-morpholin-4-yl-cyclohexanecarbonyl)-amino]-isoxazole-3-carboxylic acid ethylamide trifluoroacetate (119c). ¹H NMR (300 MHz) δ : 1.08 (t, $J = 7.1$ Hz, 3H), 1.1 (d, $J = 6.9$ Hz, 6H), 1.53-1.57 (m, 2H), 1.78-1.89 (m, 4H), 2.03-2.13 (m, 2H), 2.56 (m, $1/2$ Wh=12.5Hz, 1H), 3.03-3.33 (m, 8H), 3.69-3.77 (m, 2H), 3.92-3.96 (m, 2H), 6.51 (s, 1H), 7.12 (s, 1H), 8.58 (t, $J = 5.6$ Hz, 1H), 9.09 (s, 1H), 9.85-9.98 (mb, 3H); m/z 501.3 [M+H]⁺. Anal. (C₂₆H₃₆N₄O₆ HCl) C, H, N.

5-(2,4-Dihydroxy-5-isopropyl-phenyl)-4-[(4-*cis*-morpholin-4-yl-methyl-cyclohexane carbonyl)-amino]-isoxazole-3-carboxylic acid ethylamide (119d). ¹H NMR (300 MHz) δ : 1.07 (t, $J = 7.6$ Hz, 3H), 1.08 (d, $J = 7.3$ Hz, 6H), 1.52 (bs, 6H), 1.72 (m, 2H), 1.98 (bs, 1H), 2.40 (bs, 1H), 3.01 (m, 5H), 3.19 (q, $J = 7.0$ Hz, 2H), 3.40 (d, $J = 11.9$ Hz, 2H), 3.78 (t, $J = 11.3$ Hz, 2H), 3.90 (d, $J = 11.9$ Hz, 2H), 6.53 (s, 1H), 7.11 (s, 1H), 8.51 (t, $J = 5.2$ Hz, 1H), 8.99 (s, 1H), 9.84 (s, 1H), 9.97 (s, 2H); m/z 514.2 [M-H]⁻. Anal. (C₂₇H₃₈N₄O₆ HCl) C, H, N.

5-(2,4-Dihydroxy-5-isopropyl-phenyl)-4-[(4-*trans*-morpholin-4-yl-methylcyclohexane carbonyl)-amino]-isoxazole-3-carboxylic acid ethylamide hydrochloride (119e). ¹H NMR (300 MHz) δ : 0.95-1.1 (m, 11H), 1.30-1.42 (m, 2H), 1.7-1.88 (m, 5H), 2.22 (m, 1H), 2.92-3.11 (m, 5H), 3.19 (m, 2H), 3.40 (d, $J = 12.5$ Hz, 2H), 3.78 (t, $J = 11.6$ Hz, 2H), 3.90 (d, $J = 9.8$ Hz, 2H), 6.51 (s, 1H), 7.09 (s, 1H), 8.50 (t, $J = 5.7$ Hz, NH), 9.04 (s, 1H), 9.83 (s, 1H), 9.91 (s, 1H), 10.12 (bs, 1H); m/z 515.7 [M+H]⁺. Anal. (C₂₇H₃₈N₄O₆ HCl) C, H, N.

5-(5-Chloro-2,4-dihydroxy-phenyl)-4-(3-morpholin-4-yl-propionylamino)-isoxazole-3-carboxylic acid ethylamide (121a). White solid. ¹H NMR (400 MHz) δ : 1.09 (t, $J = 7.4$ Hz, 3H), 2.36-2.40 (m, 4H), 2.51-2.55 (m, 4H), 3.19-3.25 (m, 2H), 3.33-3.39 (m, 2H), 3.49-3.54 (m, 2H), 6.73 (s, 1H), 7.29 (s, 1H), 8.65 (br, 1H), 10.09 (br, 1H), 10.81 (br, 1H); m/z 439.4/440.5 [M+H]⁺. Anal. (C₁₉H₂₃ClN₄O₆) C, H, Cl, N.

5-(2,4-Dihydroxy-5-isopropyl-phenyl)-4-(3-morpholin-4-yl-propionylamino)-isoxazole-3-carboxylic acid ethylamide (121b). White solid. ¹H NMR (400 MHz CD₃OD) δ : 1.19-1.24 (m, 9H), 2.51-2.54 (m, 6H), 2.71 (t, $J = 6.8$ Hz, 1H), 3.17-3.23 (m, 1H), 3.38 (d, $J = 7.2$ Hz, 2H), 3.61-3.63 (m, 4H), 6.43 (s, 1H), 7.23 (s, 1H); m/z 447.6 [M+H]⁺. Anal. (C₂₂H₃₀N₄O₆) C, H, N.

4-[3-(4-Methylpiperazin-1-yl)propionylamino]-5-(2,4-dihydroxy-5-isopropylphenyl)-isoxazole-3-carboxylic acid ethylamide (121c). White solid. ¹H NMR (400 MHz CD₃OD) δ: 1.19-1.24 (m, 9H), 2.40 (s, 3H), 2.52 (t, *J* = 6.4 Hz, 2H), 2.55-2.71 (m, 8H), 2.75 (t, *J* = 6.4 Hz, 2H), 3.14-3.25 (m, 1H), 3.34-3.39 (m, 2H), 6.44 (s, 1H), 7.23 (s, 1H). *m/z* 460.4 [M+H]⁺. Anal. (C₂₃H₃₃N₅O₅) C, H, N.

5-(2,4-Dihydroxy-5-chlorophenyl)-4-amino-isoxazole-3-carboxylic acid ethylamide (122). Yellow solid. ¹H NMR (200 MHz CD₃OD), δ: 1.23 (t, *J* = 7.2 Hz, 3H), 3.40 (q, *J* = 7.2 Hz, 2H), 6.56 (s, 1H), 7.42 (s, 1H). *m/z* 298.05/300.05[M+H]⁺.

General procedure for preparation of amines 123a-d by reductive amination.

A solution of 5-(2,4-dihydroxy-5-chlorophenyl)-4-amino-isoxazole-3-carboxylic acid ethylamide (298 mg, 1 mmol) and opportune aldehyde (2 mmol) in a mixture di MeOH/AcOH (0.1%) (15 mL) was refluxed over night. Sodium cyanoborohydride (125 mg, 2 mmol) was added to the cooled suspension and the mixture was stirred for 3 hours at r.t. The residue was treated with aqueous 5% NaHCO₃ (10 mL) and extracted with AcOEt. The combined organic extracts were washed with brine, dried, and evaporated under reduced pressure. The crude reaction material was purified by chromatography (AcOEt/light petroleum).

4-[(3-Methylthiophen-2-yl)-methylamino]-5-(5-chloro-2,4-dihydroxyphenyl)-isoxazole-3-carboxylic acid ethylamide (123a). Yield 57%. Light-yellow solid. ¹H NMR (400 MHz CDCl₃) δ: 1.24 (t, *J* = 7.2 Hz, 3H), 2.10 (s, 3H), 3.42-3.46 (m, 2H), 4.02 (s, 2H), 4.89 (br, 1H), 5.75 (s, 1H), 6.67-6.71 (m, 3H), 7.08-7.09 (m, 1H), 7.64 (s, 1H), 11.68 (br, 1H); *m/z* 408.2/410.2 [M+H]⁺. Anal. (C₁₈H₁₈ClN₃O₄S) C, H, N, S.

4-(4-Methoxybenzylamino)-5-(5-chloro-2,4-dihydroxyphenyl)-isoxazole-3-carboxylic acid ethylamide (123b). Yield 58%. ¹H NMR (400 MHz CDCl₃) δ: 1.25 (t, *J* = 7.6 Hz, 3H), 3.44-3.48 (m, 2H), 3.76 (s, 3H), 3.83-3.85 (m, 2H), 4.84 (br, 1H), 5.76 (s, 1H), 6.67 (s, 1H), 6.71 (br, 1H), 6.78 (d, *J* = 8.2 Hz, 2H), 7.14 (d, *J* = 8.2 Hz, 2H), 7.62 (s, 1H), 12.02 (br, 1H); *m/z* 418.3/420.2. [M+H]⁺. Anal. (C₂₀H₂₀ClN₃O₅) C, H, N.

5-(5-Chloro-2,4-dihydroxyphenyl)-4-(cyclohexylamino)-isoxazole-3-carboxylic acid ethylamide (123c). Yield 42%. White solid. ¹H NMR (400 MHz CDCl₃) δ: 1.10-1.29 (m, 7H), 1.57-1.82 (m, 6H), 2.61 (br, 1H), 3.45-3.53 (m, 2H), 4.48 (br, 1H), 5.80 (br, 1H), 6.65 (s, 1H), 6.85 (br, 1H), 7.69 (s, 1H), 12.18 (br, 1H); *m/z* 380.4/382.3 [M+H]⁺. Anal. (C₁₃H₂₂ClN₃O₄) C, H, N.

4-(1-Methylpiperidin-4-yl-amino)-5-(5-chloro-2,4-dihydroxyphenyl)-N-isoxazole-3-carboxylic acid ethylamide (123d). Yield 40%. White solid. ¹H NMR (400 MHz CD₃OD) δ: 1.22 (t, *J* = 7.6 Hz, 3H), 1.62-1.70 (m, 2H), 2.05-2.09 (m, 2H), 2.78 (s, 3H), 2.87-2.96 (m, 2H), 3.11-3.17 (m, 1H), 3.38-3.48 (m, 4H), 6.49 (s, 1H), 7.59 (s, 1H); *m/z* 395.4/397.3 [M+H]⁺. Anal. (C₁₈H₂₃ClN₄O₄) C, H, N.

Synthesis of 4,5,6,7-tetrahydro-isoxazolo-[4,5-c]pyridine

5-Acetyl-4,5,6,7-tetrahydro-isoxazolo[4,5,c]pyridine-3-carboxylic acid ethyl ester (136).

A mixture of **133** (2.2 g, 15.6 mmol), **134** (1.4 mL, 17.16 mmol), 40 ml of toluene and a catalytic quantity of p-TSA was heated for 12 h with Dean-Stark apparatus. The solvent was concentrated under vacuo. The crude residue was used without further purification. A solution of 2-chlorohydroxyiminoacetic acid methyl ester (3 g, 21.84 mmol) in 10 ml of DCM was added dropwise to a solution of crude residue in 30 ml of DCM. After cooling to 0°C (ice bath), TEA (3 mL, 21.84 mmol) was added dropwise. The mixture was stirred for 12 h at RT and then washed, firstly with 5% citric acid solution, and then with brine. The organic phase was dried and concentrated under vacuo. The residue was used without further purification. A mixture of **135** (2 g, 6.7 mmol) in 15 ml of DCM and TFA (0.8 mL, 10 mmol) was heated for 8 h. The reaction was quenched with 10 ml of H₂O, and the product extracted with DCM. The organic layers were combined, dried (Na₂SO₄), filtered, and evaporated in vacuo. The residue was purified by flash chromatography (AcOEt-MeOH 9:1). **136** (1.37 g) was obtained in the form of a brown-yellow oil.

Yield 91%. ¹H NMR (200 MHz, CDCl₃) δ 2.19 (s, 3H), 2.7-2.9 (m, 2H), 3.75 (t, *J* = 8 Hz, 1H), 3.93-3.99 (m, 4H), 4.57 (s, 1H), 4.70 (s, 1H); *m/z* 225 [M + H]⁺.

4,5,6,7-Tetrahydro-isoxazolo[4,5-c]pyridine-3-carboxylic acid ethyl ester hydrochloride (137)

To a solution of **136** (130 mmol) in 30 ml of EtOH was added 30 ml (260 mmol) of 32% (weight percent) HCl solution. The mixture was heated for 2 h, the solvent was removed in vacuo. To a crude material was added 500ml of cooled EtOAc. The resultant precipitate was separated by filtration and dried under vacuo.

Yield: 58%. ^1H NMR (200 MHz, DMSO) δ 1.32 (t, $J = 7$ Hz, 3H), 3.12-3.18 (m, 2H), 3.38-3.45 (m, 2H), 4.32 (s, 2H), 4.35-4.43 (q, $J = 7$ Hz, 2H), 10.01 (br, 1H); m/z 230 $[\text{M} + \text{H}]^+$.

N-ethyl-4,5,6,7-tetrahydroisoxazolo[4,5-c]pyridine-3-carboxamide (140)

To a solution of ethylamine in MeOH solution 2M (51.7 mmol) was added **137** (4.3 mmol). The mixture was stirred in argon atmosphere overnight, concentrated in vacuo, purified by flash chromatography (DCM-MeOH 9.5:0.5).

Yield: 65%. ^1H NMR (200 MHz, DMSO) δ 1.33 (t, $J = 7.2$ Hz, 3H), 3.12-3.18 (m, 2H), 3.38-3.45 (m, 2H), 4.32 (s, 2H), 4.37-4.44 (q, $J = 7.2$ Hz, 2H), 10.01 (br, 1H); m/z 229 $[\text{M} + \text{H}]^+$.

General synthesis of N-resorcinol-4,5,6,7-tetrahydroisoxazolo[4,5-c]pyridine 139a-b, 141a-b..

A mixture of the amina (0.56 mmol), EDCxHCl (0.67 mmol), HOBt (0.67 mmol), TEA (1.7 mmol) and the acid (0.56 mmol) in 10 ml of DMF was stirred at room temperature overnight and then the solvent was removed in vacuo. The residue was partitioned between AcOEt and 5% acid citric solution, the organic layer was separated and washed successively with saturated sodium bicarbonate solution, brine, dried over Na_2SO_4 , filtered and evaporated in vacuo. The crude material was purified by flash chromatography (DCM-MeOH 9.5:0.5) to give the desired compound.

Ethyl 5-(5-chloro-2,4-dihydroxybenzoyl)-4,5,6,7-tetrahydroisoxazolo[4,5-c]pyridine-3-carboxylate (139a). (Yield: 60%) ^1H NMR (200 MHz, DMSO, 120°C) δ 1.31 (t, 3H, $J = 7$ Hz), 2.92 (t, $J = 5.6$ Hz, 2H), 3.77 (t, $J = 5.6$ Hz, 2H), 4.34-4.41 (q, $J = 7$ Hz, 2H), 4.57 (s, 2H), 6.57 (s, 1H), 7.11 (s, 1H); m/z 366.9 $[\text{M} + \text{H}]^+$.

5-(5-Chloro-2,4-dihydroxybenzoyl)-N-ethyl-4,5,6,7-tetrahydroisoxazolo[4,5-c]pyridine-3-carboxamide (141a). (Yield: 65%) ^1H NMR (200 MHz, DMSO, 120°C) δ 1.14 (t, 3H, $J = 7.2$ Hz), 2.89 (t, $J = 5.8$ Hz, 2H), 3.26-3.36 (q, $J = 7.2$ Hz, 2H), 3.76 (t, $J = 5.8$ Hz, 2H), 4.55 (s, 2H), 6.51 (s, 1H), 7.09 (s, 1H), 8.19 (brt, 1H); m/z 366.0 $[\text{M} + \text{H}]^+$.

Ethyl 5-(2,4-dihydroxy-5-isopropylbenzoyl)-4,5,6,7-tetrahydroisoxazolo[4,5-c]pyridine-3-carboxylate (139b). (Yield: 70%) ^1H NMR (400 MHz, CDCl_3) δ 1.20 (s, 3H), 1.22 (s, 3H), 1.38 (t, $J = 7.2$ Hz, 3H), 3.054 (t, $J = 5.6$ Hz, 2H), 3.16 (sept, 1H), 3.93-3.95 (t, $J = 5.6$ Hz, 2H), 4.39-4.444 (q, $J = 7.2$ Hz, 2H), 4.80 (s, 2H), 6.44 (s, 1H), 7.12 (s, 1H); m/z 374.15 $[\text{M} + \text{H}]^+$.

5-(2,4-Dihydroxy-5-isopropylbenzoyl)-N-ethyl-4,5,6,7-tetrahydroisoxazolo[4,5-c]pyridine-3-carboxamide (141b). (Yield: 68%) ^1H NMR (400 MHz, DMSO) δ 1.06-1.10 (m, 9H), 2.88 (t, $J = 5.6$ Hz, 2H), 3.06 (sept, 1H), 3.23 (t, $J = 5.6$ Hz, 2H), 3.6 (brt, 2H), 4.53 (s, 2H), 6.37 (s, 1H), 6.88 (s, 1H), 8.77 (t, 1H), 9.55 (s, 1H), 9.57 (s, 1H); m/z 373 $[\text{M} + \text{H}]^+$.

Synthesis of resorcinol acid

Methyl 2-benzyloxy-4-isopropoxybenzoate (143).

To a stirred solution of 2,4-dihydroxybenzoic acid (12.0 g, 77.9 mmole) in MeOH (60 mL) at 0 °C was added a solution of sulfuric acid (5 mL, 98.1 mmole) in MeOH (5 mL) over 10 min. The resulting mixture was heated to reflux for 22 h. After cooling, the reaction was concentrated to give crude which was poured directly into water/ice mixture. The resulting precipitates were collected and triturated with 20% EtOAc/hexanes. After filtration, the solid was washed successively with 20% EtOAc/hexanes (5 x 10 mL) until the filtrate was colorless and then with hexanes (2 x 15 mL) to furnish the methyl ester **143** as solid (10.6 g, 63.3 mmole). The material was used in the next step without further purification.

Yield 81%. ^1H NMR (CDCl_3): δ 7.72 (d, $J = 8.6$, 1H), 6.42 (d, $J = 2.1$, 1H), 6.39 (d x d, $J = 8.6$ and 2.4, 1H), 3.91(s, 3H).

Methyl 5-chloro-2,4-dihydroxybenzoate (144).

Methyl 2,4-dihydroxy-benzoate (8.0 g, 47.6 mmol) was dissolved in CH₂Cl₂ (500 mL) and cooled to 0°C before addition of surfuryl chloride (4 mL, 49.4 mmol). The mixture was warmed to 25°C and stirred for 13 h. Additional surfuryl chloride (2 mL, 24.7 mmol) was added and the solution stirred for 6 h before quenching with saturated aqueous NaHCO₃ (150 mL). The organic layer was removed and the aqueous layer washed with CH₂Cl₂ (3 × 100 mL). The combined organic layers were dried (Na₂SO₄), filtered, and concentrated. Chromatography (SiO₂, 6% EtOAc in hexanes) afforded **144** (4.97 g) as a white solid.

Yield 62%. ¹H NMR (CDCl₃, 400 MHz) δ 10.86 (s, 1H), 7.84 (s, 1H), 6.63 (s, 1H), 5.99 (s, 1H), 3.95 (s, 3H); *m/z* 202 [M + H]⁺.

Methyl 5-acetyl-2,4-dihydroxybenzoate (146)

Ac₂O (35.67 mmol) was added to **145** (23.78 mmol) in BF₃OEt (95.15 mmol) and the mixture was stirred at 90°C for 3 h, then allowed to cool to room temperature, Water (70 ml) was added and the mixture stirred at room temperature for 30 minutes. The mixture was diluted with DCM. The organic layer was separated and washed successively with saturated sodium bicarbonate solution and brine, then dried over Na₂SO₄, filtered and evaporated in vacuo. The crude material was purified by flash chromatography (Petroleum Ether-AcOEt 9.5:0.5) to give the desired compound **146**.

Yield: 60%. ¹H NMR (DMSO) δ 12.58 (1H, s), 11.22 (1H, s), 8.33 (1H, s), 6.45 (1 H, s), 3.90 (3H, s), 2.62 (3H, s); *m/z* 211 [M + H]⁺.

Methyl 5-acetyl-2,4-bis(benzyloxy)benzoate (147)

BnBr (51 mmol) was added to a stirred mixture of **146** (20.4 mmol) and anhydrous potassium carbonate (51 mmol) in CH₃CN (40 ml). The mixture was heated at reflux for 6 h and then allowed to cool to room temperature and then evaporated. The residue was partitioned between AcOEt and water. The organic layer was separated and washed successively with brine, dried over Na₂SO₄, filtered and evaporated in vacuo. The residue was triturated with exane and filtered to give an off-white solid.

Yield: 91%. ¹H NMR (DMSO) δ 8.21 (1H, s), 7.55 (4H, m), 7.43 (4H, m), 7.37 (2H, m), 7.04 (1H, s), 5.38 (4H, s), 3.79 (3H, s), 2.48 (3H, s); *m/z* 391 [M + H]⁺.

Methyl 2,4-bis(benzyloxy)-5-(prop-1-en-2-yl)benzoate (148)

To a suspension of $\text{CH}_3\text{P}^+(\text{Ph}_3)\text{Br}^-$ (2 mmol) in toluene (15 ml) were added NaH 60% (5mmol), **147** (1.02 mmol) at 0°C . When the addition was complete, the ice bath was removed, and the reaction mixture was heated at reflux 5 h and then allowed to cool to room temperature, then MeOH and water were added dropwise. The mixture was extract with toluene and the organic layer was separated, washed, with brine, dried over Na_2SO_4 , filtered and evaporated in vacuo.

Yield: 96%. ^1H NMR (DMSO) δ 7.59 (1H, s), 7.52 (2H, d), 7.64-7.32 (8H, m), 6.97 (1H, s), 5.28 (2H, s), 5.22 (2H, S), 5.09 (1H, s), 5.04 (1H, s), 3.76 (3H, s), 2.02 (3H, s); m/z 389 $[\text{M} + \text{H}]^+$.

Methyl 2,4-dihydroxy-5-isopropylbenzoate (149)

Compound **148** (0.96 mmol) was dissolved in EtOH (20ml) and carefully added to 10% palladium on carbon, prewetted with water under argon atmosphere. Then the mixture was stirred under hydrogen atmosphere overnight. The catalyst was filtered from the reaction mixture, and the filtrate solvents were removed in vacuo to give the title compound **149**. (

Yield: 95%. ^1H NMR (DMSO) δ 10.54 (1H, s), 10.44 (1H, br s), 7.52 (1H, s), 6.37 (1H, s), 3.85 (3H, s), 3.08 (1H, m), 1.13 (6H, d) ; m/z 211 $[\text{M} + \text{H}]^+$.

General procedure for preparation of carboxylic acid 138a-d by hydrolysis.

To a solution of ester (0.91 mmol) in MeOH (10 ml) were added NaOH (1.1 mmol) and H_2O (2.5 ml). The mixture was heated at reflux overnight and then allowed to cool to room temperature and then evaporated. The residue was partitioned between AcOEt and 5% HCl solution. The organic layer was separated and washed with brine, then dried over Na_2SO_4 , filtered and evaporated in vacuo to give the desired acid.

5-Chloro-2,4-dihydroxybenzoic acid (138a). Yield 96%. ^1H NMR (CD_3OD , 400 MHz) δ 7.75 (s, 1H), 6.43 (s, 1H); m/z 187 $[\text{M} + \text{H}]^+$.

2,4-Dihydroxy-5-isopropylbenzoic acid (138b). Yield 61%. ^1H NMR (DMSO) δ 11.88 (1H, br s), 10.11 (1H, s), 7.54 (1H, s), 6.51 (1H, s), 3.75 (3H, s), 3.11 (1H, m), 1.13 (6H, d); m/z 233 $[\text{M} + \text{H}]^+$.

Chapter 7

Reference

- [1] Workman, P. Combinatorial attack on multistep oncogenesis by inhibiting the Hsp90 molecular chaperone. *Cancer Letters* **2004**, *206*, 149-157
- [2] Pratt, W. B.; Morishima, Y.; Peng, H. M.; Osawa, Y. Proposal for a role of the Hsp90/Hsp70-based chaperone machinery in making triage decisions when proteins undergo oxidative and toxic damage. *Experimental Biology and Medicine* **2010**, *235*, 278-289.
- [3] Dymock, B. W.; Barril, X.; Brough, P. A.; Cansfield, J. E.; Massey, A.; McDonald, E.; Hubbard, R. E.; Surgenor, A.; Roughley, S. D.; Webb, P.; Workman, P.; Wright, L.; Drysdale, M. J. Novel, Potent Small-Molecule Inhibitors of the Molecular Chaperone Hsp90 Discovered through Structure-Based Design. *J. Med. Chem.* **2005**, *48*, 4212-4215.
- [4] Söti, C.; Nagy, E.; Giricz, Z.; Vigh, L.; Csermely, P.; Ferdinandy, P. Heat shock proteins as emerging therapeutic targets. *British Journal of Pharmacology* **2005**, *146*, 769-780.
- [5] Jolly, C; Morimoto, R I. Role of the Heat Shock Response and Molecular Chaperones in Oncogenesis and Cell Death. *J. Natl. Cancer Inst.* **2000**, *92*, 1564-1572.
- [6] Isaacs, J. S.; Xu, W.; Neckers, L. Heat shock protein 90 as a molecular target for cancer therapeutics. *Cancer Cell* **2003**, *3*, 213-217.
- [7] He, H.; Zatorska, D.; Kim, J.; Aguirre, J.; Llauger, L.; She, Y.; Wu, N.; Immormino, R. M.; Gewirth, D. T.; Chiosis, G. Identification of Potent Water Soluble Purine-Scaffold Inhibitors of the Heat Shock Protein 90. *J. Med. Chem.* **2006**, *49*, 381-390.
- [8] Mosser, D. D.; Morimoto, R. I. Molecular chaperones and the stress of oncogenesis. *Oncogene* **2004**, *23*, 2907-2918.

- [9] Brough, P. A.; Barril, X.; Beswick, M. : Dymock, B. W.; Drysdale, M. J.; Wright, L.; Grant K, Massey A, Surgenor A, Workman P. 3-(5-Chloro-2,4-dihydroxyphenyl)-pyrazole-4-carboxamides as inhibitors of the Hsp90 molecular chaperone. *Bioorganic & Medicinal Chemistry Letters* **2005**, *15*, 5197-5201.
- [10] Lia, Y.; Zhanga, D.; Xua, J.; Shia, J.; Jiange, L.; Yao, N.; Ye, W. Discovery and development of natural heat shock protein 90 inhibitors in cancer treatment. *Acta Pharmaceutica Sinica B* **2012**, *2*, 238-245.
- [11] Csermely, P.; Schnaider, T.; Söti, C.; Prohászkaand, Z.; Nardai, G. The 90-kDa Molecular Chaperone Family: Structure, Function, and Clinical Applications. *Pharmacol. Ther.* **1998**, *79*, 129-168.
- [12] Smith, J. R.; Workman, P. Targeting the cancer chaperone HSP90. *Drug Discov Today Ther Strateg.* **2007**, *4*, 219-227.
- [13] Sreedhar1, A. S.; Söti, C.; Csermely, P. Inhibition of Hsp90: a new strategy for inhibiting protein kinases. *Biochim. Biophys. Acta.* **2004**, *1697*, 233-242.
- [14] Jego, G.; Hazoumé, A.; Seigneuric, R.; Garrido, C. Targeting heat shock proteins in cancer. *Cancer Lett.* **2010**
- [15] Gusev, N. B.; Bogatcheva, N. V.; Marston, S. B. Structure and Properties of Small Heat Shock Proteins (sHsp) and Their Interaction with Cytoskeleton Proteins Biochemistry. *Biochemistry* **2002**, *67*, 511-519. *Translated from Biokhimiya* **2002**, *67*, 613-623.
- [16] Ehrnsperger, M.; Gaestel, M.; Buchner, J. Analysis of Chaperone Properties of Small Hsp'. *Stress Response , Methods in Molecular Biology* **2000**, *99*, 421-429.
- [17] Hennessy, F.; Nicoll, W. S.; Zimmermann, R.; Cheetham, M. E.; Blatch, G. L. Not all J domains are created equal: implications for the specificity of Hsp40-Hsp70 interactions. *Protein science : a publication of the Protein Society* **2005**, *14*, 1697-709.
- [18] Mayer, M. P.; Bukau; B. Hsp70 chaperones: Cellular functions and molecular mechanism. *Cell. Mol. Life Sci.* **2005**, *62*, 670-684.
- [19] Bukau, B.; Horwich, A. L. The Hsp70 and Hsp60 Chaperone Machines. *Cell* **1998**, *92*, 351-366.
- [20] Pratt, W. B.; Toft, D. O. Regulation of Signaling Protein Function and Trafficking by the hsp90/hsp70-Based Chaperone Machinery. *Exp. Biol. Med.* **2003**, *228*, 111-133.

- [21] Neckers, L.; Mimnaugh, E.; Schulte, T. W. Hsp90 as an anti-cancer target. *Drug Resistance Updates* **1999**, *2*, 165-172.
- [22] Manu, A.; Katiyar-Agarwal, S.; Sahi, C.; Gallie, D. R.; Grover, A. *Arabidopsis thaliana* Hsp100 proteins: kith and kin. *Cell Stress Chaperones* **2001**, *6*, 219-224.
- [23] Schirmer, E. C.; Glover, J. R.; Singer, M. A.; Lindquist, S. HSP100/Clp proteins: a common mechanism explains diverse functions. Review Article *Trends in Biochemical Sciences* **1996**, *21*, 289-296.
- [24] Sreedhar, A. S.; Soti, C.; Csermely, P. Inhibition of Hsp90: a new strategy for inhibiting protein kinases. *Biochim. Biophys. Acta.* **2004**, *1697*, 233–242.
- [25] Workman, P. Altered states: selectively drugging the Hsp90 cancer chaperone. *Trends Mol. Med.* **2004**, *10*, 47-51.
- [26] Buchner, J. Hsp90 & Co. a holding for folding. *Trends Biochem. Sci.* **1999**, *24*, 136-141.
- [27] Isaacs, J. S.; Xu, W.; Neckers, L. Heat shock protein 90 as a molecular target for cancer therapeutics. *Cancer Cell* **2003**, *3*, 213-317.
- [28] Maloney, A.; Workman, P. Hsp90 as a new therapeutic target for cancer therapy: the story unfolds. *Expert Opin. Biol. Ther.* **2002**, *2*, 3-24.
- [29] Solit, D. B.; Chiosis, G. Development and application of Hsp90 Inhibitors. *Drug Discovery Today* **2008**, *13*, 38-43.
- [30] Barril, X.; Beswick, M. C.; Collier, A.; Drysdale, M. J.; Dymock, B. W.; Fink, A.; Grant, K.; Howes, R.; Jordan, A. M.; Massey, A.; Surgenor, A; Wayne, J.; Workman, P.; Wright, L. 4-Amino derivatives of the Hsp90 inhibitor CCT018159. *Bioorg Med Chem Lett.* **2006**, *16*, 2543-8.
- [31] Howes, R.; Barril, X.; Dymock, B. W.; Grant, K.; NorthWeld, C. J.; Robertson, A. G. S.; Surgenor, A.; Wayne, J.; Wright, L.; James, K.; Matthews, T.; Cheung, K.M.; McDonald, E.; Workman, P.; Drysdale, M. J. A Xuorescence polarization assay for inhibitors of Hsp90. *Analytical Biochemistry*, **2006**, *350*, 202-213.
- [32] Prodromou, C.; Piper, P. W.; Pearl, L. H. Expression and crystallisation of the yeast Hsp82 chaperone, and preliminary X-ray diffraction studies of the amino-terminal domain. *Prot. Struct. Funct. Genet.* **1996**, *25*, 517-522.
- [33] Prodromou, C.; Roe, S. M.; O'Brien, R.; Ladbury, J. E.; Piper, P. W.; Pearl, L. H. Identification and structural characterization of the ATP/ADP-binding site in the Hsp90 molecular chaperone. *Cell.* **1997**, *90*, 65-75.

- [34] Wright, L.; Barril, X.; Dymock, B.; Sherida, L.; Surgenor, A.; Beswick, M.; Drysdale, M.; Collier, A.; Massey, A.; Davies, N.; Fink, A.; Workman, P.; Hubbard, E. Structure-activity relationships in purine-based inhibitor binding to HSP90 isoforms. *Chemistry & Biology* 2004, *11*, 775-785.
- [35] Scheibel, T.; Johannes, B. The Hsp90 Complex-A Super-Chaperone Machine as a Novel Drug Target. *Biochemical Pharmacology* **1998**, *56*, 675-682.
- [36] Minami, Y.; Kimura, Y.; Kawasaki, H.; Suzuki, K.; Yahara, I.; The carboxy-terminal region of mammalian HSP90 is required for its dimerization and function in vivo. *Mol. Cell. Biol.* **1994**, *14*, 1459.
- [37] Nemoto, T. N.; Sato, N.; Iwanari, H.; Yamashita, H.; Takagi, T. J. Domain structures and immunogenic regions of the 90-kDa heat-shock protein (HSP90). Probing with a library of anti-HSP90 monoclonal antibodies and limited proteolysis. *Biol. Chem.* 1997, *272*, 26179-87.
- [38] Young, J. C.; Schneider, C.; Hartl, F. U. In vitro evidence that hsp90 contains two independent chaperone sites. *FEBS Lett.* 1997, *418*, 139.
- [39] Calderwood, S. K.; Khaleque, A.; Sawyer, D. B.; Ciocca, D. R. Heat shock proteins in cancer: chaperones of tumorigenesis. *TRENDS in Biochem. Science* 2006, *31*, 164.
- [40] Brown, M. A.; Zhu, L.; Schimdt, C.; Tucker, P. W. Hsp90-from signal transduction to cell transformation. *Biochem. Biophys. Res. Commun.* 2007, *363*, 241.
- [41] Chiosis, G.; Rodina, A.; Moulick, K. Emerging Hsp90 inhibitors: from discovery to clinic. *Anti-Cancer Agents-Med-Chem.* 2006, *6*, 1.
- [42] Solit, D. B.; Chiosis, G. Development and application of Hsp90 inhibitors. *Drug Discov. Today* 2008, *13*, 38.
- [43] Marcu, M. G.; Chadli, A.; Bouhouche, I.; Catelli, M.; Neckers, L. M. The heat shock protein 90 antagonist novobiocin interacts with a previously unrecognized ATP-binding domain in the carboxyl terminus of the chaperone. *Biol. Chem.* 2000, *275*, 37181.
- [44] Meyer, P.; Prodromou, C.; Hu, B.; Vaughan, C.; Roe, S. M.; Panaretou, B.; Piper, P. W.; Pearl, L. H. Structural and Functional Analysis of the Middle Segment of Hsp90: Implications for ATP Hydrolysis and Client Protein and Cochaperone. *Mol. Cell.* **2003**, *11*, 647-658.
- [45] Sgobba, M.; Rastelli, G. Structure-based and in silico design of Hsp90 inhibitor. *Chem. Med. Chem.* 2009, *4*, 1399-409.

- [46] Pearl, L. H.; Prodromou, C. Structure and *in vivo* function of Hsp90. *Curr. Opin. Struct. Bio.* **2000**, *10*, 46-51.
- [47] Powers, M. V.; Workman, P. Inhibitors of the heat shock response: biology and pharmacology. *FEBS Lett.* 2007, *581*, 3758.
- [48] Neckers, L. Hsp90 inhibitors as novel cancer chemotherapeutic agents. *Trends Mol. Med.* **2002**, *8*, S55-S61.
- [49] Kamal, A.; Kasibhatla, S.; Biamonte, M.; Zhang, H.; Zhang, L.; Lunsgren, K.; Boehm, M. F.; Burrows, F. J. *Heat Shock Proteins in Cancer*; Calderwood, S. K., Sherman, M. Y., Ciocca, D. R. Eds; *Springer-Verlag.* **2007**; 275.
- [50] Howes, R.; Barril X.; Dymock, B. W.; Grant, K.; Northfield, C. J.; Robertson, A. G.; Surgenor, A.; Wayne, J.; Wright, L.; James, K.; Matthews, T.; Cheung, K. M.; McDonald, E.; Workman, P.; Drysdale, M. J. A fluorescence polarization assay for inhibitors of Hsp90. *Anal. Biochem.* 2006, *350*, 202-13.
- [51] Kamal, A.; Thao, L.; Sensintaffar, J.; Zhang, L.; Boehm, M. F.; Fritz, L. C.; Burrows, F. J. A high-affinity conformation of Hsp90 confers tumor selectivity on Hsp90 inhibitors. *Nature* **2003**, *425*, 407-410.
- [52] Onuoha, S. C.; Mukund, S. R.; Coulstock, E. T.; Sengerová, B.; Shaw J.; McLaughlin S. H.; Jackso, S. E. Mechanistic Studies on Hsp90 Inhibition by Ansamycin Derivatives. *J. Mol. Biol.* **2007**, *372*, 287-297
- [53] Kamal, A.; Boehm, M. F.; Burrows, F. J. Therapeutic and diagnostic implications of Hsp90 activation. *Trends Mol. Med.* **2004**, *10*, 283-290.
- [54] Biamonte, M. A.; Van de Water, R.; Arndt, J. W.; Scannevin, R. H.; Perret, D.; Lee, W.C. Heat Shock Protein 90: Inhibitors in Clinical Trials. *J. Med. Chem.* **2010**, *53*, 3–17.
- [55] Le Bras, G.; Radanyi, C.; Peyrat, J. F.; Brion, J. D.; Alami, M.; Marsaud, V.; Stella, B.; Renoir, J. M. New Novobiocin Analogues as Antiproliferative Agents in Breast Cancer Cells and Potential Inhibitors of Heat Shock Protein 90. *J. Med. Chem.* **2007**, *50*, 6189
- [56] Burlison, J. A.; Neckers, L. M.; Smith, A. B.; Maxwell, A.; Blagg, B. S. Novobiocin: Redesigning a DNA Gyrase Inhibitor for Selective Inhibition of Hsp90. *J. Am. Chem. Soc.* **2006**, *128*, 15529.
- [57] De Boer, C.; Meulman, P. A.; Wnuk, R. J.; Peterson, D. H. Geldanamycin, a new antibiotic. *J. Antibiot.* **1970**, *23*, 442–447.
- [58] Cheng, H.; Cao, X.; Xian, M.; Fang, L.; Cai, T. B.; Ji, J. J.; Tunac, B.; Sun, D.; Wang P. G. Synthesis and Enzyme-Specific Activation of Carbohydrate-

- Geldanamycin Conjugates with Potent Anticancer Activity. *J. Med. Chem.* **2005**, *48*, 645-652.
- [59] Whitesell, L.; Shifrin, S. D.; Schwab, G.; Neckers, L. M. Benzoquinonoid ansamycins possess selective tumoricidal activity unrelated to src kinase inhibition. *Cancer Res* **1992**, *52*, 1721-8.
- [60] Sgobba, M.; Rastelli, G. *Minireviews*, **2009**, *4*, 1399.
- [61] Burlison, J. A.; Neckers, L. M.; Smith, A. B.; Maxwell, A.; Blagg, B. S. *J. Am. Chem. Soc.* **2006**, *128*, 15529.
- [62] Taldone, T.; Sun, W.; Chiosis, G. Discovery and development of heat shock protein 90 inhibitors. *Bioorganic & Medicinal Chemistry* **2009**, *17*, 2225-2235.
- [63] Ge, J.; Normant, E.; Porter, J. R.; Ali, J. A.; Dembski, M. S.; Gao, Y.; Georges, A. T.; Grenier, L.; Pak, R. H.; Patterson, J.; Sydor, J. R.; Tibbitts, T. T.; Tong, J. K.; Adams, J.; Palombella, V. J. Design, Synthesis, and Biological Evaluation of Hydroquinone Derivatives of 17-Amino-17-demethoxygeldanamycin as Potent, Water-Soluble Inhibitors of Hsp90. *J. Med. Chem.* **2006**, *49*, 4606-4615.
- [64] Infinity Pharmaceuticals, Inc. Product Candidates. <http://www.infi.com/product-candidates-pipeline.asp>.
- [65] Roe, S. M.; Prodromou, C.; O'Brien, R.; Ladbury, J. E.; Piper, P. W.; Pearl, L. H. Structural Basis for Inhibition of the Hsp90 Molecular Chaperone by the Antitumor Antibiotics Radicicol and Geldanamycin. *J. Med. Chem.* **1999**, *42*, 260-266.
- [66] Schulte, T. W.; Akinaga, S.; Soga, S.; Sullivan, W.; Stensgard, B.; Toft, D.; Neckers, L. M. Antibiotic radicicol binds to the N-terminal domain of Hsp90 and shares important biologic activities with geldanamycin. *Cell Stress & Chaperones* **1998**, *3*, 100-108.
- [67] Sharma, S. V.; Agatsuma, T.; Nakano, H. Oncogene. Targeting of the protein chaperone, HSP90, by the transformation suppressing agent, radicicol. **1998**, *16*, 2639-45.
- [68] Sgobba, M.; Rastelli, G. *Minireviews*, **2009**, *4*, 1399.
- [69] Biamonte, M.; Van de Water, R.; Arndt, J. W.; Scannevin, R. H.; Perret, D.; Lee, W. C. *J. Med. Chem.* **2010**, *53*, 3.
- [70] Wright, L.; Barril, X.; Dymock, B.; Sheridan, L.; Surgenor, A.; Beswick, M.; Drysdale, M.; Collier, A.; Massey, A.; Davies, N.; Fink, A.; Fromont, C.; Aherne, W.; Boxall, K.; Sharp, S.; Workman, P.; Hubbard, R. E. Structure-activity

- relationships in purine-based inhibitor binding to Hsp90 isoforms. *Chem Biol.* **2004**, *11*, 775-85.
- [71] He, H.; Zatorska, D.; Kim, J.; Aguirre, J.; Llauger, L.; She, Y.; Wu, N.; Immormino, R. M.; Gewirth, D. T.; Chiosis, G. Identification of Potent Water Soluble Purine-Scaffold Inhibitors of the Heat Shock Protein 90. *J. Med. Chem.* **2006**, *49*, 381-390.
- [72] Llauger, L.; He, H.; Kim, J.; Aguirre, J.; Rosen, N.; Peters, U.; Davies, P.; Chiosis, G. Evaluation of 8-arylsulfanyl, 8-arylsulfoxyl, and 8-arylsulfonyl adenine derivatives as inhibitors of the heat shock protein 90. *J. Med. Chem.* **2005**, *48*, 2892-905.
- [73] Zhang, L.; Fan, J.; Vu, K.; Hong, K.; Le Brazidec, J. Y.; Shi, J.; Biamonte, M.; Busch, D. J.; Lough, R. E.; Grecko, R.; Ran, Y.; Sensintaffar, J. R.; Kamal, A.; Ludgren, K.; Burrows, F. J.; Mansfield, R.; Timony, G. A.; Ulm, E. H.; Kasibhatla, S. R.; Boehm, M. F. 7'-substituted benzothiazolothio- and pyridinethiazolothio-purines as potent heat shock protein 90 inhibitors. *J. Med. Chem.* **2006**, *49*, 5352.
- [74] Kasibhatla, S. R.; Hong, K. D.; Boehm, M. F. U.S. Patent 0113339 A1 **2005**.
- [75] Kasibhatla, S. R.; Biamonte, M. A.; Hong, K. D.; Hurst, D.; Boehm, M. F. U.S. Patent 0119282 A1 **2005**.
- [76] Shi, J.; Le Brazidec, J. Y.; Biamonte, M. A.; Hong, K.D.; Boehm, M. F. U.S. Patent 0107343 A1 **2005**.
- [77] Kim, S. H.; Bajji, A.; Tangallapally, R.; Markovitz, B.; Trovato, R.; Shenderovich, M.; Baichwal, V.; Bartel, P.; Cimbora, D.; McKinnon, R.; Robinson, R.; Papac, D.; Wettstein, D.; Carlson, R.; Yager, K. M. Discovery of (2S)-1-[4-(2-{6-Amino-8-[(6-bromo-1,3-benzodioxol-5-yl)sulfanyl]-9H-purin-9-yl}ethyl)piperidin-1-yl]-2-hydroxypropan-1-one (MPC-3100), a Purine-Based Hsp90 Inhibitor. *J. Med. Chem.* **2012**, *55*, 7480-7501.
- [78] Sgobba, M.; Rastelli, G. Structure-based and in silico design of Hsp90 inhibitors. *Chem. Med. Chem.*, **2009**, *4*, 1399-409.
- [79] Huang, K. H.; Veal, J. M.; Fadden, R. P.; Rice, J. W.; Eaves, J.; Strachan, J. P.; Hall, S. E. Discovery of novel 2-aminobenzamide inhibitors of heat shock protein 90 as potent, selective and orally active antitumor agents. *J. Med.Chem.* **2009**, *52*, 4288-305.
- [80] Woodhead, A. J.; Angove, H.; Carr, M. G.; Chessari, G.; Congreve, M.; Coyle, J. E.; Cosme, J.; Graham, B.; Day, P. J.; Downham, R.; Fazal, L.; Feltell, R.;

- Figueroa, E.; Frederickson, M.; Lewis, J.; McMEnamin, R.; Murray, C. W.; O'Brien, M. A.; Parra, L.; Patel, S.; Phillips, T.; Rees, D. C.; Rich, S.; Smith, D.-M.; Gary Trewartha, G.; Vinkovic, M.; Williams, B.; Woolford, A. J.-A. Discovery of (2,4-dihydroxy-5-isopropylphenyl)-[5-(4-methylpiperazin-1-ylmethyl)-1,3-dihydroisoindol-2-yl]methanone (AT13387), a novel inhibitor of the molecular chaperone Hsp90 by fragment based drug design. *J. Med. Chem.* **2010**, *53*, 5956–5969.
- [81] Cheung, K. J.; Matthews, T. P.; James, K.; Rowlands, M. G.; Boxall, K. J.; Sharp, S. Y.; Maloney, A.; Roe, S. M.; Prodromou, C.; Pearl, L. H.; Aherne, G. W.; McDonald, E.; Workman, P. The identification, synthesis, protein crystal structure and in vitro biochemical evaluation of a new 3,4-diarylpyrazole class of Hsp90 inhibitors. *Bioorg. Med. Chem. Lett.* **2005**, *15*, 3338-43.
- [82] Kreusch, A.; Han, S.; Brinker, A.; Zhou, V.; Choi, H.; He, Y.; Lesley, S.A.; Caldwell, J.; Gu, X. Crystal structures of human Hsp90 alpha-complexed with dihydroxyphenylpyrazoles. *Bioorg. Med. Chem Lett* **2005**, *15*, 1475-8.
- [83] Sharp, S. Y.; Boxall, K.; Rowlands, M.; Prodromou, C.; Roe, S. M.; Maloney, A.; Powers, M.; Clarke, P. A.; Box, G.; Sanderson, S.; Patterson, L.; Matthews, T. P.; Cheung, K. M. J.; Ball, K.; Hayes, A.; Raynaud, F.; Marais, R.; Pearl, L.; Eccles, S.; Aherne, W.; McDonald, E.; Workman, P. *In vitro* Biological Characterization of a Novel, Synthetic Diaryl Pyrazole Resorcinol Class of Heat Shock Protein 90 Inhibitors. *Cancer Res* **2007**, *6*, 2206-16.
- [84] Cheung, K. M.; Matthews, T. P.; James, K.; Rowlands, M. G.; Boxall, K. J.; Sharp, S. Y.; Maloney, A.; Roe, S. M.; Prodromou, C.; Pearl, L. H.; Aherne, G. W.; McDonald, E.; Workman P. The identification, synthesis, protein crystal structure and in vitro biochemical evaluation of a new 3,4-diarylpyrazole class of Hsp90 inhibitors. *Bioorg. Med. Chem. Lett.* **2005**, *15*, 3338-43.
- [85] Dymock, B. W.; Barril, X.; Brough, P. A.; Cansfield, J. E.; Massey, A.; McDonald, E.; Hubbard, R. E.; Surgenor, A.; Roughley, S. D.; Webb, P.; Workman, P.; Wright, L.; Drysdale, M. J. Novel, Potent Small-Molecule Inhibitors of the Molecular Chaperone Hsp90 Discovered through Structure-Based Design. *J. Med. Chem.* **2005**, *48*, 4212-4215.
- [86] Barril, X.; Beswick, M. C.; Collier, A.; Drysdale, M. J.; Dymock, B. W.; Fink, A.; Grant, K.; Howes, R.; Jordan, A. M.; Massey, A.; Surgenor, A.; Wayne, J.; Workmanb, P.; Wrighta, L. 8 4-Amino derivatives of the Hsp90 inhibitor CCT018159. *Bioorg. Med. Chem. Lett.* **2006**, *16*, 2543–254.

- [87] Brough, P. A.; Aherne, W.; Barril, X.; Borgognoni, J.; Boxall, K.; Cansfield, J. E.; Cheung, K. M.; Collins, I.; Davies, N. G.; Drysdale, M. J.; Dymock, B.; Eccles, S. A.; Finch, H.; Fink, A.; Hayes, A.; Howes, R.; Hubbard, R. E.; James, K.; Jordan, A. M.; Lockie, A.; Martins, V.; Massey, A.; Matthews, T. P.; McDonald, E.; Northfield, C. J.; Pearl, L. H.; Prodromou, C.; Ray, S.; Raynaud, F. I.; Roughley, S. D.; Sharp, S. Y.; Surgenor, A.; Walmsley, D. L.; Webb, P.; Wood, M.; Workman, P.; Wright, L. 4,5-Diarylisoxazole Hsp90 Chaperone Inhibitors: Potential Therapeutic Agents for the Treatment of Cancer. *J. Med. Chem.* **2008**, *51*, 196–218.
- [88] Sharp, S. Y.; Prodromou, C.; Boxall, K.; Powers, M. V.; Holmes, J. L.; Box, G.; Matthews, T. P.; Cheung, K. M.; Kalusa, A.; James, K.; Hayes, A.; Hardcastle, A.; Dymock, B.; Brough, P. A.; Barril, X.; Cansfield, J. E.; Wright, L.; Surgenor, A.; Foloppe, N.; Hubbard, R. E.; Aherne, W.; Pearl, L.; Jones, K.; McDonald, E.; Raynaud, F.; Eccles, S.; Drysdale, M.; Workman, P. Inhibition of the heat shock protein 90 molecular chaperone in vitro and in vivo by novel, synthetic, potent resorcinyl pyrazole/isoxazole amide analogues. *Mol. Cancer Ther.* **2007**, *6*, 1198–211.
- [89] Wright, L.; Barril, X.; Dymock, B.; Sheridan, L.; Surgenor, A.; Beswick, M.; Drysdale, M.; Collier, A.; Massey, A.; Davies, N.; Fink, A.; Fromont, C.; Aherne, W.; Boxall, K.; Sharp, S.; Workman, P.; Hubbard, R. E. Structure-Activity Relationships in Purine-Based Inhibitor Binding to HSP90 Isoforms *Chem. Bio.* **2004**, *11*, 775–785.
- [90] Kreusch, A.; Han, S.; Brinker, A.; Zhou, V.; Choi, H. S.; He, Y.; Lesley, S. A.; Caldwell, J.; Gu, X. J. Crystal structures of human Hsp90a-complexed with dihydroxyphenylpyrazoles. *Bioorg. Med. Chem. Lett.* **2005**, *15*, 1475–1478.
- [91] Eccles, S. A.; Massey, A.; Raynaud, F. I.; Sharp, S. Y.; Box, G.; Valenti, M.; Patterson, L.; de Haven Brandon, A.; Gowan, S.; Boxall, F.; Aherne, W.; Rowlands, M.; Hayes, A.; Martins, V.; Urban, F.; Boxall, K.; Prodromou, C.; Pearl, L.; James, K.; Matthews, T. P.; Cheung, K. M.; Kalusa, A.; Jones, K.; McDonald, E.; Barril, X. NVP-AUY922: A Novel Heat Shock Protein 90 Inhibitor Active against Xenograft Tumor Growth, Angiogenesis, and Metastasis *Cancer Res.* **2008**, *68*, 2850–2860.
- [92] Wang, Y.; Trepel, J. B.; Neckers, L. M.; Giaccone, G. STA-9090, a small-molecule Hsp90 inhibitor for the potential treatment of cancer. *Curr. Opin. Invest. Drugs* **2010**, *11*, 1466–1476.

- [93] Ohba, S.; Hirose, Y.; Yoshida, K.; Yazaki, T.; Kawase, T. Inhibition of 90-kD heat shock protein potentiates the cytotoxicity of chemotherapeutic agents in human glioma cells. *J. Neurosurg.* **2010**, *112*, 33-42.
- [94] .., Pisano C., Cabri W. Novel 3,4-Isoxazolidiamides as Potent Inhibitors of Chaperone Heat Shock Protein 90 *J. Med. Chem.*, **2011**, *54*, 8592-8604.
- [95] Dymock, B. W.; Barril, X.; Brough, P. A.; Cansfield, J. E.; Massey, A.; McDonald, E.; Hubbard, R. E.; Surgenor, A.; Roughley, S. D.; Webb, P.; Workman, P.; Wright, L.; Drysdale, M. J. Novel potent small-molecule inhibitors of the molecular chaperone Hsp90 discovered through structure-based design. *J. Med. Chem.* **2005**, *48*, 4212-4215.
- [96] Biamonte, M. A.; Van de Water, R.; Arndt, J. W.; Scannevin, R. H.; Perret, D.; Lee W-C. *J. Med. Chem.* **2010**, *53*, 3-17.
- [97] Gopalsamy, A.; Shi, M.; Golas, J.; Vogan, E.; Jacob, J.; Johnson, M.; Lee, F.; Nilakantan, R.; Petersen, R.; Svenson, K.; Chopra, R.; Tam, M. S.; Wen, Y.; Ellingboe, J.; Arndt, K.; Boschelli, F. *J. Med. Chem.* **2008**, *51*, 373-375.
- [98] Taldone, T.; Sun, W.; Chiosis, G. *Bioorg. Med. Chem.* **2009**, *17*, 2225-35.
- [99] Kim, J.; Felts, S.; Llauger, L.; He, H.; Huezo, H.; Rosen, N.; Chiosis, G. Development of a fluorescence polarization assay for the molecular chaperone Hsp90. *J. Biomol. Screening* **2004**, *9*, 375-381.
- [100] Woodhead, A. J.; Angove, H.; Carr, M. G.; Chessari, G.; Congreve, M.; Coyle, J. E.; Cosme, J.; Graham, B.; Day, P. J.; Downham, R.; Fazal, L.; Feltell, R.; Figueroa, E.; Frederickson, M.; Lewis, J.; McMenamin, R.; Murray, C. W.; O'Brien, M. A.; Parra, L.; Patel, S.; Phillips, T.; Rees, D. C.; Rich, S.; Smith, D. M.; Trewartha, G.; Vinkovic, M.; Williams, B.; Woolford, A. J. A. Discovery of (2,4-Dihydroxy-5-isopropylphenyl)-[5-(4-methylpiperazin-1-ylmethyl)-1,3-dihydroisoindol-2-yl]methanone (AT13387), a Novel Inhibitor of the Molecular Chaperone Hsp90 by Fragment Based Drug Design. *J. Med. Chem.* **2010**, *53*, 5956-5969.